

Discovery, SAR Study and ADME Properties of methyl 4-amino-3-cyano-1-(2-benzyloxyphenyl)-1H-pyrazole-5-carboxylate as an HIV-1 Replication Inhibitor

Jeanne Fichez^a, Cathia Soulie^b, Laurent Le Corre^a, Sophie Sayon^b, Stéphane Priet^{c,d}, Karine Alvarez^c, Olivier Delelis^e, Patrick Gizzi^f, Guillaume Prestat^a, Christine Gravier-Pelletier^a, Anne-Geneviève Marcelin^b, Vincent Calvez^b and Patricia Busca^{*a}

^a LCBPT, UMR CNRS 8601, Université de Paris, Paris, France

^b Laboratoire de Virologie-CERVI, UMR S 1136, Hôpital Pitié Salpêtrière - Sorbonne Université, Paris, France

^c Laboratoire AFMB, UMR CNRS 7257, Université Aix-Marseille, Marseille, France

^d *Present Address*: UMR EPV, Université Aix-Marseille - IRD 190 - INSERM 1207 - EHESP, Marseille, France

^e LBPA, UMR CNRS 8113, ENS Paris-Saclay, Cachan, France

^f PCBIS, UMS CNRS 3286, ESBS - Université de Strasbourg, Illkirch, France

Table of contents

I. Biology.....	2
1. General information.....	2
2. Evaluation of the antiviral effect in a single-round infection.....	2
3. Evaluation of cytotoxicity.....	3
4. Evaluation of the antiviral effect in a multiple-round infection.....	3
5. Evaluation of ADME properties.....	3
6. Evaluation as RT inhibitor.....	5
7. Evaluation as IN inhibitor.....	6
8. Biological results of the first screening.....	6
9. Dose-response curves, EC ₅₀ and CC ₅₀ values of the three selected hits.....	35
II. Chemistry.....	37
1. General information.....	37
2. General procedures.....	37
3. Description of hydrazones II.....	37
4. Description of pyrazoles A.....	40
5. ¹ H and ¹³ C Nuclear Magnetic Resonance Spectra.....	45

I. Biology

1. General information

Chemicals and consumables

DMSO, acetonitrile, formic acid, sodium chloride, potassium chloride, sodium hydrogenophosphate, potassium dihydrogenophosphate, octanol, dodecane, L- α -Phosphatidylcholine, NADP (nicotinamide adenine dinucleotide phosphate), G6PDH (glucose-6-phosphate dehydrogenase), G6P (glucose-6-phosphate), magnesium chloride, UDPGA (uridine 5'-diphospho-glucuronic acid) and LY (Lucifer Yellow dilithium salt) were purchased from Sigma Aldrich. Deionized water was obtained from a purification system (Millipore Milli-Q plus). The RED plate (Rapid Equilibrium Dialysis) was purchased from Thermo Fisher Scientific. The 96 well MultiScreen-IP PAMPA plate was purchased from Millipore. CD1 mouse liver microsomes were obtained from Xenotech and pooled mouse plasma was obtained from CD1 mice weighing 25 – 30 g.

Instrumentation

Sample analysis for solubility and lipophilicity measurements were performed using a Gilson HPLC system with a photodiode array detector DAD 172, an autosampler GX-271 and a Valco injector. Data acquisition and processing were done with Trilution LC V3.0 software. Measurements were carried out at room temperature. A 2.6 μ m Kinetex column (50 X 4.6 mm) purchased from Phenomenex was used. The injection volume was 20 μ L, the mobile phase flow rate was set at 2 mL/min and the following program was applied for the elution: 0-0.1 min, 95% A, 5% B; 2.6-3.1 min, 5% A, 95% B; 3.3-6 min, 95% A, 5% B. Solvent A was 0.05% trifluoroacetic acid in water and solvent B was HPLC grade acetonitrile. The detection wavelength was 315 nm.

For plasma stability, metabolic stability, plasma protein binding and permeability assay, as the samples are less concentrated and in more complex matrices, analyzes were performed using an UHPLC-MS/MS system (LC-MS 8030, Shimadzu with LabSolutions version 5 software). Chromatographic separations were carried out at 40 °C. A 2.6 μ m Kinetex column (50 X 2.1 mm) purchased from Phenomenex was used. The mobile phase flow rate was set at 0.5 mL/min and the following program was applied for the elution: 0 min, 95% A, 5% B; 1.2-1.4 min, 5% A, 95% B; 1.42-2.8 min, 95% A, 5% B. Solvent A consisted of 0.05% formic acid in water and solvent B was HPLC grade acetonitrile. 1 μ L was injected. The mass spectrometer was interfaced with the liquid chromatograph using an electrospray ion source. The nitrogen nebulizing gas flow was set at 1.5 L/min and the drying gas flow at 15 mL/min. 4500 V were used for the interface voltage. Temperatures of the block heater and the desolvation line were set respectively at 400 °C and 250 °C. The collision gas used was argon at 230 kPa. The MRM transition was m/z 349.1 \rightarrow 91.1 for **A.20** and **A.21** and collision energy was set at -25.

2. Evaluation of the antiviral effect in a single-round infection

Human Hela-p4 cells, containing a stably integrated LTR linked to a Lac Z reporter gene, were cultured in 96-well microplates at 1.10^4 cells per well and maintained in DMEN with 10% (vol/vol) heat-inactivated fetal calf serum (Gibco), 100 units/mL penicillin and 100 μ g/mL streptomycin (Gibco). All cells were grown in a humidified incubator at 37 °C with 5% CO₂.

After 24 hours of culture, cells were incubated with 50 μM or varying concentrations of drugs (2.5, 7.5, 15 and 50 μM) for 48 hours. The tenofovir was evaluated in the same conditions. As control, media alone or zidovudine (0.05, 0.5 and 5 μM ; Sigma-Aldrich) was used in the same culture conditions. After 2 hours, the HIV-1 Laï (1 ng equivalent p24 antigen/well) was added for 48 hours. All experiments were performed in duplicate wells for each condition and repeated at least twice.

The HIV infection was assessed using a CPRG based beta-galactosidase detection assay kit (OZBiosciences). The levels of active beta-galactosidase expression was quickly measured by its catalytic hydrolysis of Chlorophenol red-b-D-galactopyranoside (CPRG), substrate to a dark red product. Briefly, cells were lysed and CPRG was added in a dilution buffer. The plate was incubated at 37 °C until the dark red product developed. The absorbance was read at 575 nm with a micro titer spectrophotometer (10, 30, 60, 120, 180, and 240 min).

3. Evaluation of cytotoxicity

The cytotoxicity of the tested compounds was evaluated in the same culture condition, but without HIV-1, with [3-(4,5-dimethylthiazol-2-yl)-5-(3-carboxymethoxyphenyl)-2-(4-sulfophenyl)-2H-tetrazolium, inner salt; MTS] and an electron coupling reagent (phenazine ethosulfate; PES)-based colorimetric assay according to the manufacturer's instructions (CellTiter 96® AQueous One Solution Cell Proliferation Assay, Promega). After 10, 30, 60, 120, 180, and 240 min of incubation, the absorbance was recording at 490 nm with a 96-well plate reader. The quantity of formazan product is directly proportional to the number of living cells in culture.

4. Evaluation of the antiviral effect in a multiple-round infection

The human lymphoblastoid MT2 were obtained through the NIH AIDS Research and Reference Reagent Program. This cell line was used to test the antiviral effect of the three first selected compounds in a multiple-round infection. The MT2 cells were first incubated 2 hours with each compound (5, 10, 25 and 50 μM) and then infected with the HIV-1 Laï at MOI 3 (3.10^6 cells/ 10^7 virus) and cultivated for 3 days in RPMI-1640 Glutamax supplemented with 10% (vol/vol) heat-inactivated fetal calf serum (Gibco) at 37 °C in 5% CO₂. As control, media alone or zidovudine (0.05, 0.5 and 5 μM ; Sigma-Aldrich) was used in the same culture conditions. All experiments were repeated at least twice.

The HIV-1 RNA viral load in cell culture supernatant was quantified by a real-time PCR assay using the Amplicor monitors assay (Cobas Taqman® v.2.0, Roche Diagnostics).

5. Evaluation of ADME properties

Compounds stock solutions were prepared in DMSO at 10 mM, aliquoted and then stored at -20 °C until use. All the studies were done in duplicate except PAMPA assay that was done in triplicate.

Solubility

Thermodynamic solubility was measured by dissolving compounds until saturation, in a pH 7.4 phosphate buffered saline (PBS) containing various excipients. Samples were shaken during 24 hours at 20 ± 1 °C. After centrifugation (10 min at 15000 g), the concentration in saturated solutions was measured by an HPLC procedure using a calibration curve by diluting the 10 mM DMSO stock solution to adapted concentrations.

Lipophilicity

Lipophilicity was determined by a miniaturized octanol/buffer shake flask method. 10 μL of the DMSO stock solution were added to three different volume ratios of octanol to buffer (respectively in μL , 20/970, 200/790 and 660/330). The preparations were shaken during an hour at room temperature to allow distribution of the compound between the two phases. After centrifugation at 15000 g for 5 minutes, aqueous phases were analyzed by HPLC. 1 mL of reference solution was prepared at 100 μM by diluting the stock solution in water. Knowing that $\log D$ of DMSO is -1.35 and 10 μL of DMSO were added, it is assumed that 9.6 μL of DMSO were mixed to the aqueous phase and 0.4 μL to octanol. The equation below was used to calculate $\log D$ value.

$$\log D = \log (V_{\text{ref}} \times A_{\text{ref}} - V_{\text{aq}} \times A_{\text{aq}}) / (V_{\text{oct}} \times A_{\text{aq}})$$

V_{ref} : Reference solution volume = 1 mL
 A_{ref} : Area under the peak of the reference solution
 V_{aq} : Aqueous phase volume (979.6 μL ; 799.6 μL ; 339.6 μL)
 A_{aq} : Area under the peak of the aqueous phase for the test solution
 V_{oct} : organic phase volume (20.4 μL ; 200.4 μL ; 660.4 μL)

Stability in mouse plasma

Plasma stability was determined in CD1 mouse plasma at 37 $^{\circ}\text{C}$ for 1 h. The 10 mM DMSO stock solution was diluted to a final incubation concentration of 1 μM with 0.01% DMSO. The mixture was incubated at 37 $^{\circ}\text{C}$ for various times up to 60 min. The incubation of each aliquot was stopped at 30 s, 15, 30, 45 and 60 min by adding 150 μM of ice-cold acetonitrile. Samples were stirred during 3 min, sonicated during 3 min and then centrifuged (15 000 g, 4 $^{\circ}\text{C}$) before LC-MS/MS analysis. The percentage of the remaining test compound relative to t_0 was determined by monitoring the peak area on the chromatogram. Procaine was used as positive control.

Metabolic stability (mouse liver microsomes)

Incubations in phosphate buffer containing 0.5 mg/mL of mouse liver microsomes were used to determine metabolic stability. The 10 mM DMSO stock solution was diluted to a final incubation concentration of 1 μM with 0.01% DMSO. For cytochrome P450 reactions study, a NADPH regenerating system was used consisting of 1 mM NADP, 3 mM G6P, 0.4 u/mL G6PDH and 3 mM MgCl_2 . The resulting mixture was incubated at 37 $^{\circ}\text{C}$ for various times up to 60 min. The incubation of each aliquot was stopped at 30 s, 15, 30, 45 and 60 min by adding 60 μM of ice-cold acetonitrile. Samples were vortexed, sonicated and liquid chromatography-mass spectrometry was performed on the supernatant. The percentage of the remaining test compound relative to t_0 was measured by monitoring the peak area on the chromatogram. An incubation was performed in the absence of NADPH to reveal any chemical instability or non-NADPH dependent enzymatic degradation. Testosterone was used as positive control. Half-life ($t_{1/2}$) was estimated from the slope of the logarithmic curve of the compound remaining (%) against time, assuming first-order kinetics.

Plasma protein binding

Plasma protein binding was determined by using the Thermo Scientific Single-Use RED Plate (Rapid Equilibrium Dialysis) composed of dialysis inserts with a membrane cutoff of 25 kDa. Plasma was centrifuged at 2000 g and 4 $^{\circ}\text{C}$ to remove fibrin. The 10 mM DMSO stock solution was diluted in plasma to a final concentration of 1 μM with 0.01% DMSO. 200 μL of

spiked plasma solution were placed into the sample chamber and 350 μL of PBS into the adjacent chamber. The plate was covered with a sealing tape and incubated at 37 $^{\circ}\text{C}$ on an orbital shaker set at 100 RPM for 4 hours. At the end of the incubation, the seal was removed and the volume of each side of the insert was confirmed. 50 μL of each chamber were pipetted and dispensed to microcentrifuge tubes. 50 μL of plasma or PBS are added to the appropriate tubes to obtain samples with identical final compositions in plasma and buffer. Proteins were precipitated and compound released by addition of 350 μL of acetonitrile. The tubes were then vortexed, sonicated and finally centrifuged at 15000 g for 10 min. The percentage of the test compound bound to protein is calculated as follows:

$$\% \text{ free} = (\text{peak area of buffer chamber} / \text{peak area of plasma chamber}) \times 100$$

$$\% \text{ bound} = 100 - \% \text{ free}$$

Antipyrine and verapamil were used respectively, as lowly and highly bound control compounds.

Parallel artificial membrane permeability assay (PAMPA)

Compound passage through a lipid barrier (phosphatidylcholine) was carried out in a 96-well, MultiScreen-IP PAMPA filter plate to determine apparent permeability. The artificial membrane was prepared by applying 5 μL of a L- α -Phosphatidylcholine solution in dodecane (1%, w/v) on a PVDF filter dividing each well of the plate into 2 chambers (donor and acceptor).

10 μM compound solutions were prepared in PBS pH 7.4 with 1% Lucifer yellow and 1% DMSO. LY was used to assess membrane integrity. Immediately after the application of the lipid, 150 μL of test solution were added to the donor chamber. Then, 300 μL of PBS were added to the acceptor compartment. The drug-filled donor plate was placed carefully into the acceptor plate making sure the underside of the membrane was in contact with the buffer.

Solutions at the theoretical equilibrium was prepared by mixing 150 μL test solution and 300 μL PBS (i.e., the resulting concentration if the donor and acceptor solutions were simply combined). The plate was incubated at room temperature for about 16 hours. Concentrations were then measured using LC-MS/MS in donor chamber, acceptor chamber and solution at the theoretical equilibrium.

Permeability was calculated from the following equation:

$$P_e = -C \times \text{Ln} \left[1 - \frac{\text{Area peak Acceptor}}{\text{Area peak equilibrium}} \right]$$

$$\text{where : } C = \frac{(\text{Volume}_{\text{Donor}} \times \text{Volume}_{\text{Acceptor}})}{(\text{Volume}_{\text{Donor}} + \text{Volume}_{\text{Acceptor}}) \times \text{Area}_{\text{membrane}} \times \text{time}} = 7.23\text{E-}6 \quad \text{cm/sec}$$

Antipyrine and verapamil were used respectively, as low and high permeability controls.

6. Evaluation as RT inhibitor

The p66RTB gene construct allowing the bacterial expression of the wild-type (WT) HIV-1 RT was described elsewhere.^{1, 2} The recombinant clade B WT HIV-1 RT was co-expressed

with HIV-1 protease in *Escherichia coli* in order to obtain p66/p51 heterodimers, which were later purified using affinity chromatography. Enzymes were quantitated by active-site titration before biochemical studies. Activated Calf Thymus DNA was purchased from GE Healthcare. [³H]-labelled deoxythymidine 5'-triphosphate was purchased from Perkin Elmer.

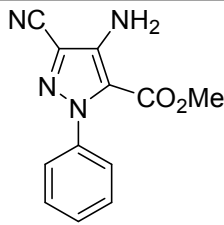
In vitro drug susceptibility assays with recombinant subtype B WT HIV-1 RT

Standard RT activity was assayed using 250 µg/mL of activated calf thymus DNA. To determine IC₅₀ values, reactions were performed with 10 nM enzyme and 5 µM of each dNTP as a mixture (dATP, dCTP, dGTP, dTTP) containing 100 µCi/mmol of [³H]-labelled deoxythymidine 5'-triphosphate (Perkin Elmer), for 15 min with increasing amounts of **A.20** and AZT and Nevirapin as references. Each aliquot was spotted in duplicate on DE81 ion-exchange paper discs. After washing in 0.3 M ammonium formate, pH 8.0, the radioactivity bound to the discs was determined by liquid scintillation counting. Values of IC₅₀ are the average from at least three independent experiments.

7. Evaluation as IN inhibitor

Recombinant HIV-1 IN was purified under non-denaturing conditions as described previously.³ Oligonucleotides mimicking the 3'-processed extremity (U5B-2: 5'-GTGTGGAAAATCTCTAGCA-3') were radiolabelled with T4 polynucleotide kinase (NEB) and [γ -³²P]ATP (Amersham), then purified on a Sephadex G-10 column. Double-stranded oligonucleotides were obtained by mixing equimolar amounts of U5B-2 with the complementary strand (U5A: 5'-ACTGCTAGAGATTTTCCACAC-3') in the presence of 100 mM NaCl. Strand-transfer reactions were carried out at 37 °C with 300 nM IN in a buffer containing 20 mM HEPES (pH 6.8), 1 mM dithiothreitol (DTT), 7.5 mM MgCl₂ and 50 mM NaCl in the presence of 12.5 nM U5A/U5B-2. Products were separated in a 16% acrylamide/urea denaturing gel, analysed with a Typhoon TRIO variable mode imager (GE Healthcare) and quantified with ImageQuant TL software. The susceptibility of IN to **A.20** was determined *in vitro* by measuring IN activity in the presence of various concentrations of ranging from 100 nM to 333 µM.

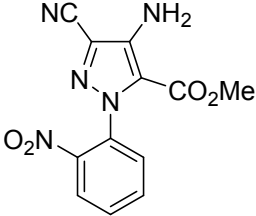
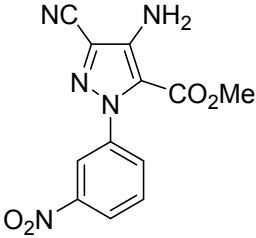
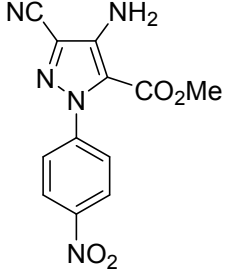
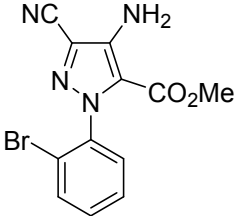
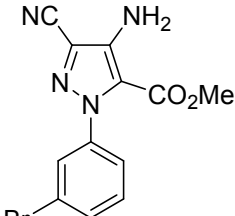
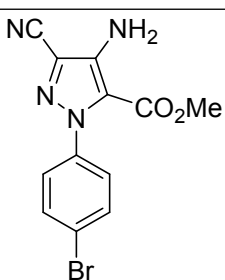
8. Biological results of the first screening

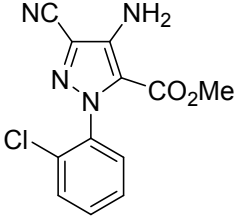
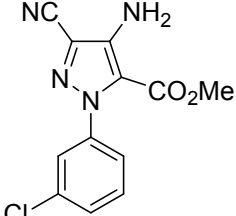
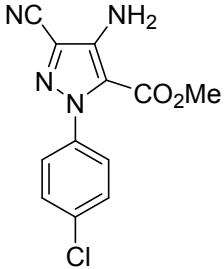
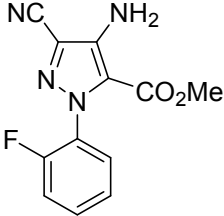
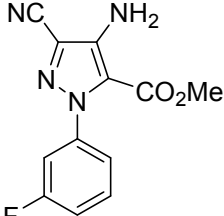
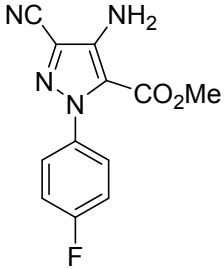
Compound	Structure	HIV activity inhibition	Cell toxicity
A.1		<30	7.0

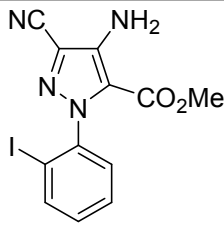
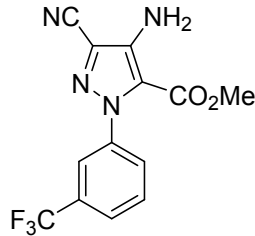
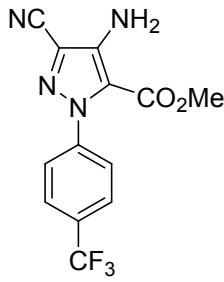
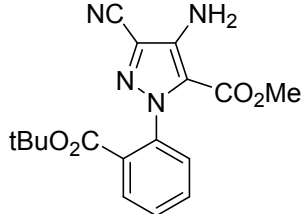
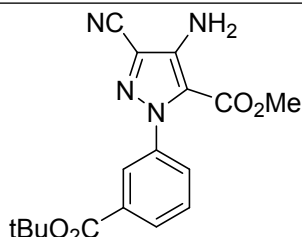
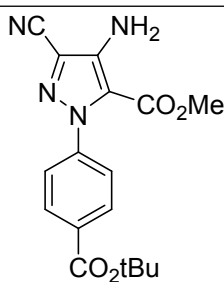
¹ J. Boretto, S. Longhi, J.-M. Navarro, B. Selmi, J. Sire and B. Canard, *Anal. Biochem.*, 2001, **292**, 139.

² B. Selmi, J. Boretto, J.-M. Navarro, J. Sire, S. Longhi, C. Guerreiro, L. Mulard, S. Sarfati and B. Canard, *J. Biol. Chem.*, 2001, **276**, 13965.

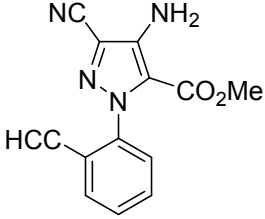
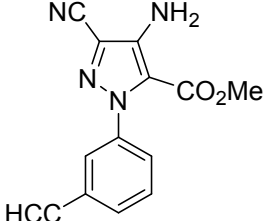
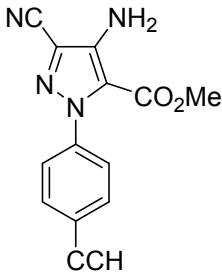
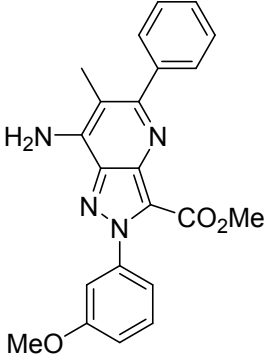
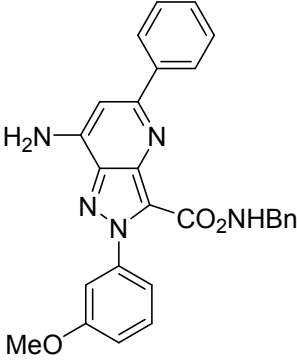
³ O. Delelis, V. Parissi, H. Leh, G. Mbemba, C. Petit, P. Sonigo, E. Deprez and J.-F. Mouscadet, *PLoS One*, 2007, **2**, e608.

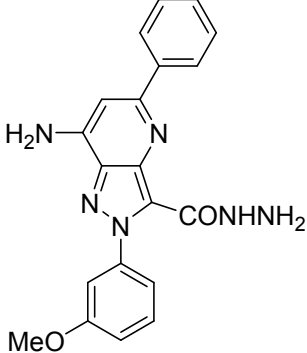
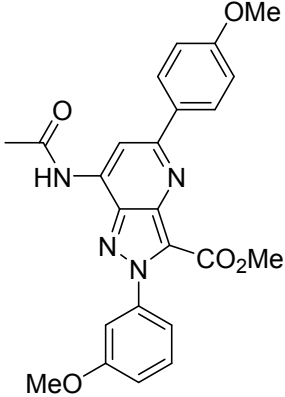
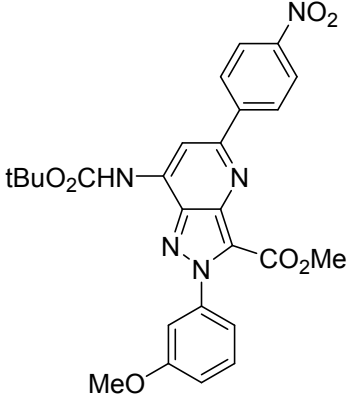
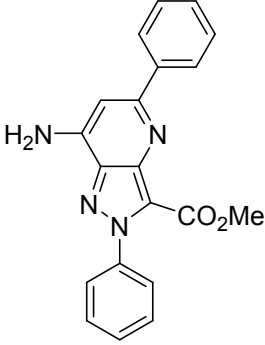
A.2		42	-5.0
A.3		47	-19.0
A.4		43	-9.0
A.5		32	4.8
A.6		42	9.0
A.7		67	20.0

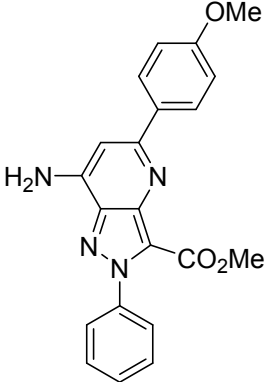
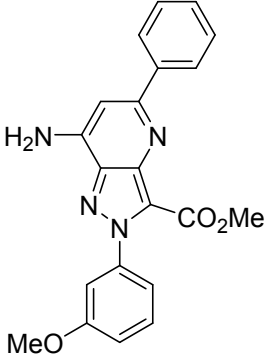
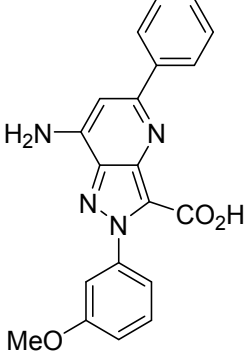
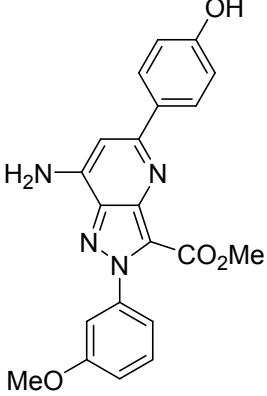
A.8		30	2.4
A.9		<30	11.0
A.10		60	12.0
A.11		<30	3.6
A.12		48	0.0
A.13		<30	6.0

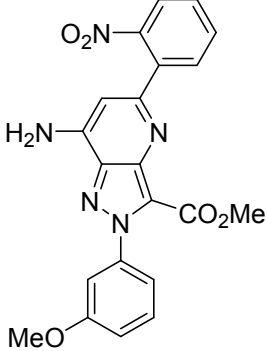
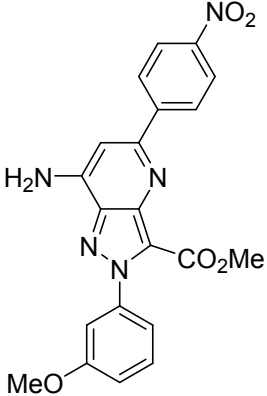
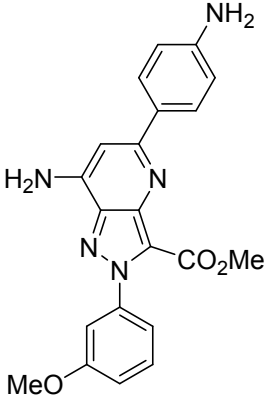
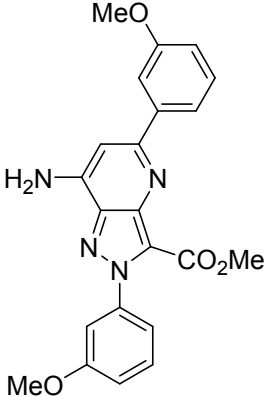
A.14	 <p>Chemical structure: 1-(4-iodophenyl)-2-amino-4-cyano-5-methylimidazole. The imidazole ring is substituted with a cyano group (NC), an amino group (NH₂), and a methyl ester group (CO₂Me). It is attached to a 4-iodophenyl ring.</p>	<30	19.0
A.15	 <p>Chemical structure: 1-(4-(trifluoromethyl)phenyl)-2-amino-4-cyano-5-methylimidazole. The imidazole ring is substituted with a cyano group (NC), an amino group (NH₂), and a methyl ester group (CO₂Me). It is attached to a 4-(trifluoromethyl)phenyl ring (F₃C).</p>	<30	39.0
A.16	 <p>Chemical structure: 1-(4-(trifluoromethyl)phenyl)-2-amino-4-cyano-5-methylimidazole. The imidazole ring is substituted with a cyano group (NC), an amino group (NH₂), and a methyl ester group (CO₂Me). It is attached to a 4-(trifluoromethyl)phenyl ring (CF₃).</p>	<30	14.0
A.17	 <p>Chemical structure: 1-(4-(tert-butoxycarbonyl)phenyl)-2-amino-4-cyano-5-methylimidazole. The imidazole ring is substituted with a cyano group (NC), an amino group (NH₂), and a methyl ester group (CO₂Me). It is attached to a 4-(tert-butoxycarbonyl)phenyl ring (tBuO₂C).</p>	<30	2.8
A.18	 <p>Chemical structure: 1-(4-(tert-butoxycarbonyl)phenyl)-2-amino-4-cyano-5-methylimidazole. The imidazole ring is substituted with a cyano group (NC), an amino group (NH₂), and a methyl ester group (CO₂Me). It is attached to a 4-(tert-butoxycarbonyl)phenyl ring (tBuO₂C).</p>	36	-15.0
A.19	 <p>Chemical structure: 1-(4-(tert-butoxycarbonyl)phenyl)-2-amino-4-cyano-5-methylimidazole. The imidazole ring is substituted with a cyano group (NC), an amino group (NH₂), and a methyl ester group (CO₂Me). It is attached to a 4-(tert-butoxycarbonyl)phenyl ring (CO₂tBu).</p>	47	14.0

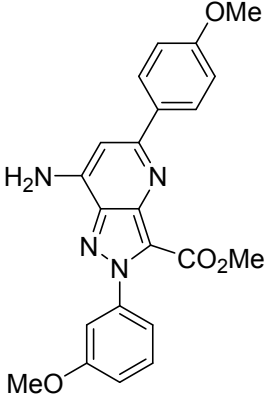
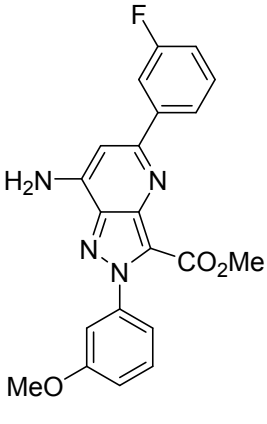
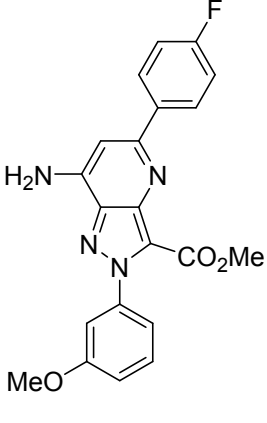
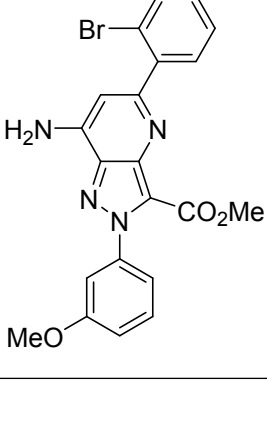
A.20		63	9.0
A.21		65	11.0
A.22		<30	3.8
A.23		<30	9.2
A.24		<30	6.0
A.25		<30	14.6

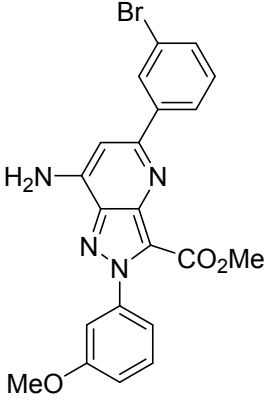
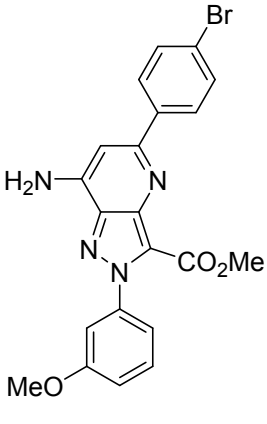
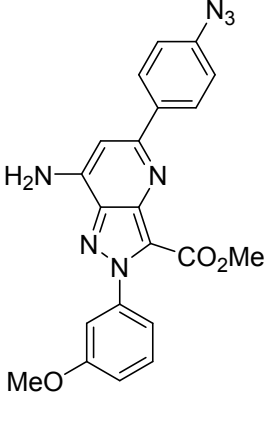
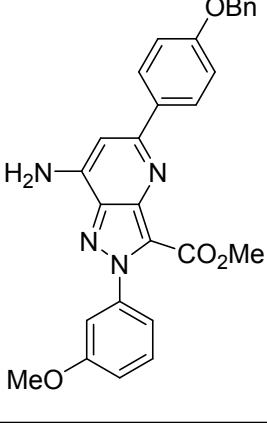
A.26		<30	7.0
A.27		<30	14.0
A.28		N.T	N.T
B.1		34	2.0
B.2		<30	55.0

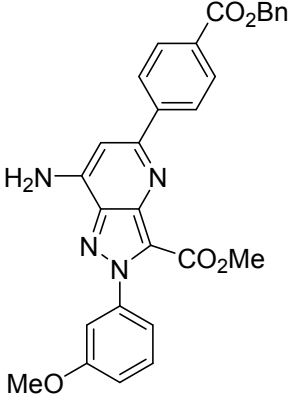
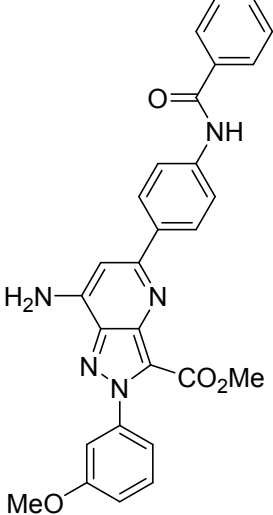
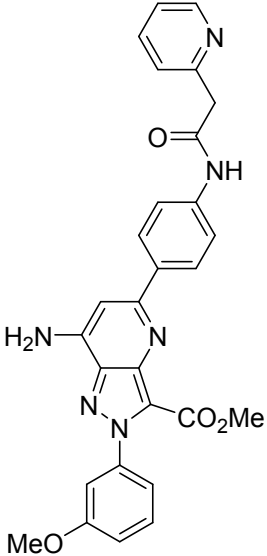
B.3		<30	-5.0
B.4		<30	-25.0
B.5		48	-3.0
B.6		<30	-21.0

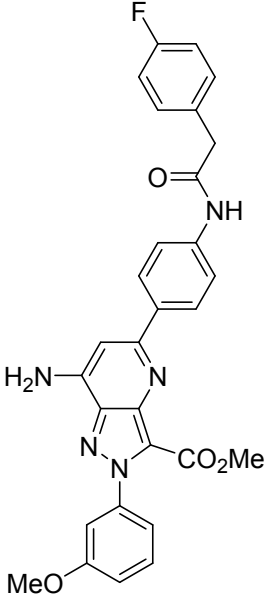
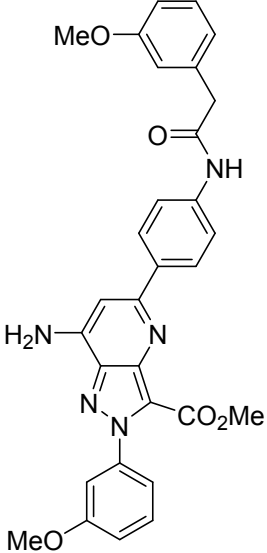
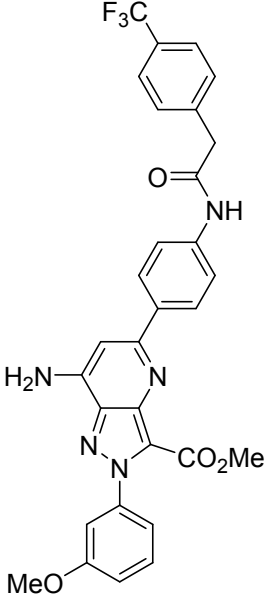
B.7		<30	-20.0
B.8		<30	-1.0
B.9		<30	17.0
B.10		<30	17.0

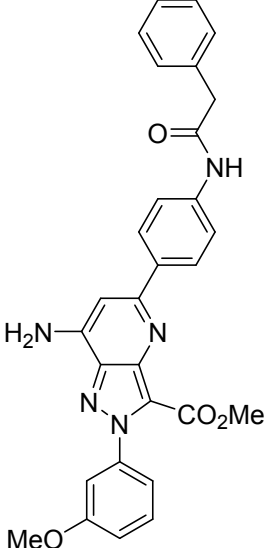
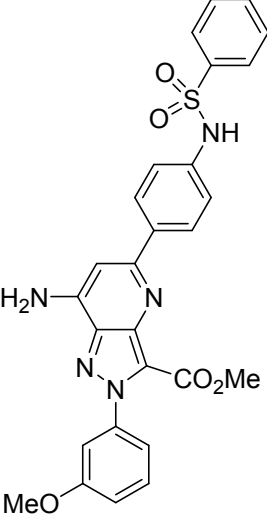
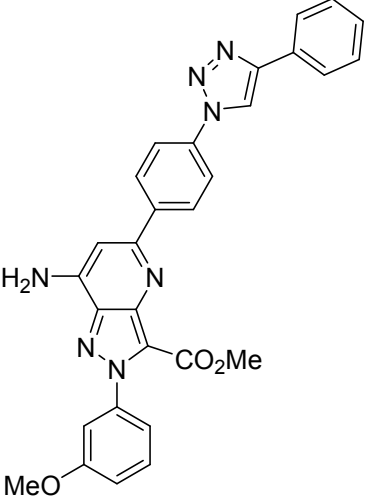
B.11		<30	3.0
B.12		<30	-37.0
B.13		<30	4.0
B.14		<30	-4.0

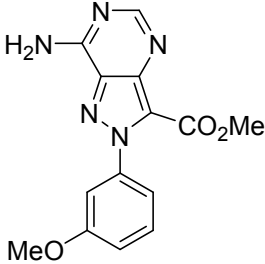
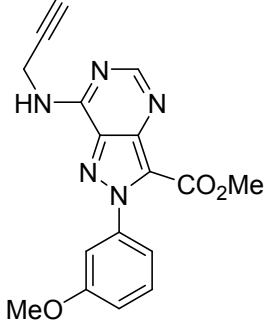
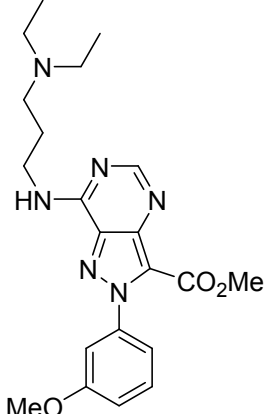
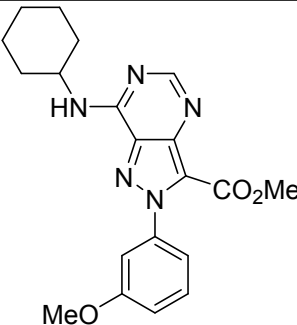
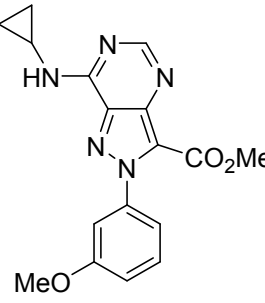
B.15		<30	-7.0
B.16		<30	-14.0
B.17		<30	-17.0
B.18		<30	-28.0

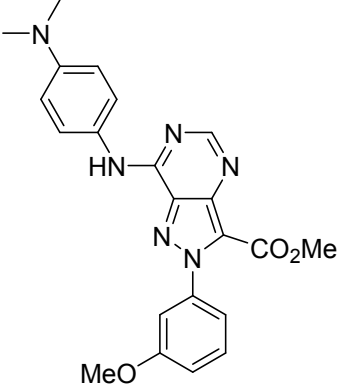
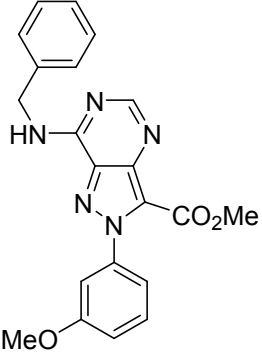
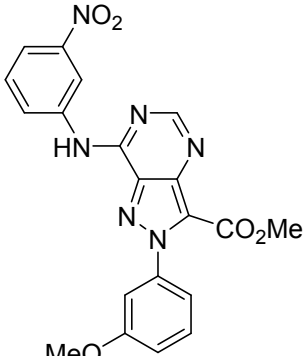
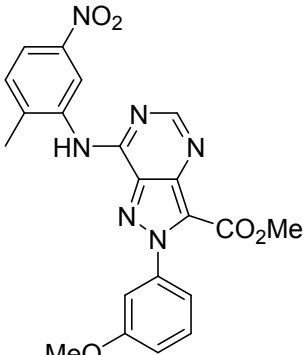
B.19		54	2.0
B.20		<30	-3.0
B.21		<30	-17.0
B.22		<30	-26.0

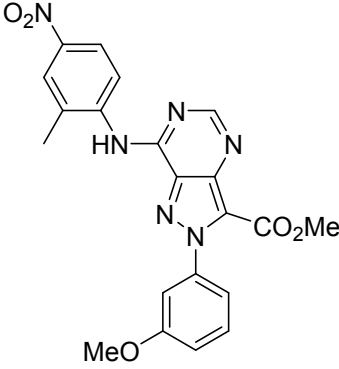
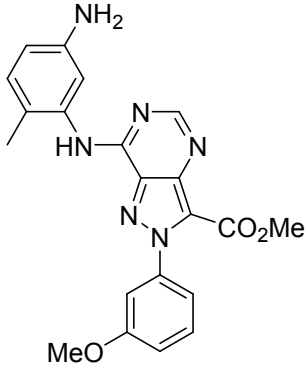
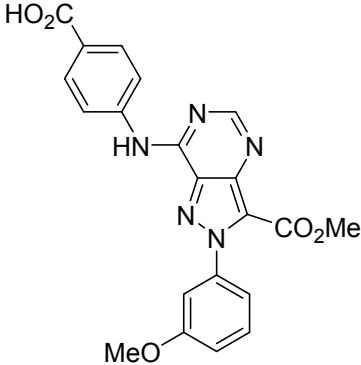
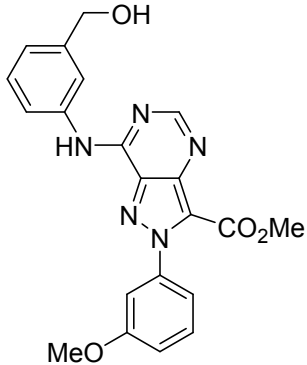
B.23		<30	10.0
B.24		<30	26.0
B.24		<30	39.0

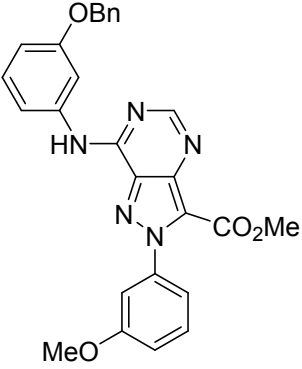
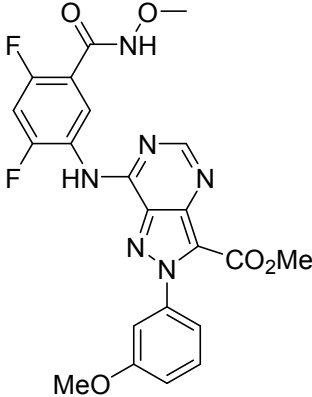
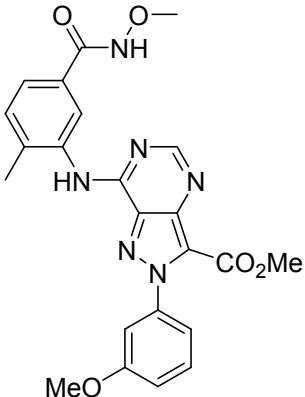
B.26		<30	51.0
B.27		33	59.0
B.28		<30	50.0

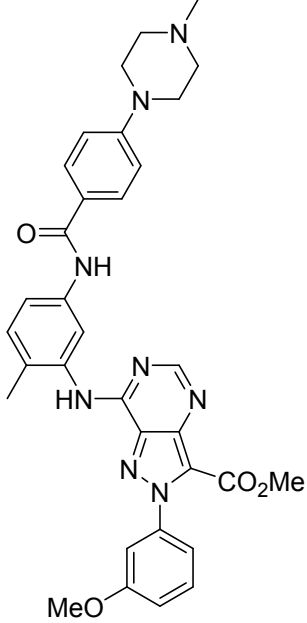
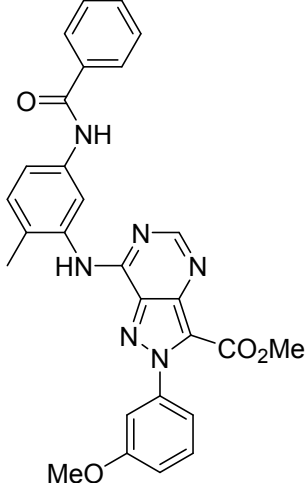
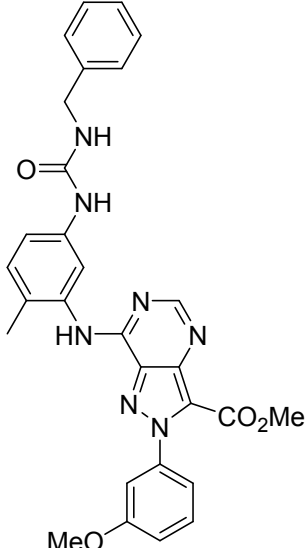
B.29		<30	11.0
B.30		<30	-8.0
B.31		<30	53.0

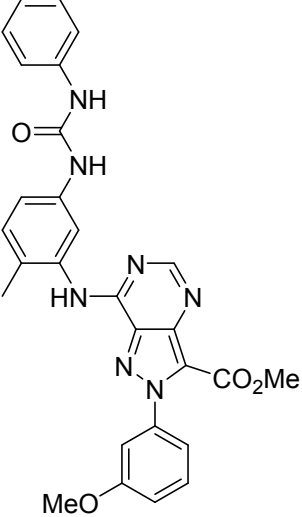
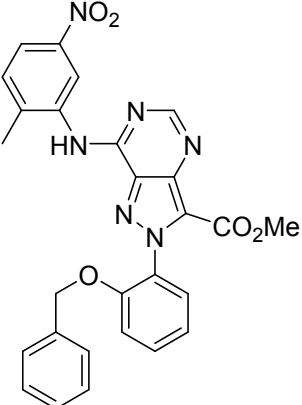
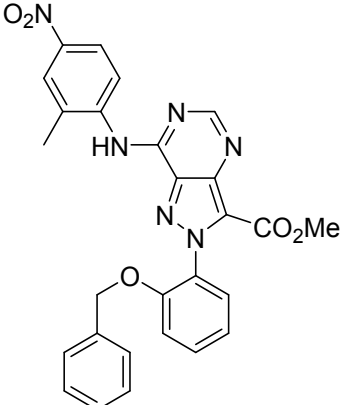
C.1		36	3.0
C.2		43	14.0
C.3		<30	18.0
C.4		35	18.0
C.5		<30	-13.0

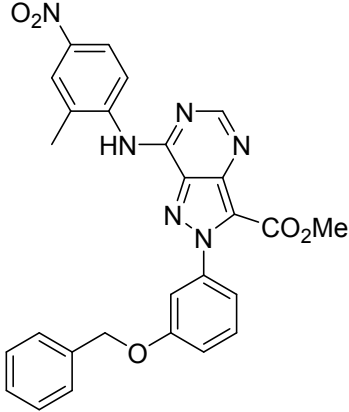
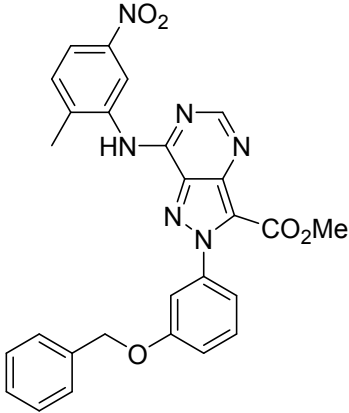
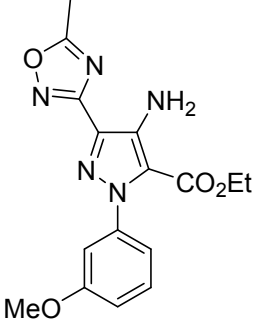
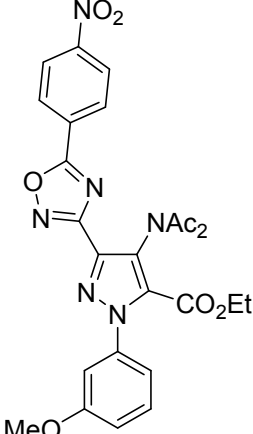
C.6		<30	-6.0
C.7		<30	-29.0
C.8		<30	-15.0
C.9		<30	-1.0

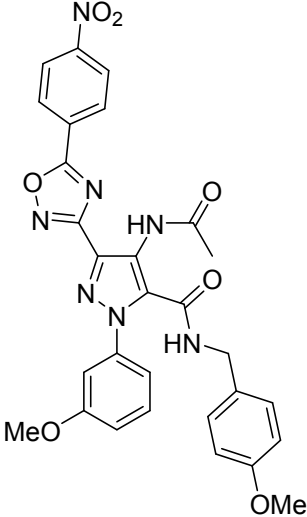
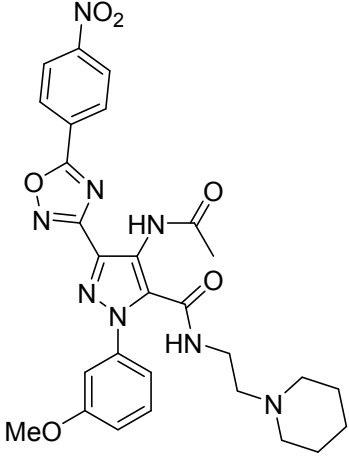
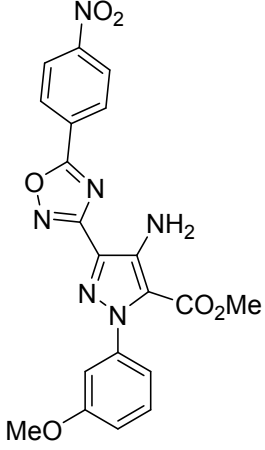
C.10		<30	-51.0
C.11		<30	-44.0
C.12		<30	-56.0
C.13		<30	-40.0

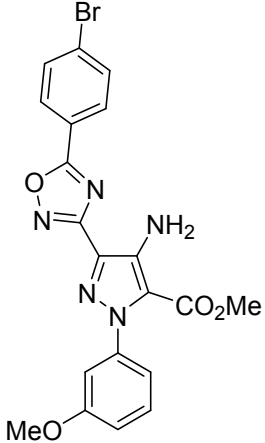
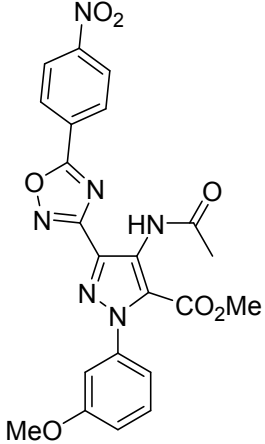
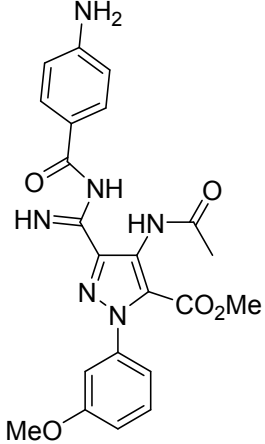
C.14		<30	-44.0
C.15		<30	-19.0
C.16		<30	-1.0

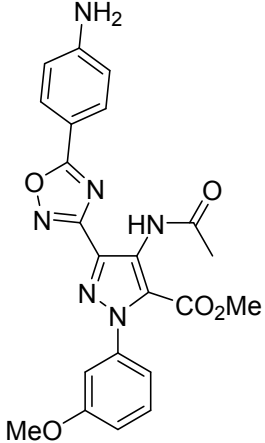
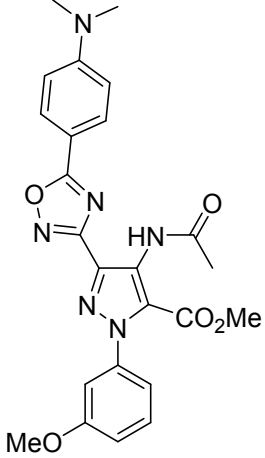
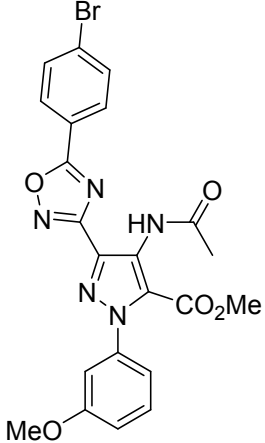
C.17		82	67.0
C.18		<30	-62.0
C.19		<30	-40.0

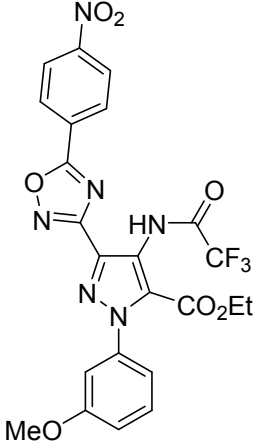
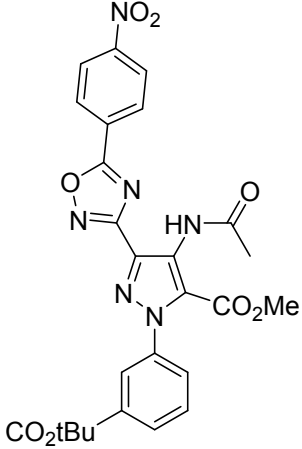
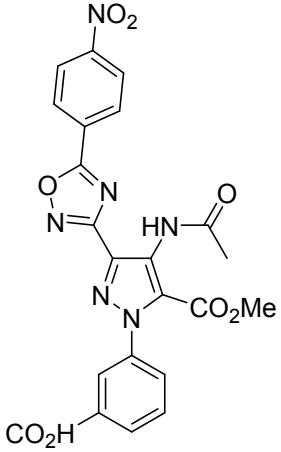
C.20		38	-2.0
C.21		<30	-28.0
C.22		<30	-25.0

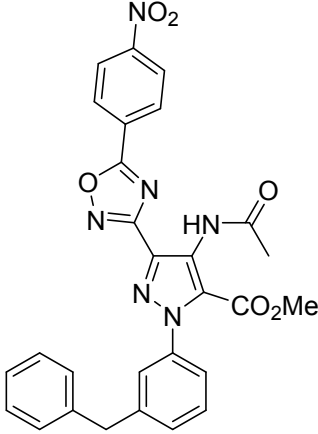
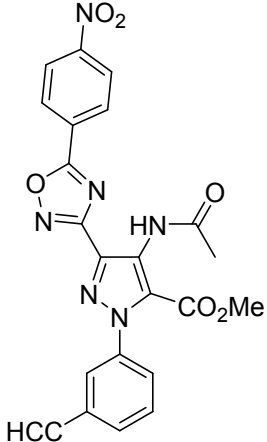
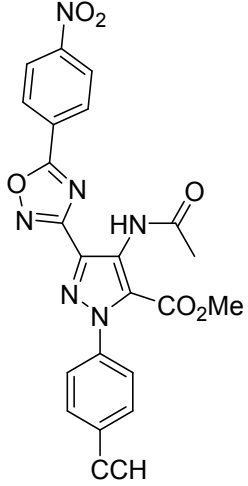
C.23		<30	-42.0
C.24		<30	23.0
D.1		<30	-32.0
D.2		<30	22.0

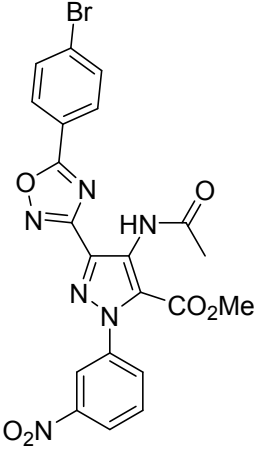
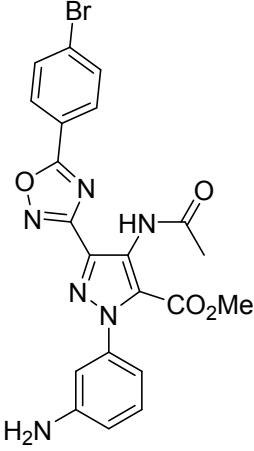
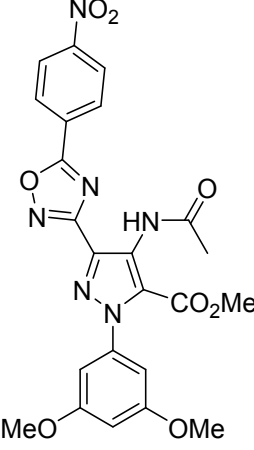
D.3	 <p>The structure shows a pyrazole ring substituted at the 4-position with a nitro group (NO₂), at the 5-position with a methoxy group (MeO), and at the 3-position with a 1,2,4-oxadiazol-5-yl group. The pyrazole ring also has two amide side chains: one at the 2-position (NH-C(=O)-CH₃) and one at the 1-position (NH-CH₂-C₆H₄-OMe).</p>	<30	-54.0
D.4	 <p>The structure shows a pyrazole ring substituted at the 4-position with a nitro group (NO₂), at the 5-position with a methoxy group (MeO), and at the 3-position with a 1,2,4-oxadiazol-5-yl group. The pyrazole ring also has two amide side chains: one at the 2-position (NH-C(=O)-CH₃) and one at the 1-position (NH-CH₂-CH₂-N(piperidine)).</p>	<30	-20.0
D.5	 <p>The structure shows a pyrazole ring substituted at the 4-position with a nitro group (NO₂), at the 5-position with a methoxy group (MeO), and at the 3-position with a 1,2,4-oxadiazol-5-yl group. The pyrazole ring also has an amino group (NH₂) at the 2-position and a methyl ester group (CO₂Me) at the 1-position.</p>	<30	-17.0

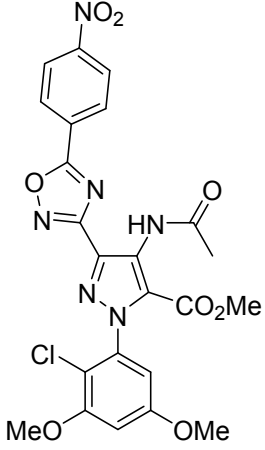
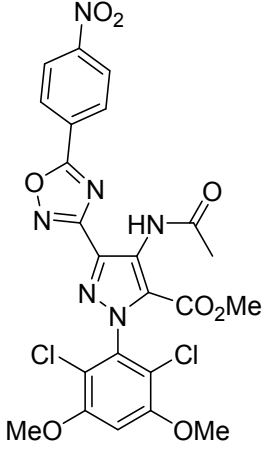
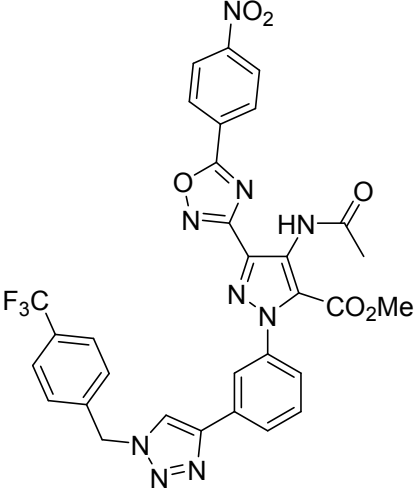
D.6		<30	-38.0
D.7		<30	-19.0
D.8		<30	-22.0

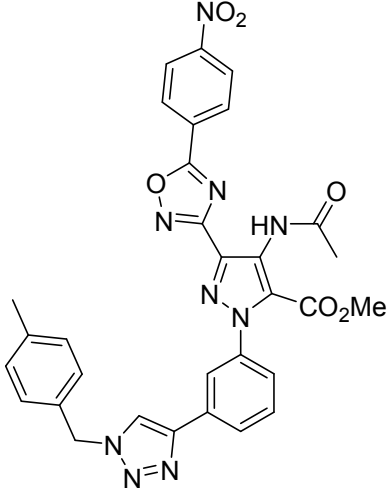
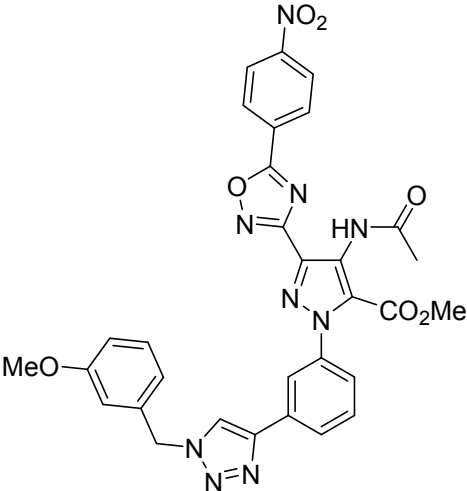
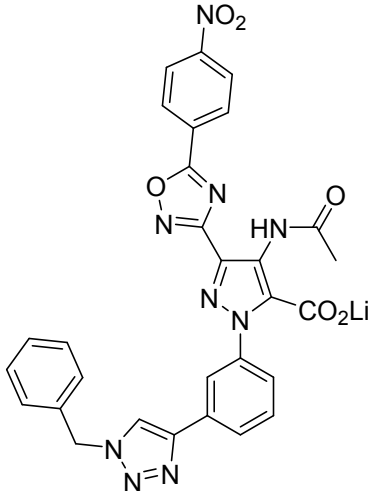
D.9		<30	1.0
D.10		30	-10.0
D.11		<30	-51.0

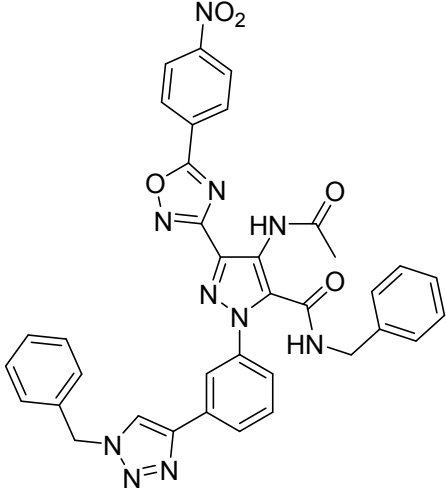
D.12		<30	-20.0
D.13		<30	-5.0
D.14		<30	-53.0

D.15		<30	-25.0
D.16		<30	-37.0
D.17		<30	-49.0

D.18		<30	-49.0
D.19		<30	-38.0
D.20		<30	-59.0

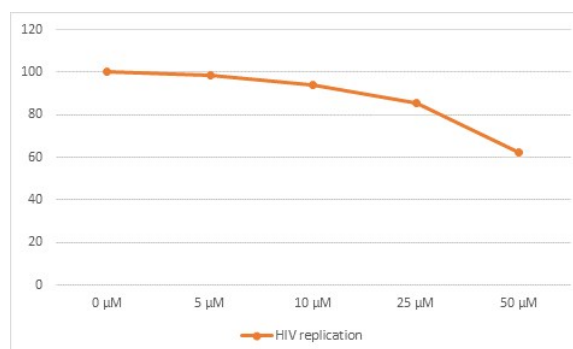
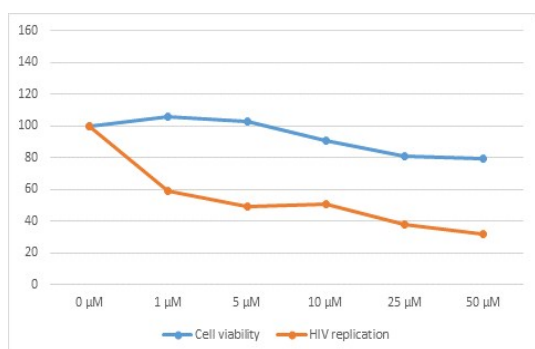
D.21		<30	-25.0
D.22		<30	-45.0
D.23		<30	7.0

D.24		<30	1.0
D.25		<30	-17.0
D.26		<30	-44.0

D.27		<30	-68.0
------	---	-----	-------

9. Dose-response curves, EC₅₀ and CC₅₀ values of the three selected hits

Compound A.20



Horizontally: inhibitor concentration.

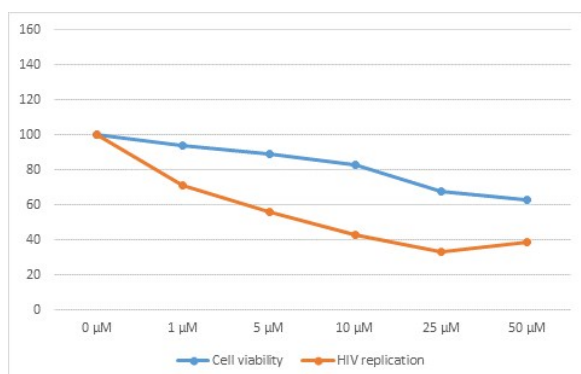
Vertically: percentage of remaining cells (blue) or viruses (orange).

$$EC_{50} = 19.4 \mu\text{M}$$

$$CC_{50} > 50 \mu\text{M}$$

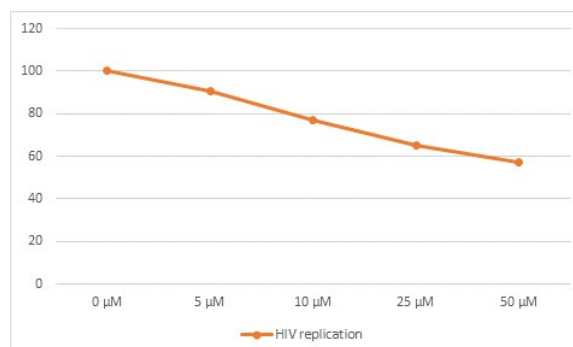
Dose-response curves in a multiple-round infection

Compound A.21



Horizontally: inhibitor concentration.

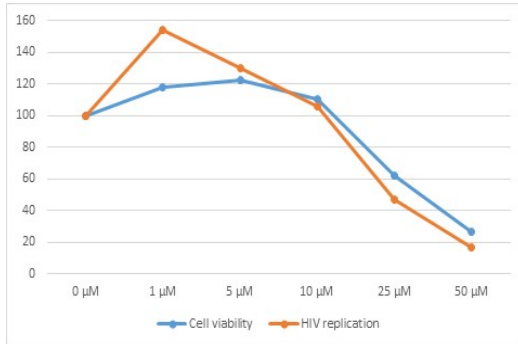
Vertically: percentage of remaining cells (blue) or viruses (orange).



Dose-response curves in a multiple-round infection

$EC_{50} = 15.2 \mu\text{M}$
 $CC_{50} > 50 \mu\text{M}$

Compound B.7



Horizontally: inhibitor concentration.
Vertically: percentage of remaining cells (blue) or viruses (orange).

EC_{50} not determined
 $CC_{50} = 35 \mu\text{M}$

II. Chemistry

1. General information

All chemicals and solvents were purchased from commercial sources and used without any further purification. All microwave assisted reactions (μW) were performed with a commercially available single-mode focused microwave reactor (model CEM Discover Benchmate). The reaction mixture temperature was monitored with an external surface sensor. The heating time was included in the measurement of reaction time.

Column chromatography was performed with silica gel 60 (40–63 μm). Thin-layer chromatography (TLC) was performed using 0.25 mm silica gel plates (60F-254). The solvent systems are given in v/v. ^1H and ^{13}C NMR spectra were recorded on Bruker Advance 500 (500 MHz). Data for ^1H and ^{13}C NMR are reported as follows: chemical shift (ppm), multiplicity (s = singlet, d = doublet, t = triplet, q = quartet, m = multiplet), and coupling constants are expressed in Hertz. IR spectra were recorded on a Perkin Elmer Spectrum one FT-IR Spectrometer (ATR), and the wavenumbers are reported in cm^{-1} . Low resolution mass spectra were obtained on a LCQ Advantage spectrometer (ThermoElectron). High resolution mass spectra were recorded with a TOF mass analyzer. Melting points were determined on a Kofler heating bench and values are expressed with a precision of $\pm 2^\circ\text{C}$.

2. General procedures

General procedure I for the synthesis of the aryl-hydrazones

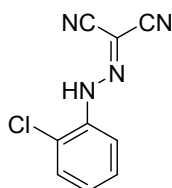
To an ice-cold solution of the aniline (1 equiv) in water (5 mL.mmol $^{-1}$) were successively added dropwise 37% aq. HCl (11 equiv) and 1 M aq. NaNO $_2$ (1 equiv). The mixture was stirred for 30 min and then added dropwise to a solution of malononitrile (1.5 equiv) and 3 M sodium acetate (31 equiv) in water with continuous stirring and cooling to 0 $^\circ\text{C}$. After 2 h, the insoluble hydrazone was filtered off and washed with water. The precipitate was dissolved in AcOEt and washed with brine. The organic layer was dried over MgSO $_4$ and concentrated under vacuum to afford the desired hydrazone which was used without further purification.

General procedure II for the synthesis of the pyrazoles

A mixture of hydrazone (1 equiv), potassium carbonate (2.7 equiv), and methyl bromoacetate (7.5 equiv) in dioxane (3 mL.mmol $^{-1}$) was irradiated at 110 $^\circ\text{C}$ (power input: 90 W) for 10 to 30 min. The reaction mixture was cooled to rt and concentrated in vacuo. The resulting residue was dissolved in DCM and washed with brine. The organic layer was dried over MgSO $_4$ and concentrated under vacuum. Flash chromatography afforded the desired pyrazole.

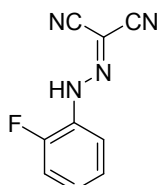
3. Description of hydrazones II

(2-Chlorophenyl)carbonohydrizonoyl dicyanide (II.8)



According to the general procedure **I**, hydrazone **II.2** was synthesized from *o*-chloroaniline (0.638 g, 5.00 mmol) and obtained as a yellow solid (1.05 g, 99 %). **mp** 121-123 °C **¹H NMR** (500 MHz, CDCl₃) δ 10.06 (bs, 1H), 7.66 (dd, *J* = 1.5, *J* = 8.5, 1H), 7.48-7.38 (m, 2H), 7.29-7.20 (m, 1H). **¹³C NMR** (125 MHz, CDCl₃) δ 135.7, 130.0, 128.7, 127.0, 121.1, 117.2, 111.7, 107.6, 89.5. **IR** ν 3274, 2234, 2215. **HRMS** [M-H]⁻ calculated *m/z* 203.0203, found *m/z* 203.0125.

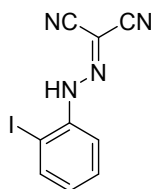
(2-Fluorophenyl)carbonohydrizonoyl dicyanide (II.11)



According to the general procedure **I**, hydrazone **II.11** was synthesized from *o*-fluoroaniline (0.56 g, 5.00 mmol) and obtained as a yellow solid (0.64 g, 68 %). **mp** 151-153 °C **¹H NMR** (500 MHz, CDCl₃) δ 9.75 (bs, 1H), 7.62-7.57 (m, 1H), 7.26-7.19 (m, 3H). **¹³C NMR** (125 MHz, CDCl₃) δ 151.2 (d, *J* = 246.5), 128.1 (d, *J* = 8.5), 127.1 (d, *J* = 7.5), 125.7 (d, *J* = 2.5), 117.3, 116.1 (d, *J* = 17.5), 111.7, 107.5, 89.4. **IR** ν 3242, 2234, 2207. **HRMS** [M-H]⁻ calculated *m/z* 187.0498, found *m/z* 187.0420.

1-Cyano-N-(2-iodophenyl)methanecarbohydrazonoyl cyanide (II.14)⁴

[CAS : 191353-22-7]



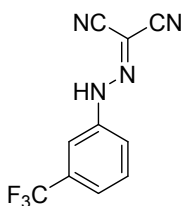
According to the general procedure **I**, hydrazone **II.14** was synthesized from commercially available 2-iodoaniline (0.400 g, 1.83 mmol) and obtained as a bright yellow solid (0.402 g, 74%). **¹H NMR** (500 MHz, CDCl₃) δ 10.03 (bs, 1H), 7.81 (dd, *J* = 8.0, *J* = 1.5, 1H), 7.55 (dd, *J* = 8.5, *J* = 2.0, 1H), 7.43 (ddd, *J* = 8.0, *J* = 7.5, *J* = 1.5, 1H), 6.99 (ddd, *J* = 8.0, *J* = 7.5, *J* = 1.5, 1H). **¹³C NMR** (125 MHz, CDCl₃) δ 139.4, 138.7, 130.2, 127.9, 117.4, 111.7, 107.8, 89.0, 84.7.

(3-(Trifluoromethyl)phenyl)carbonohydrizonoyl dicyanide (II.15)⁵

[CAS : 3720-41-0]

⁴ D.C. DeLuca, T. Hinds and C.G. Winter, *Arch. Biochem. Biophys.*, 1997, **342**, 182.

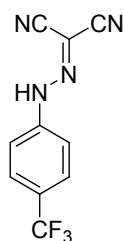
⁵ L.L. Corre, M.C.D. Lang, C. Garbay, C. Gravier-Pelletier, P. Busca, M. Ethève-Quellejeu and E. Braud, *Synthesis*, 2016, **48**, 4569.



According to the general procedure **I**, hydrazone **II.15** was synthesized from 3-aminobenzotrifluoride (0.500 g, 3.10 mmol) and obtained as an orange solid (0.73 g, 99 %). $^1\text{H NMR}$ (500 MHz, CDCl_3) δ 9.98 (bs, 1H), 7.60 (m, 1H), 7.57 (m, 1H), 7.51 (m, 2H). $^{13}\text{C NMR}$ (500 MHz, CDCl_3) δ 140.2, 132.6 (q, $J = 130$), 130.7, 124.4, 123.2 (m), 119.1, 113.0 (m), 111.7, 108.0, 88.4.

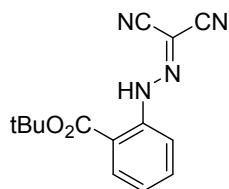
(4-(Trifluoromethyl)phenyl)carbonohydrizonoyl dicyanide (II.16)⁵

[CAS : 7089-17-0]



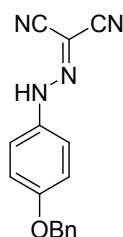
According to the general procedure **I**, hydrazone **II.16** was synthesized from 4-aminobenzotrifluoride (0.500 g, 3.10 mmol) and obtained as an orange solid (0.73 g, 99 %). $^1\text{H NMR}$ (500 MHz, CDCl_3) δ 9.87 (bs, 1H), 7.22 (d, $J = 12.5$, 2H), 7.43 (d, $J = 8.5$, 2H). $^{13}\text{C NMR}$ (500 MHz, CDCl_3) δ 142.2, 128.5, 127.4, 122.6, 116.0, 111.6, 107.8, 88.9.

tert-Butyl 2-(2-(dicyanomethylene)hydrazinyl)benzoate (II.17)



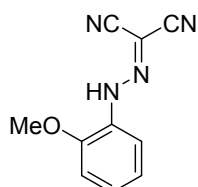
According to the general procedure **I**, hydrazone **II.17** was synthesized from *tert*-butyl 2-aminobenzoate (1.0 g, 5.18 mmol) and obtained as a brown solid (1.33 g, 95 %). **mp** 167-169 °C $^1\text{H NMR}$ (500 MHz, CDCl_3) δ 13.60 (bs, 1H), 7.66 (dd, $J = 2.0$, $J = 8.0$, 1H), 7.77 (m, 1H), 7.59 (m, 1H), 7.22 (m, 1H). $^{13}\text{C NMR}$ (125 MHz, CDCl_3) δ 167.3, 142.6, 134.6, 131.3, 124.9, 116.2, 115.9, 112.6, 108.4, 88.9, 84.0, 28.2. **IR** ν 2981, 2226, 2212. **HRMS** $[\text{M}-\text{H}]^-$ calculated m/z 269.1117, found m/z 269.1035.

(4-(Benzyloxy)phenyl)carbonohydrizonoyl dicyanide (II.22)



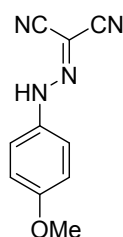
According to the general procedure I, hydrazone **II.22** was synthesized from 4-benzyloxy aniline (1.00 g, 5.02 mmol) and obtained as a yellow solid (0.98 g, 70 %). **mp** 155-157 °C **¹H NMR** (500 MHz, CDCl₃) δ 9.70 (bs, 1H), 7.37-7.42 (m, 5H), 7.27-7.24 (m, 2H) 7.04-7.00 (m, 2H), 5.09 (s, 2H). **¹³C NMR** (125 MHz, CDCl₃) δ 157.7, 136.3, 133.5, 128.7, 128.3, 127.5, 117.5, 116.2, 112.5, 108.5, 85.5, 70.5. **IR** ν 3525, 2229, 2215. **HRMS** [M+H]⁺ calculated m/z 275.1011, found m/z 275.0930.

(2-Methoxyphenyl)carbonohydrizonoyl dicyanide (II.23)



According to the general procedure I, hydrazone **II.23** was synthesized from *o*-anisidine (0.618 g, 5.02 mmol) and obtained as a brown solid (0.97 g, 97 %). **mp** 151-153 °C **¹H NMR** (500 MHz, CDCl₃) δ 10.13 (bs, 1H), 7.52 (dd, *J* = 1.0, *J* = 8.0, 1H), 7.17-7.26 (m, 1H), 7.01 (m, 2H), 3.96 (s, 3H). **¹³C NMR** (125 MHz, CDCl₃) δ 147.4, 128.8, 126.7, 121.9, 115.9, 112.5, 111.2, 108.2, 87.2, 56.1. **IR** ν 3276, 2231, 2204. **HRMS** [M-H]⁻ calculated m/z 199.0698, found m/z 199.0614.

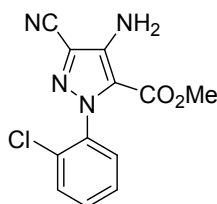
(4-Methoxyphenyl)carbonohydrizonoyl dicyanide (II.25)



According to the general procedure I, hydrazone **II.25** was synthesized from *p*-anisidine (0.618 g, 5.02 mmol) and obtained as an orange solid (0.77 g, 77 %). **mp** 155-157 °C **¹H NMR** (500 MHz, CDCl₃) δ 9.70 (bs, 1H), 7.32 (d, *J* = 9.0, 2H), 6.81 (d, *J* = 9.03, 2H), 3.78 (s, 3H). **¹³C NMR** (125 MHz, CDCl₃) δ 158.6, 133.5, 117.6, 115.2, 112.5, 108.7, 85.3, 55.7. **IR** ν 3197, 2222, 2204. **HRMS** [M-H]⁻ calculated m/z 199.0698, found m/z 199.0642.

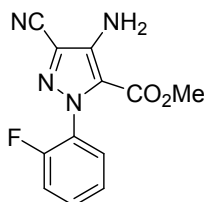
4. Description of pyrazoles A

Methyl 4-amino-1-(2-chlorophenyl)-3-cyano-1H-pyrazole-5-carboxylate (A.8)



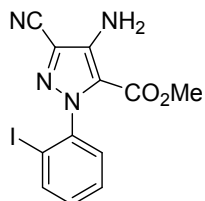
According to the general procedure **II**, pyrazole **A.8** was synthesized from the hydrazone **II.8** (1.05 g, 5.12 mmol). The mixture was irradiated for 20 min. Flash chromatography (toluene/acetone 99:1) afforded **A.8** as an orange solid (0.497 g, 35 %). **mp** 123-125 °C **¹H NMR** (500 MHz, CDCl₃) δ (ppm) 7.51 (dd, $J = 1.5$, $J = 8.0$, 1H), 7.45 (td, $J = 2.0$, $J = 8.0$, 1H), 7.42-7.36 (m, 2H), 4.80 (s, 2H), 3.73 (s, 3H). **¹³C NMR** (125 MHz, CDCl₃) δ 159.0, 141.3, 138.0, 131.8, 131.0, 129.9, 128.7, 127.4, 118.5, 114.9, 112.3, 52.0. **IR** ν 1727, 2235, 3334. **HRMS** [M+H]⁺ calculated m/z 277.0414, found m/z 277.0488.

Methyl 4-amino-1-(2-fluorophenyl)-3-cyano-1H-pyrazole-5-carboxylate (A.11)



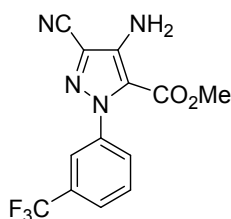
According to the general procedure **II**, pyrazole **A.11** was synthesized from the hydrazone **II.11** (0.59 g, 3.13 mmol). The mixture was irradiated for 20 min. Flash chromatography (toluene/acetone 99:1) afforded **A.11** as an orange solid (0.58 g, 71 %). **mp** 107-109 °C **¹H NMR** (500 MHz, CDCl₃) δ (ppm) 7.49-7.45 (m, 1H), 7.42 (td, $J = 2.0$, $J = 8.0$, 1H), 7.29-7.25 (m, 1H), 7.21 (td, $J = 2.0$, $J = 8.5$, 1H), 4.75 (s, 2H), 3.77 (s, 3H). **¹³C NMR** (125 MHz, CDCl₃) δ 159.07, 157.87-155.88 (d, $J = 249.0$), 141.46, 131.34-131.28 (d, $J = 8.0$), 128.35-128.23 (d, $J = 14.5$), 128.00, 124.48-124.43 (d, $J = 3.5$), 118.43, 116.19-116.03 (d, $J = 20.0$), 115.30, 112.15, 51.97. **IR** ν 1699, 2236, 3357. **HRMS** [M+H]⁺ calculated m/z 261.0710, found m/z 261.0779.

Methyl 4-amino-3-cyano-1-(2-iodophenyl)-1H-pyrazole-5-carboxylate (A.14)



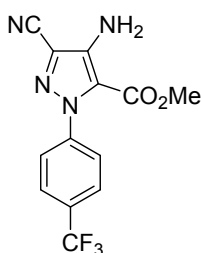
According to the general procedure **II**, pyrazole **A.14** was synthesized from hydrazone **II.14** (0.395 g, 1.33 mmol). 40 minutes were necessary to the full conversion of the substrates. Flash chromatography (toluene/acetone 98:2) afforded **A.14** as a yellow solid (0.290 g, 59%). Precipitation in pentane afforded 0.238 g of **A.14** as a clean yellow solid. **mp** 166-168 °C **¹H NMR** (500 MHz, CDCl₃) δ 7.92 (dd, $J = 8.0$, $J = 1.5$), 7.47 (ddd, $J = 8.0$, $J = 7.5$, $J = 1.5$), 7.31 (dd, $J = 8.0$, $J = 1.5$), 7.22 (ddd, $J = 8.0$, $J = 7.5$, $J = 1.5$), 4.78 (bs, 2H), 3.72 (s, 3H). **¹³C NMR** (125 MHz, CDCl₃) δ 159.0, 143.0, 141.5, 139.3, 131.2, 128.8, 128.3, 118.1, 114.6, 112.3, 96.0, 52.0. **IR** ν 3364, 2236, 1737. **HRMS** [M+H]⁺ calculated m/z 409.1513, found m/z 409.1506.

Methyl 4-amino-3-cyano-1-(3-(trifluoromethyl)phenyl)-1H-pyrazole-5-carboxylate (A.15)



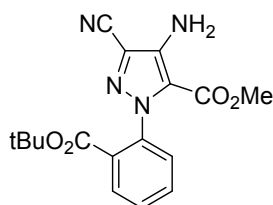
According to the general procedure **II**, pyrazole **A.15** was synthesized from the hydrazone **II.15** (0.730 g, 3.075 mmol). The mixture was irradiated for 10 min. Flash chromatography (toluene/acetone 99:1) afforded **A.15** as a white solid (0.793 g, 83 %). **mp** 155-157 °C **¹H NMR** (500 MHz, CDCl₃) δ (ppm) 7.74 (m, 1H), 7.67 (m, 1H), 7.60 (m, 2H), 4.85 (s, 2H), 3.79 (s, 3H). **¹³C NMR** (500 MHz, CDCl₃) δ 159.1, 142.6, 140.2, 131.3 (d, $J = 32.5$), 129.3, 129.0, 126.0 (m), 123.1, 122.3 (d, $J = 271.6$), 117.0, 115.2, 112.0, 52.0. **IR** ν 1721, 2236, 3373. **HRMS** [M-H]⁻ calculated m/z 309.0678, found m/z 309.0579.

Methyl 4-amino-3-cyano-1-(4-(trifluoromethyl)phenyl)-1H-pyrazole-5-carboxylate (A.16)



According to the general procedure **II**, pyrazole **A.16** was synthesized from the hydrazone **II.16** (0.700 g, 2.94 mmol). The mixture was irradiated for 10 min. Flash chromatography (toluene/acetone 99:1) afforded **A.16** as an orange solid (0.308 g, 29 %). **mp** 195-197 °C **¹H NMR** (500 MHz, CDCl₃) δ (ppm) 7.74 (d, $J = 16.5$, 2H), 7.52 (d, $J = 12.5$, 2H), 4.84 (s, 2H), 3.81 (s, 3H). **¹³C NMR** (500 MHz, CDCl₃) δ 159.1, 142.5, 131.4, 131.1, 126.1, 125.8 (d, $J = 3.5$), 122.1, 117.0, 115.2, 112.0, 52.1. **IR** ν 1731, 2231, 3370. **HRMS** [M-H]⁻ calculated m/z 309.0678, found m/z 309.0579.

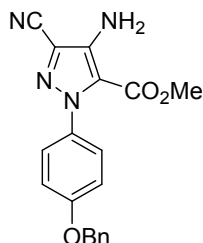
Methyl 4-amino-1-(2-(tert-butoxycarbonyl)phenyl)-3-cyano-1H-pyrazole-5-carboxylate (A.17)



According to the general procedure **II**, pyrazole **A.17** was synthesized from the hydrazone **II.17** (1.33 g, 4.91 mmol). The mixture was irradiated for 20 min. Flash chromatography (toluene/acetone 99.5:0.5) afforded **A.17** as a brown oil non isolated. After crystallization in pentane and filtration, product **A.17** was obtained as an orange solid (0.62 g, 37 %). **mp** 108-110 °C **¹H NMR** (500 MHz, CDCl₃) δ (ppm) 8.00 (dd, $J = 2.0$, $J = 7.5$, 1H), 7.61-7.55 (m, 2H), 7.1 (dd, $J = 1.5$, $J = 7.5$, 1H), 4.77 (s, 2H), 3.69 (s, 3H), 1.36 (s, 9H). **¹³C NMR**

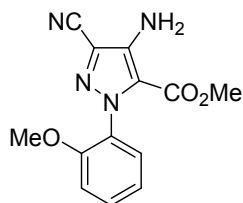
(125 MHz, CDCl₃) δ 163.9, 159.3, 141.7, 139.0, 132.0, 130.9, 130.4, 129.8, 128.3, 118.8, 113.9, 112.4, 82.2, 51.8, 27.7. **IR** ν 1685, 1715, 2232, 3343. **HRMS** [M+H]⁺ calculated m/z 343.1328, found m/z 343.1394.

Methyl 4-amino-1-(4-(benzyloxy)phenyl)-3-cyano-1H-pyrazole-5-carboxylate (A.22)



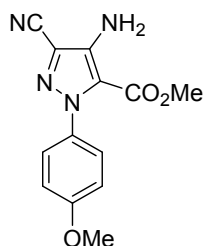
According to the general procedure **II**, pyrazole **A.22** was synthesized from the hydrazone **II.22** (0.98 g, 3.54 mmol). The mixture was irradiated for 10 min. Flash chromatography (cyclohexane/DCM 20:80 to DCM) afforded **A.22** as an orange solid non isolated. The product was washed with pentane and cyclohexane to afforded **A.22** as an orange solid (0.094 g, 8 %). **mp** 161-163 °C **¹H NMR** (500 MHz, CDCl₃) δ (ppm) 7.45-7.39 (m, 4H), 7.36-7.33 (m, 1H), 7.29-7.27 (m, 2H), 7.03-7.01 (m, 2H), 5.11 (s, 2H), 4.75 (s, 2H), 3.77 (s, 3H). **¹³C NMR** (125 MHz, CDCl₃) δ 159.4, 159.4, 142.1, 136.4, 133.2, 128.7, 128.7, 127.6, 127.1, 117.1, 114.7, 113.9, 112.5, 70.4, 51.8. **IR** ν 3354, 2227, 1720. **HRMS** [M+H]⁺ calculated m/z 349.1222, found m/z 349.1293.

Methyl 4-amino-3-cyano-1-(2-methoxyphenyl)-1H-pyrazole-5-carboxylate (A.23)



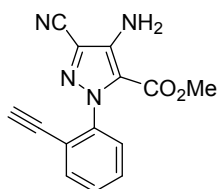
According to the general procedure **II**, pyrazole **A.23** was synthesized from the hydrazone **II.23** (0.770 g, 3.85 mmol). The mixture was irradiated for 10 min. Flash chromatography (cyclohexane/AcOEt 90:10 to cyclohexane/AcOEt 70:30) afforded N-alkylated intermediary which was further reacted with K₂CO₃ to afford **A.23** as an orange solid (0.485 g, 91 %). **mp** 149-151 °C **¹H NMR** (500 MHz, CDCl₃) δ (ppm) 7.44 (td, *J* = 1.5, *J* = 7.5, 1H), 7.30 (dd, *J* = 1.5, *J* = 7.5, 1H), 7.05 (dt, *J* = 1.5, *J* = 7.5, 1H), 6.99 (dd, *J* = 1.5, *J* = 7.5, 1H), 4.69 (s, 2H), 3.76 (s, 3H), 3.72 (s, 3H). **¹³C NMR** (125 MHz, CDCl₃) δ 159.0, 154.4, 141.1, 131.0, 129.4, 127.6, 120.6, 118.9, 114.3, 112.6, 111.6, 55.8, 51.7. **IR** ν 1717, 2228, 3358. **HRMS** [M+H]⁺ calculated m/z 273.0909, found m/z 273.0979.

Methyl 4-amino-3-cyano-1-(4-methoxyphenyl)-1H-pyrazole-5-carboxylate (A.25)



According to the general procedure **II**, pyrazole **A.25** was synthesized from the hydrazone **II.25** (0.770 g, 3.85 mmol). The mixture was irradiated for 10 min. Flash chromatography (cyclohexane/AcOEt 90:10 to cyclohexane/AcOEt 70:30) afforded **A.25** as an orange solid (0.308 g, 29 %). **mp** 157-159 °C **¹H NMR** (500 MHz, CDCl₃) δ (ppm) 7.28 (d, $J = 9.0$, 2H), 6.95 (d, 2H), 4.75 (s, 2H), 3.85 (s, 3H), 3.77 (s, 3H). **¹³C NMR** (125 MHz, CDCl₃) δ 160.2, 159.3, 142.1, 133.0, 127.0, 117.3, 113.8, 113.8, 112.5, 55.2, 51.5. **IR** ν 1720, 2232, 3368. **HRMS** [M+H]⁺ calculated m/z 273.0909, found m/z 273.0976.

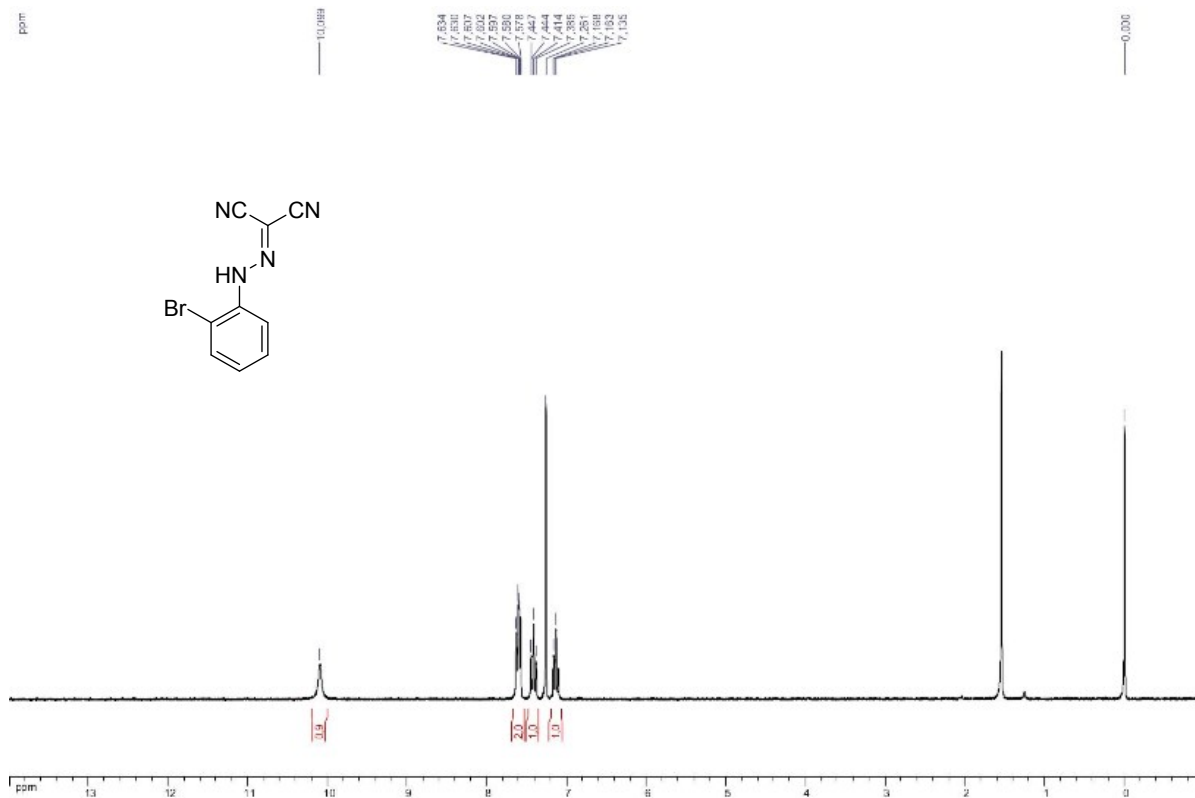
Methyl 4-amino-3-cyano-1-(2-ethynylphenyl)-1H-pyrazole-5-carboxylate (A.26)



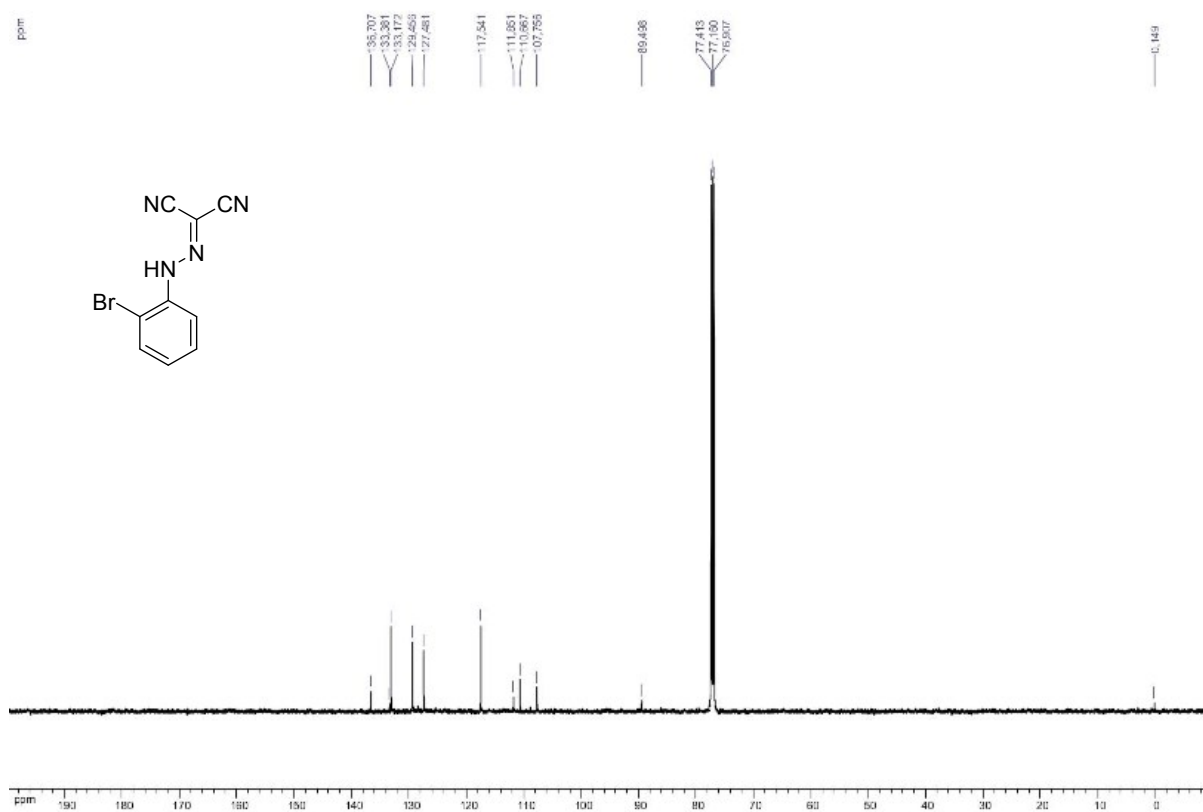
According to the general procedure **II**, pyrazole **A.26** was synthesized from the hydrazone **II.26** (1.64 g, 8.46 mmol). The mixture was irradiated for 20 min. Flash chromatography (toluene/acetone 99.5:0.5) afforded **A.26** as an orange solid (0.870 g, 40 %). **mp** 95-97 °C **¹H NMR** (500 MHz, CDCl₃) δ (ppm) 7.60 (dd, $J = 2.2$, $J = 7.1$, 1H), 7.50-7.44 (m, 2H), 7.36 (dd, $J = 2.0$, $J = 7.2$, 1H), 4.74 (s, 2H), 3.72 (s, 3H), 3.05 (s, 1H). **¹³C NMR** (125 MHz, CDCl₃) δ 159.4, 141.9, 141.3, 133.1, 129.5, 129.4, 126.9, 120.5, 118.5, 114.7, 112.4, 82.3, 77.4, 51.9. **IR** ν 1712, 2235, 3350, 3360. **HRMS** [M+H]⁺ calculated m/z 267.0804, found m/z 267.0877.

5. ^1H and ^{13}C Nuclear Magnetic Resonance Spectra

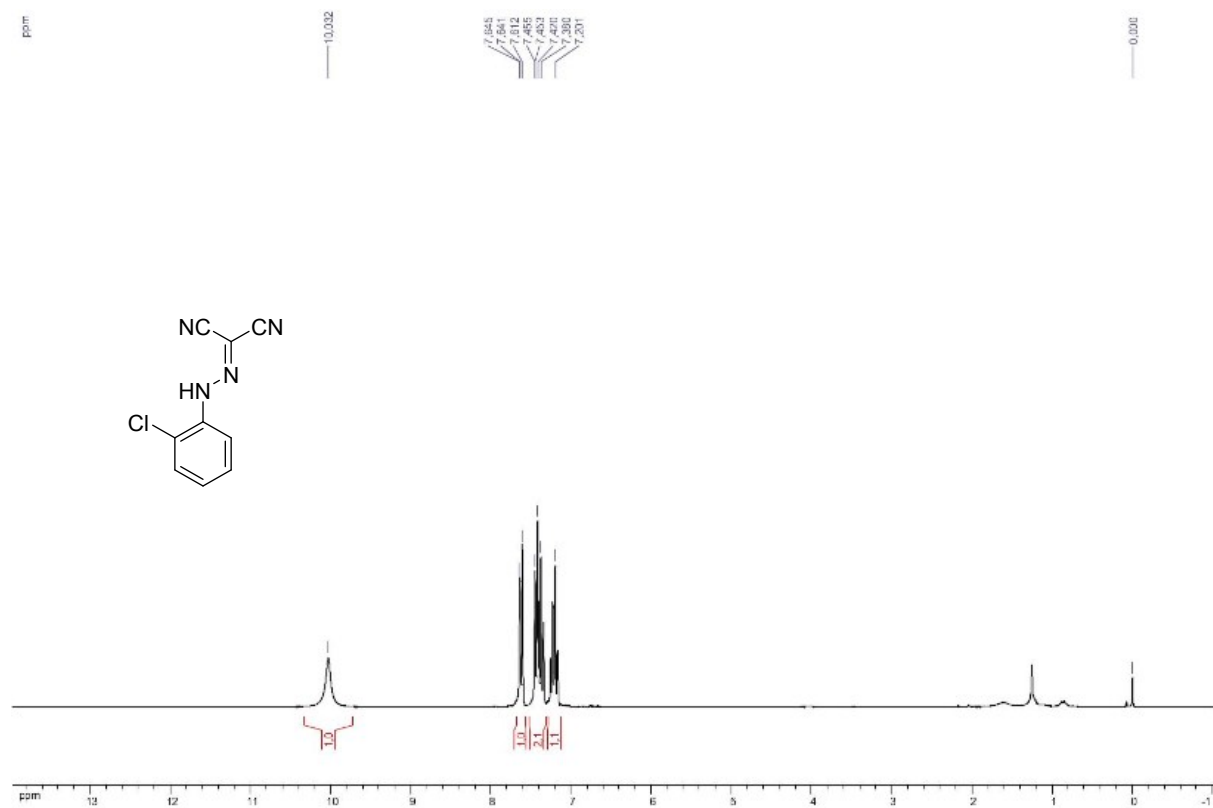
^1H NMR compound II.5



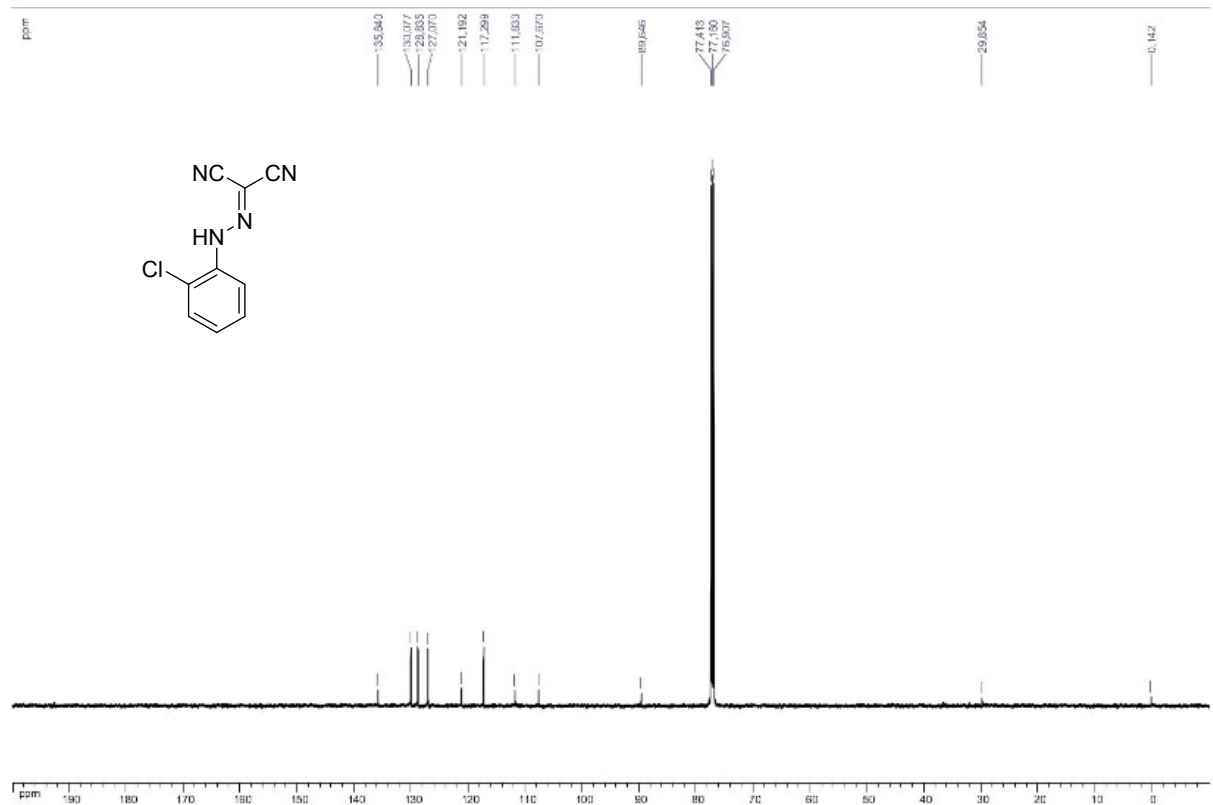
^{13}C NMR compound II.5



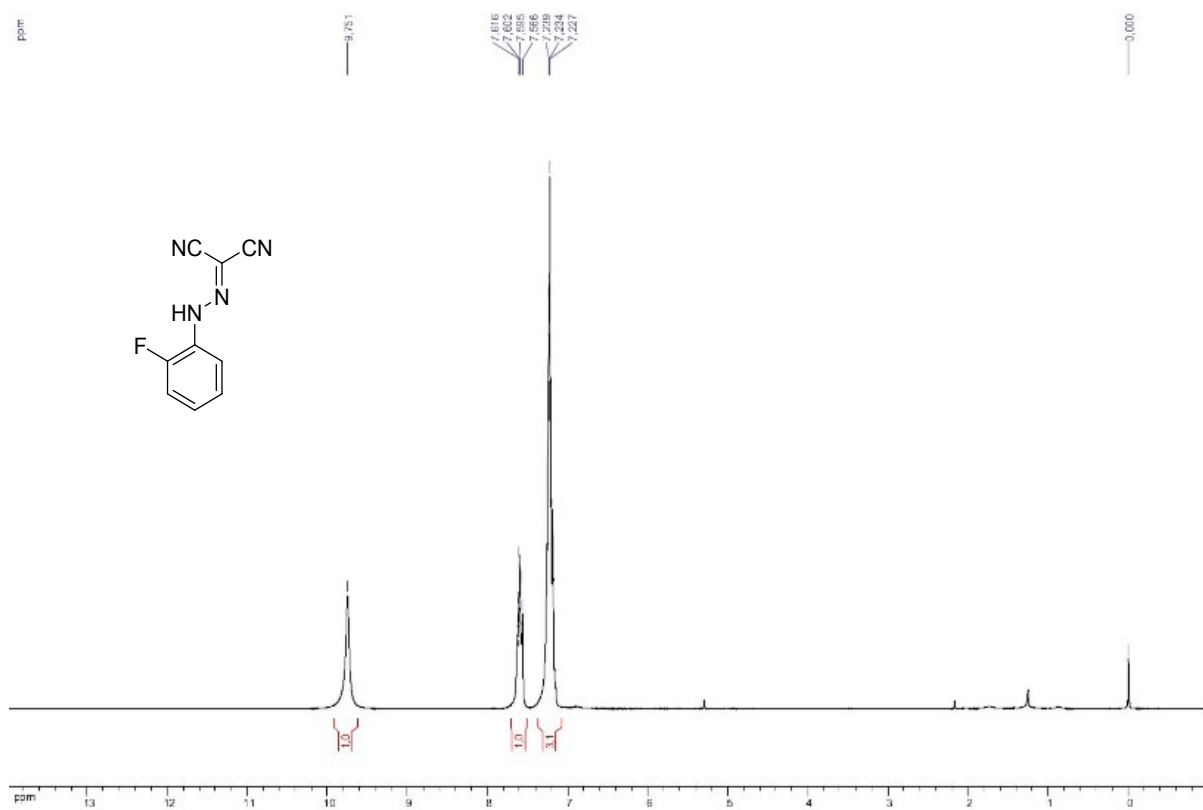
¹H NMR compound II.8



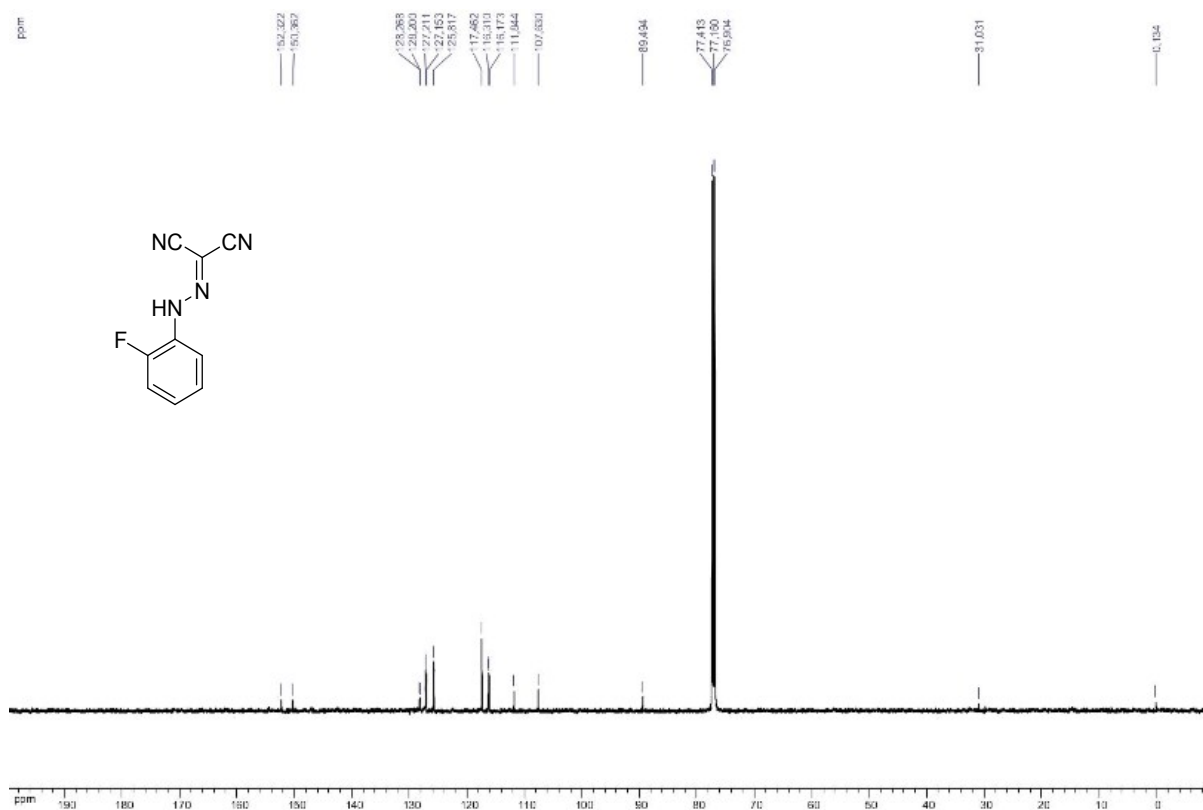
¹³C NMR compound II.8



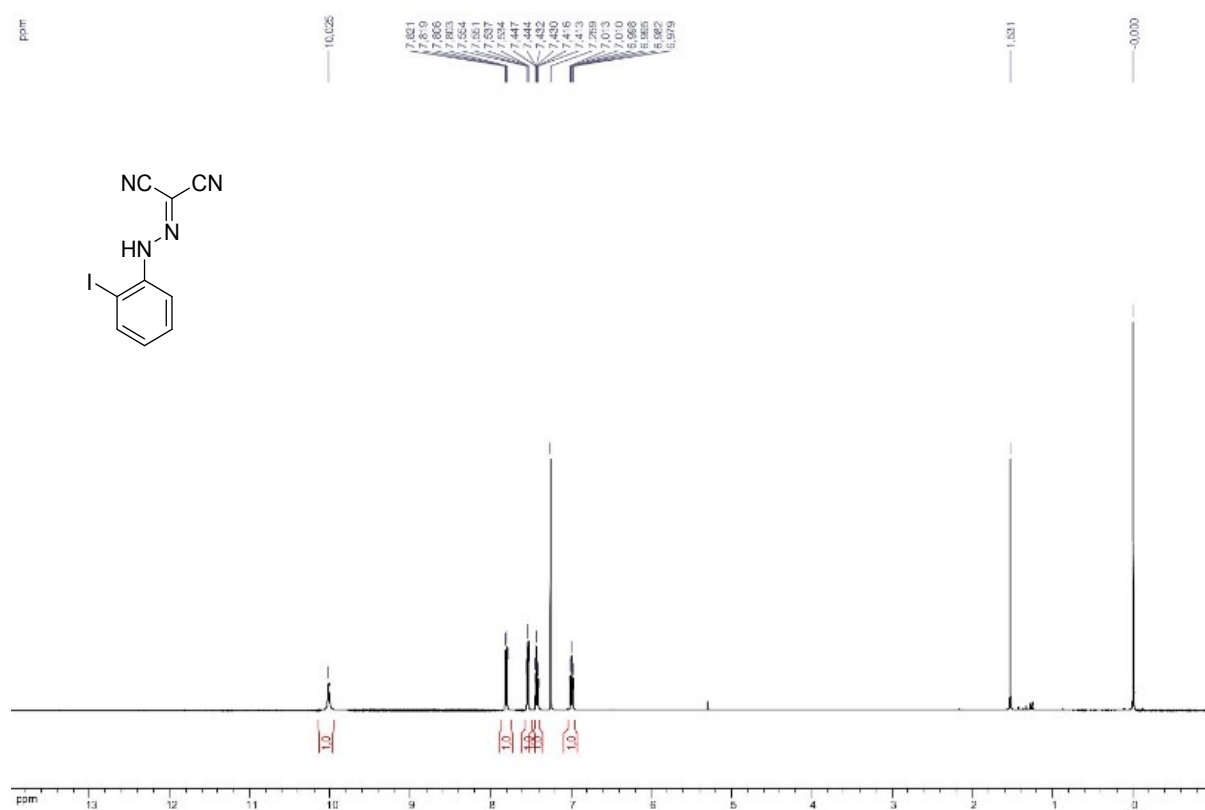
¹H NMR compound II.11



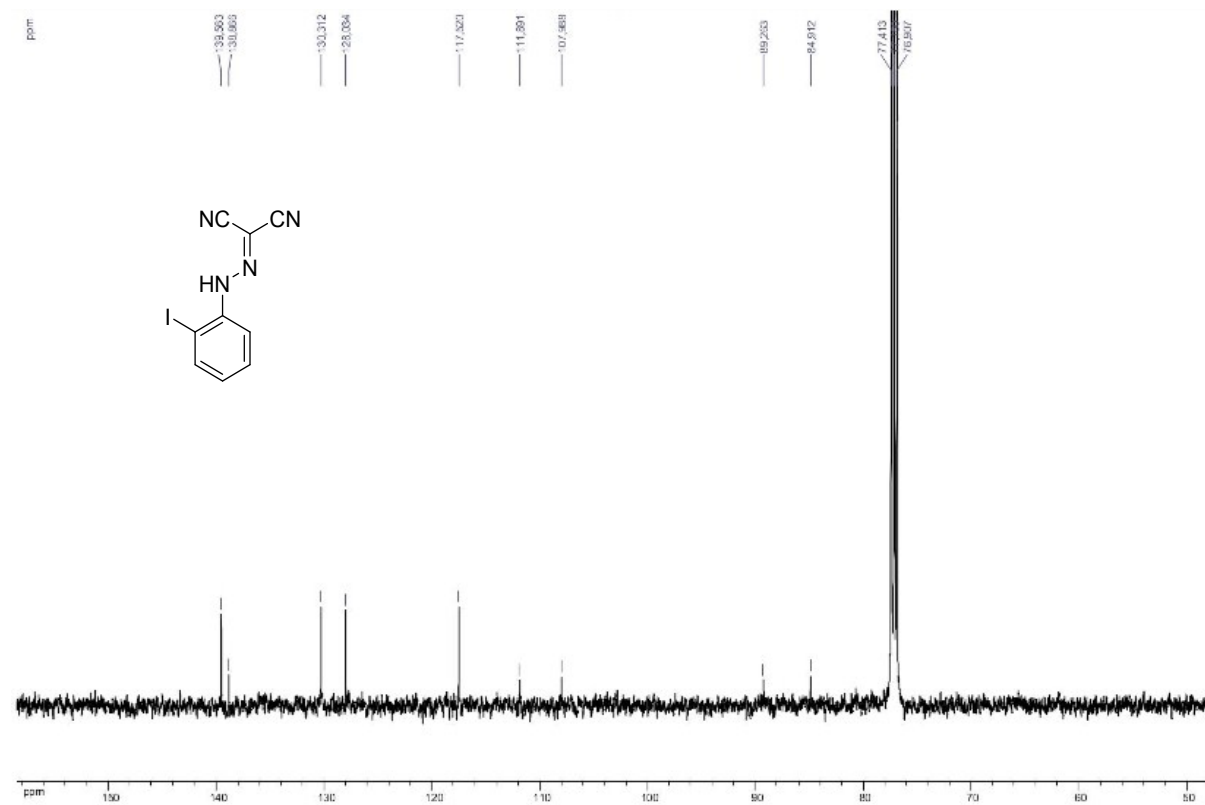
¹³C NMR compound II.11



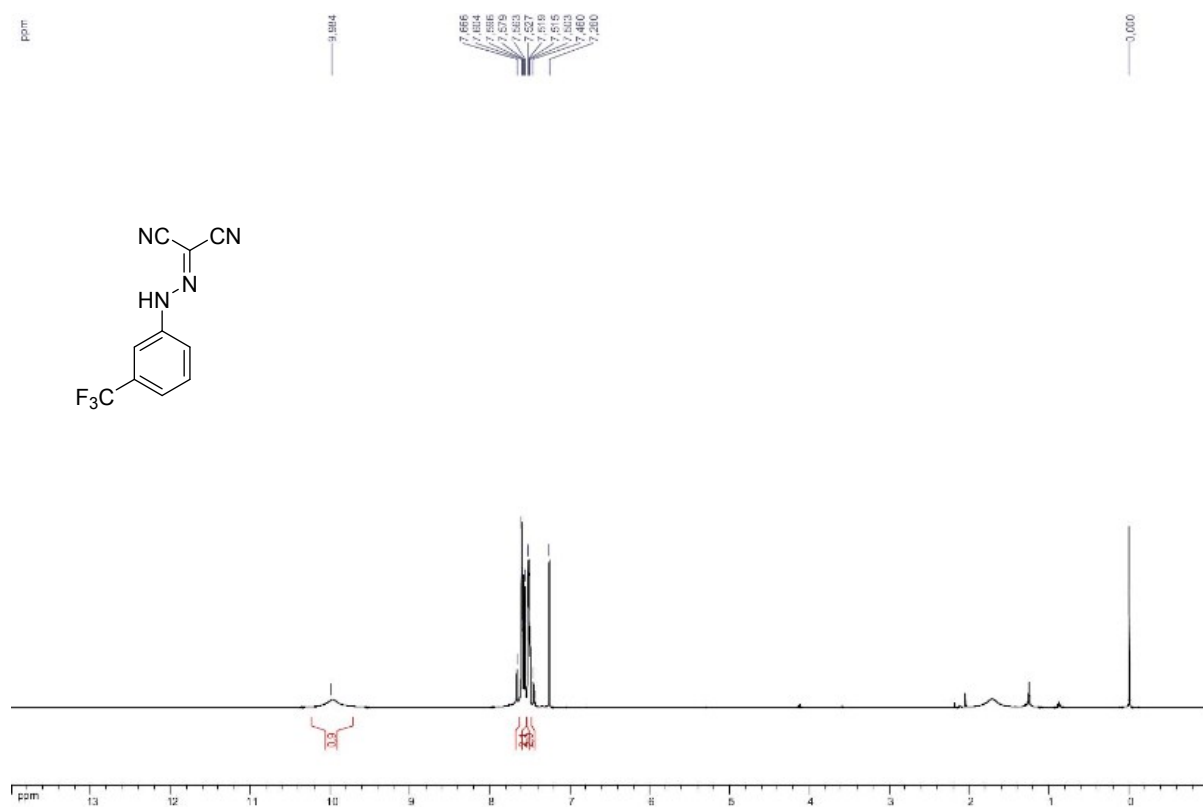
¹H NMR compound II.14



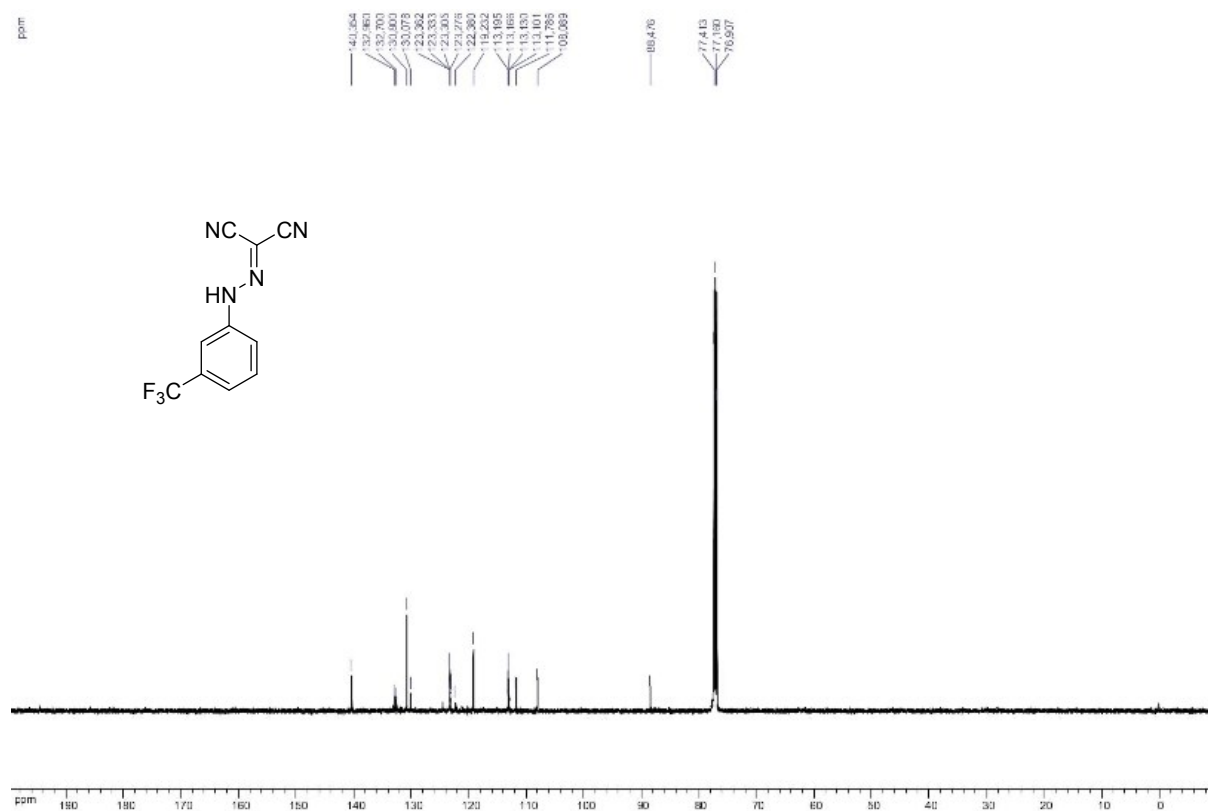
¹³C NMR spectrum of compound II.14



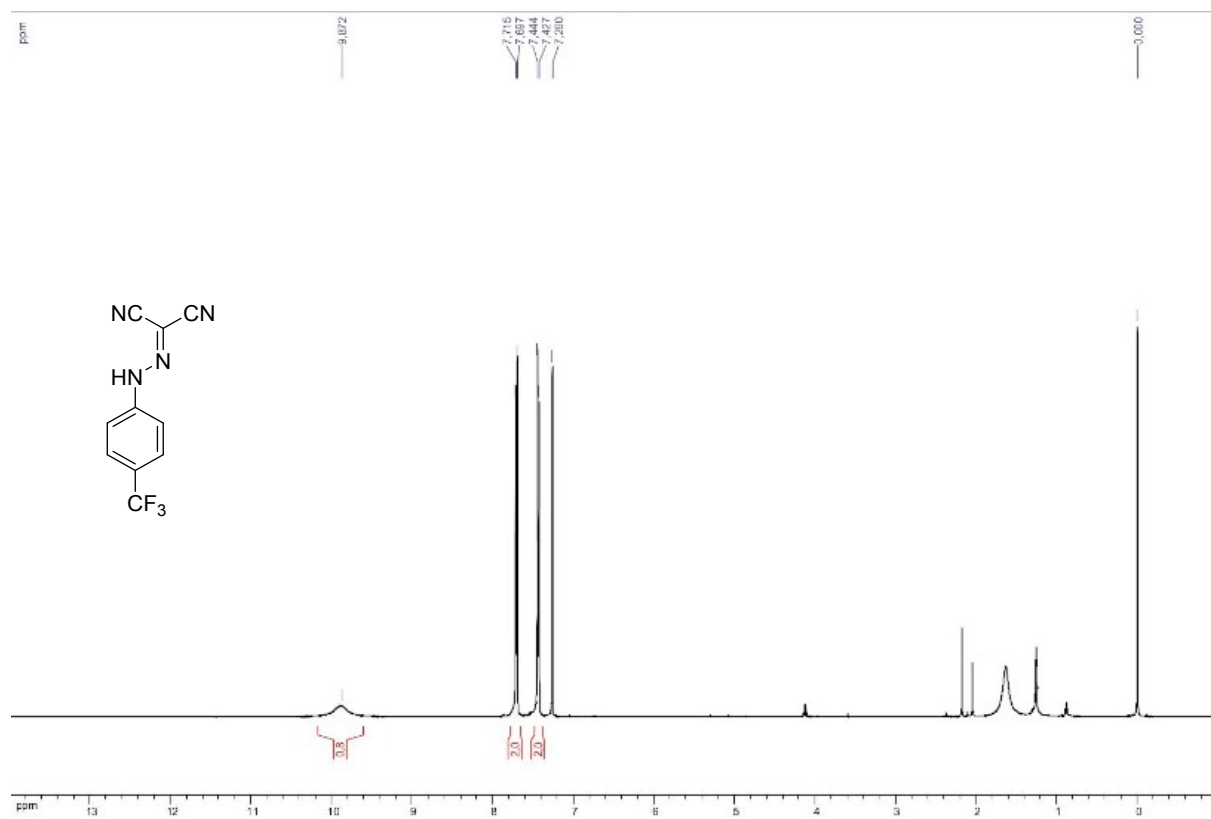
¹H NMR compound II.15



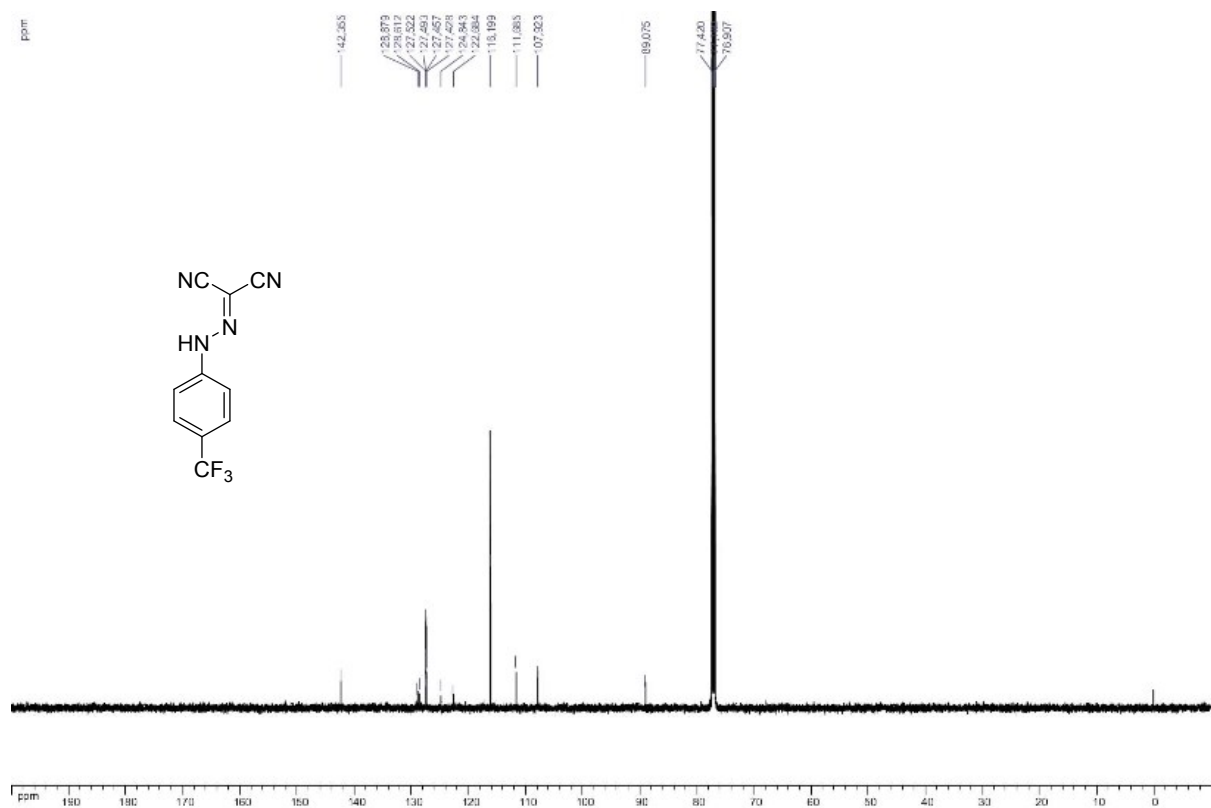
¹³C NMR compound II.15



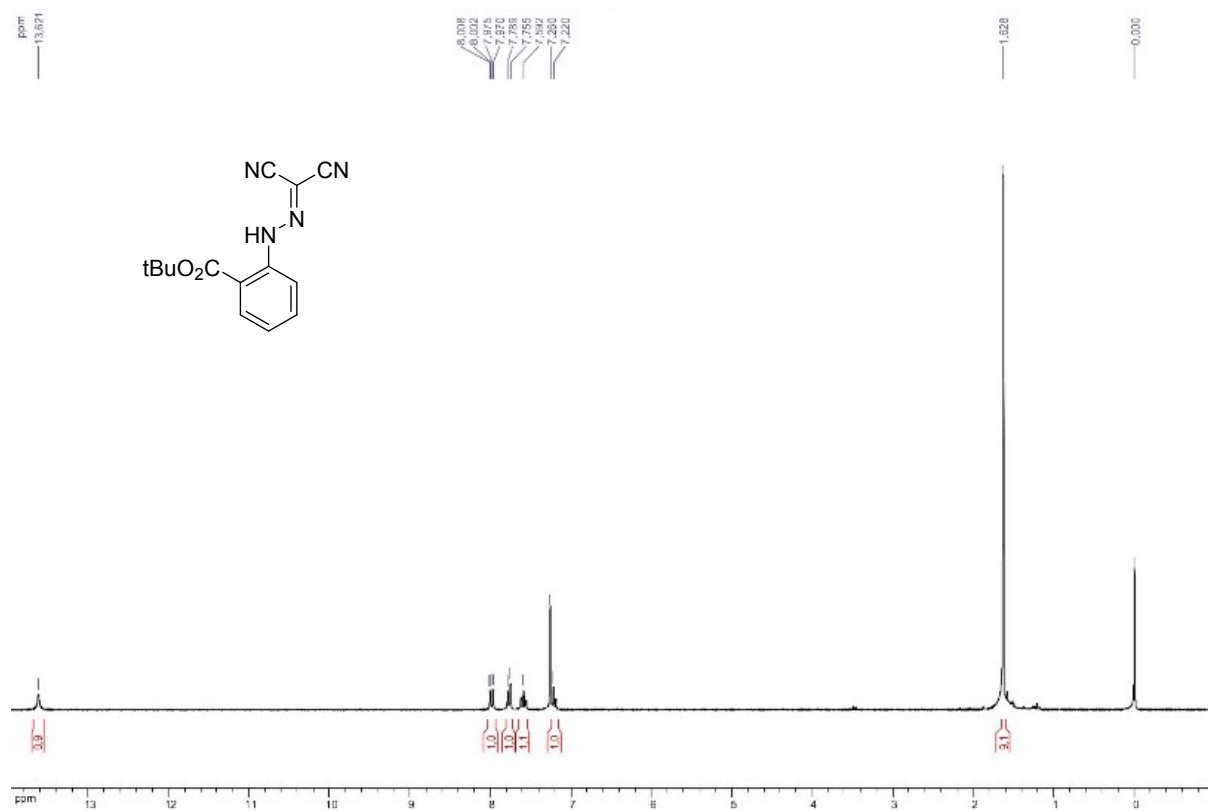
¹H NMR compound II.16



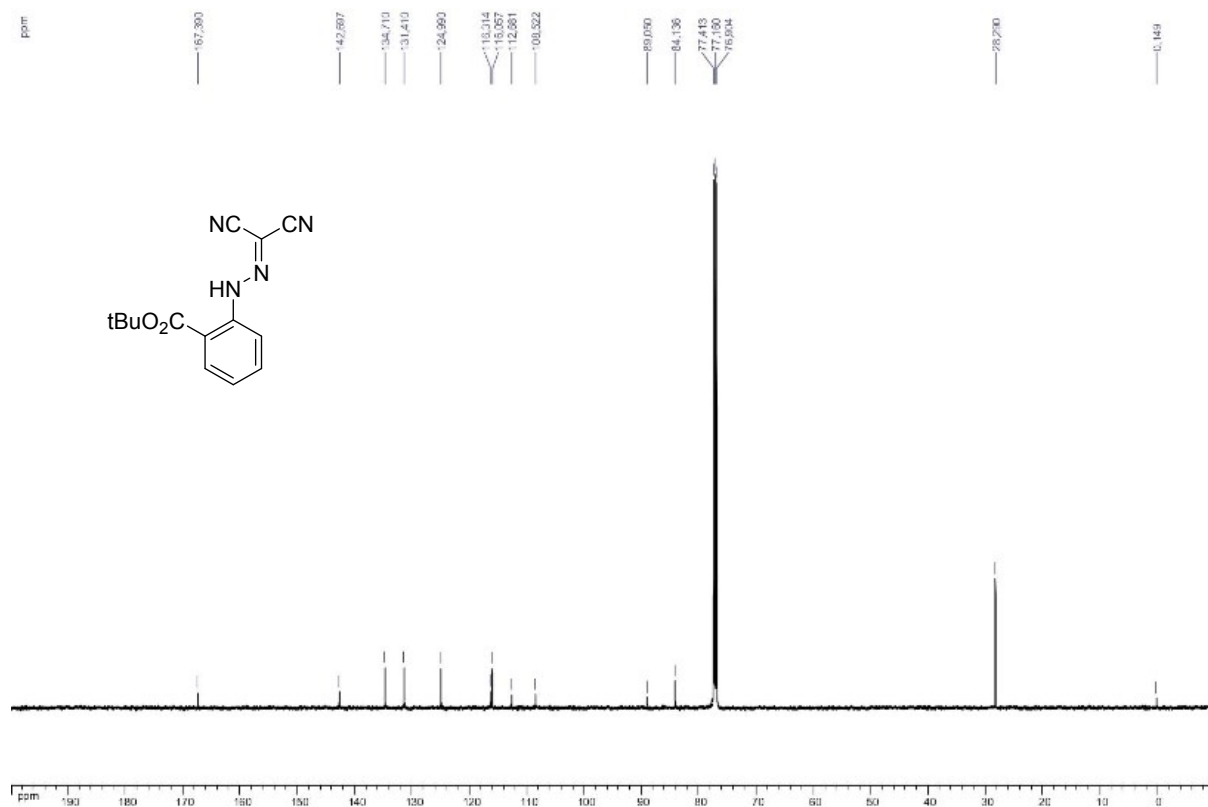
¹³C NMR compound II.16



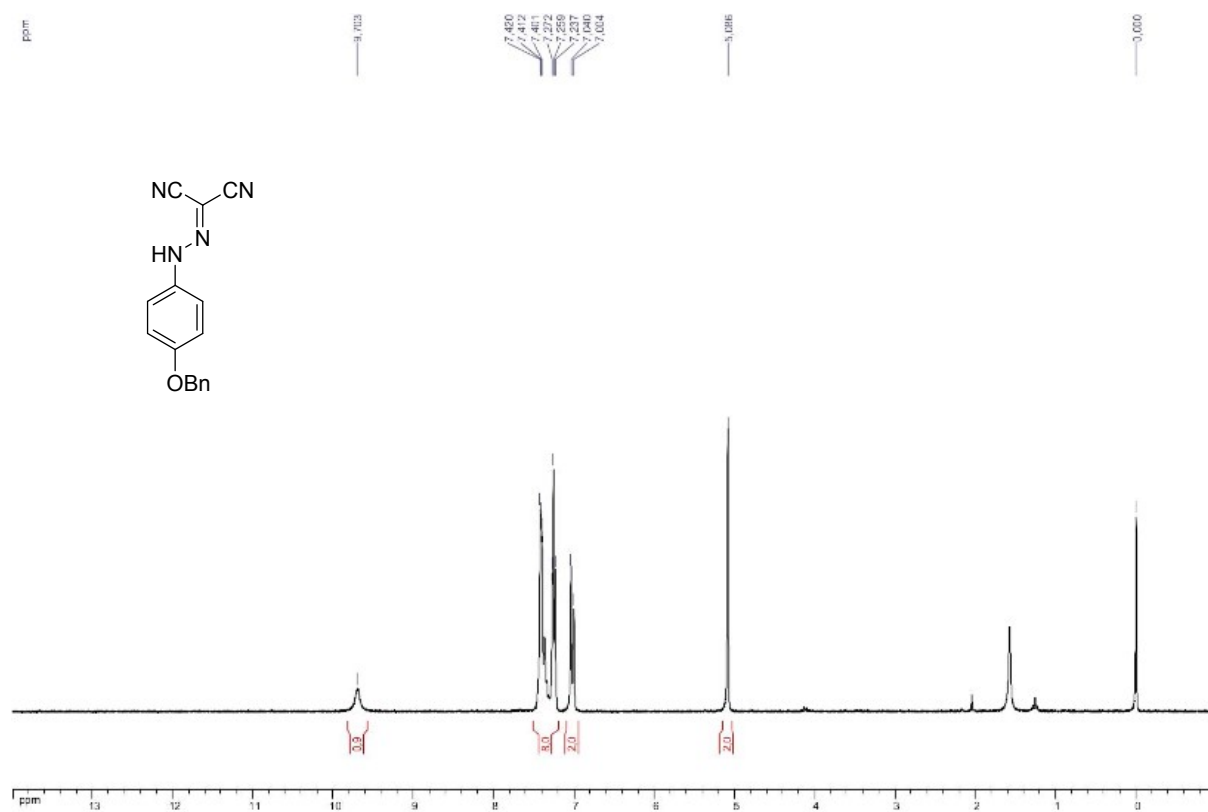
¹H NMR compound II.17



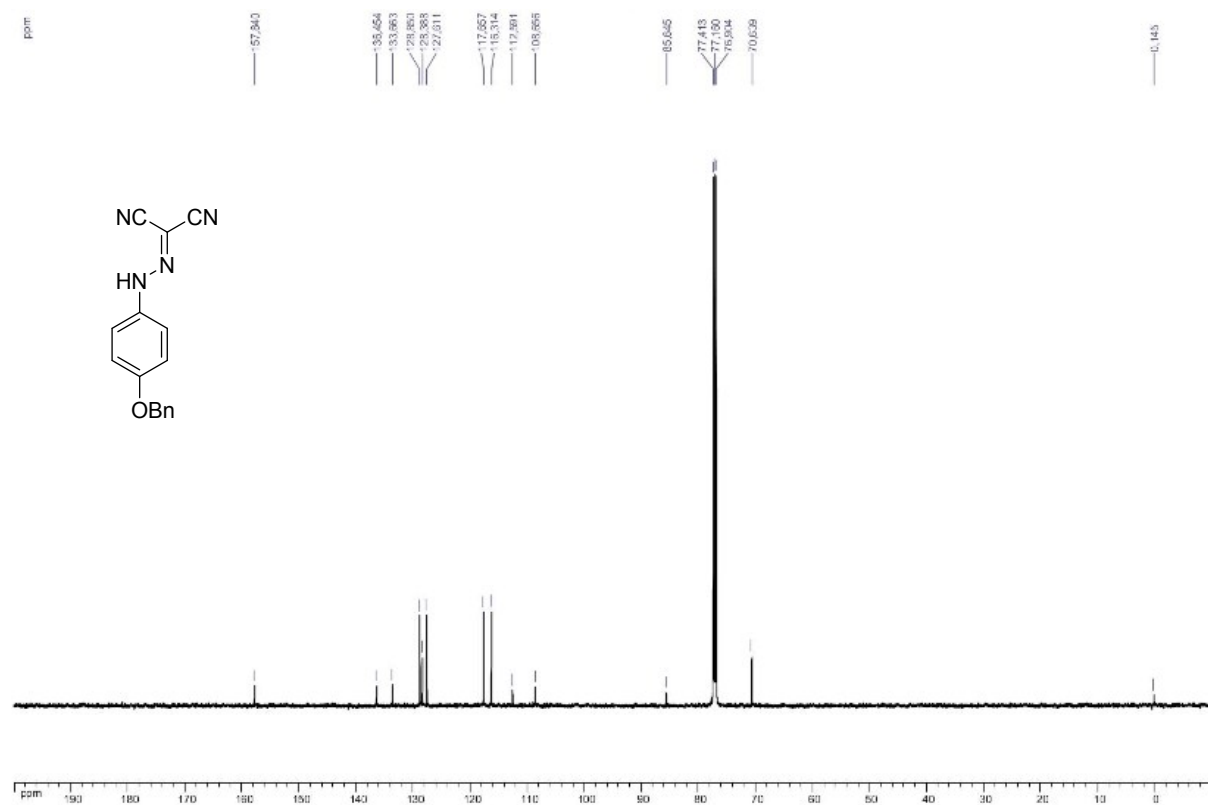
¹³C NMR spectrum of compound II.17



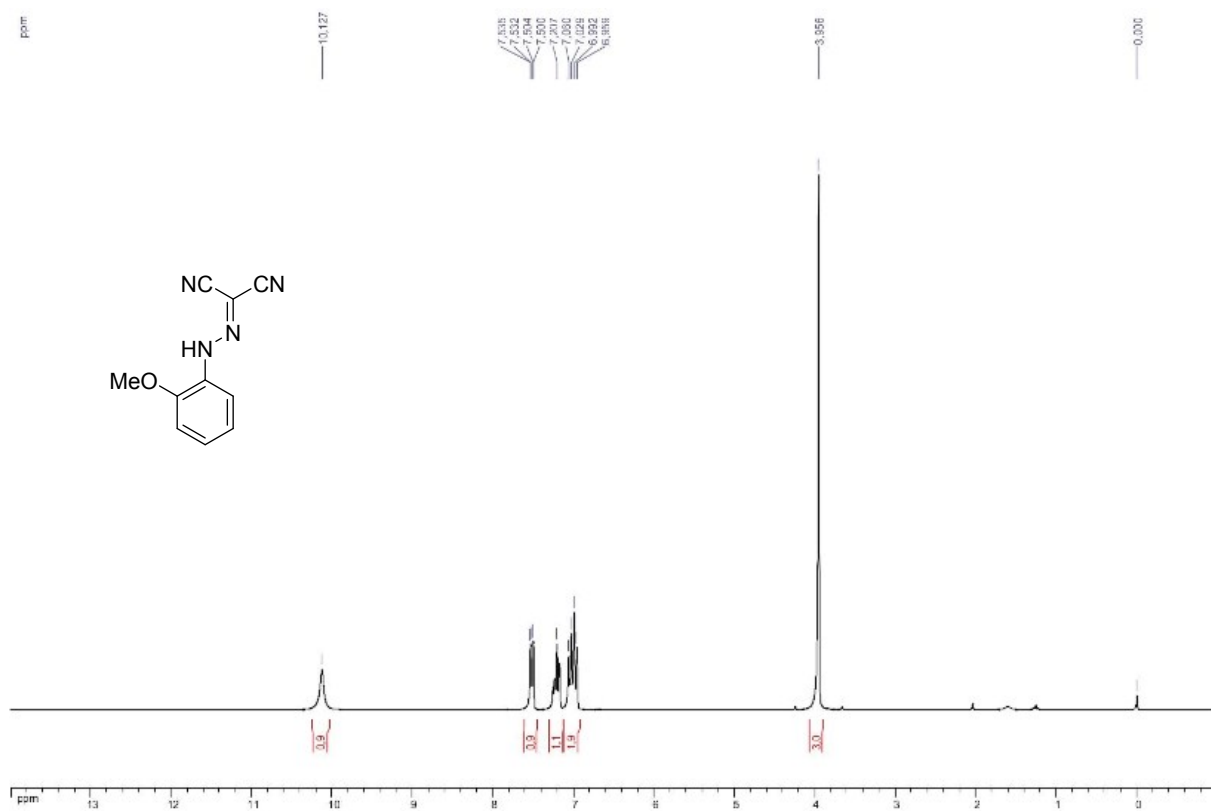
¹H NMR compound II.22



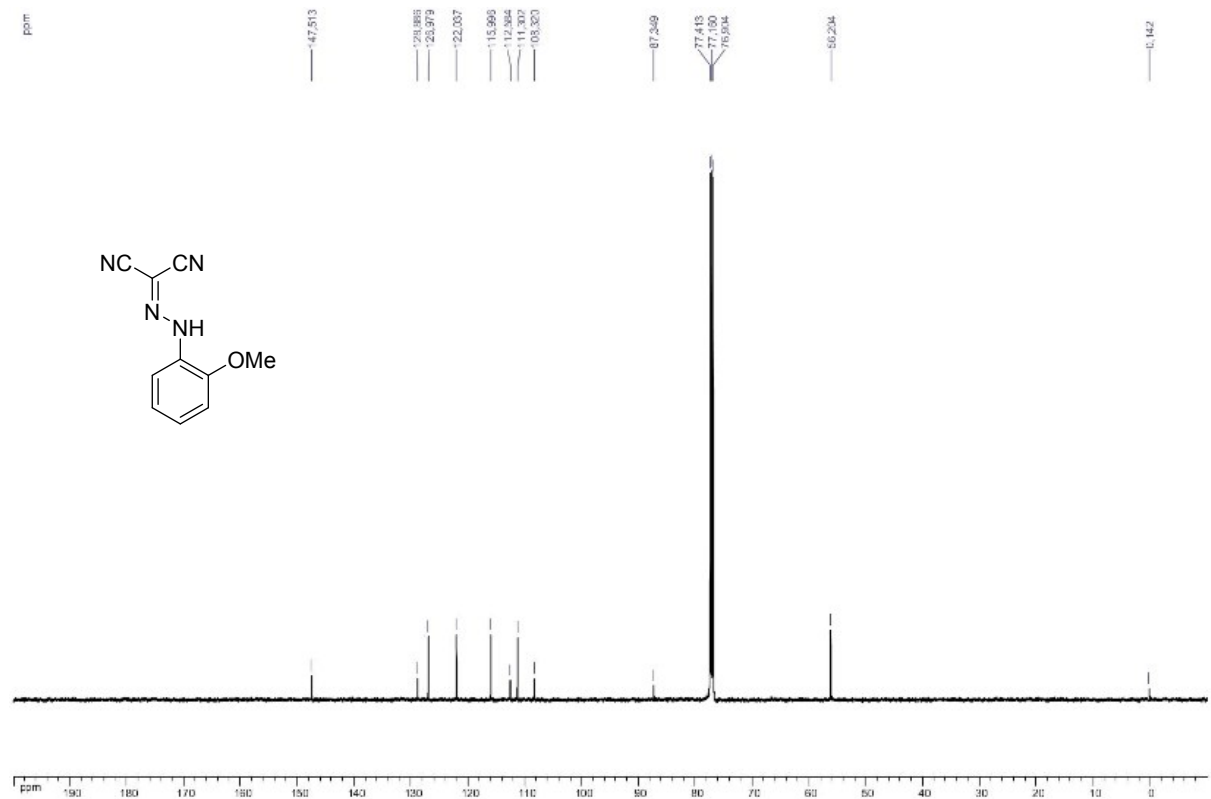
¹³C NMR compound II.22



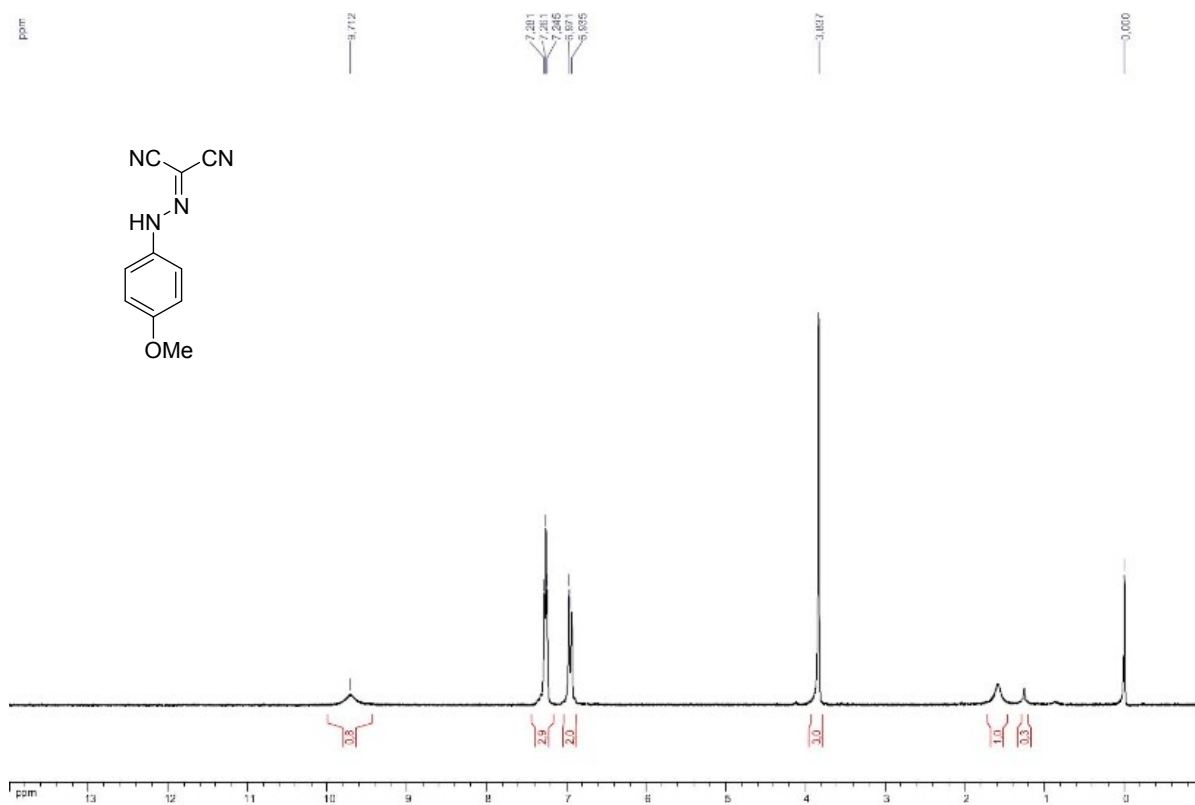
¹H NMR compound II.23



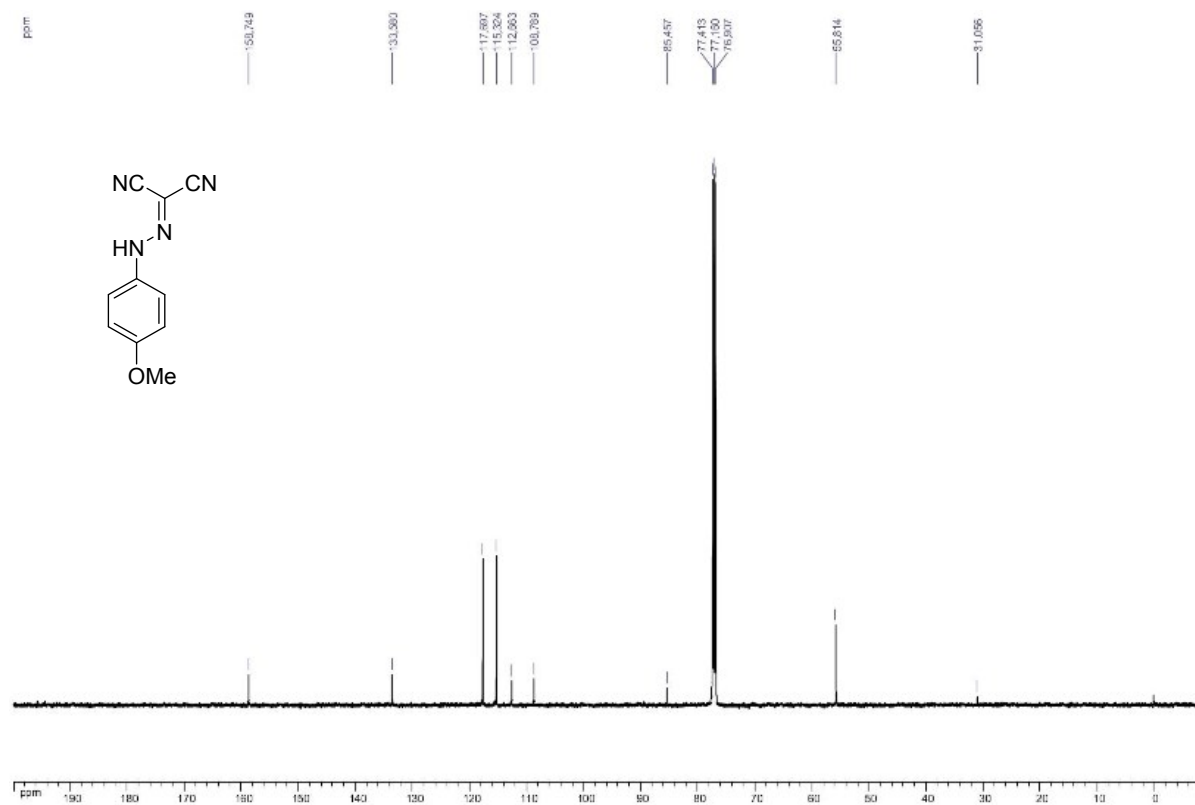
¹³C NMR compound II.23



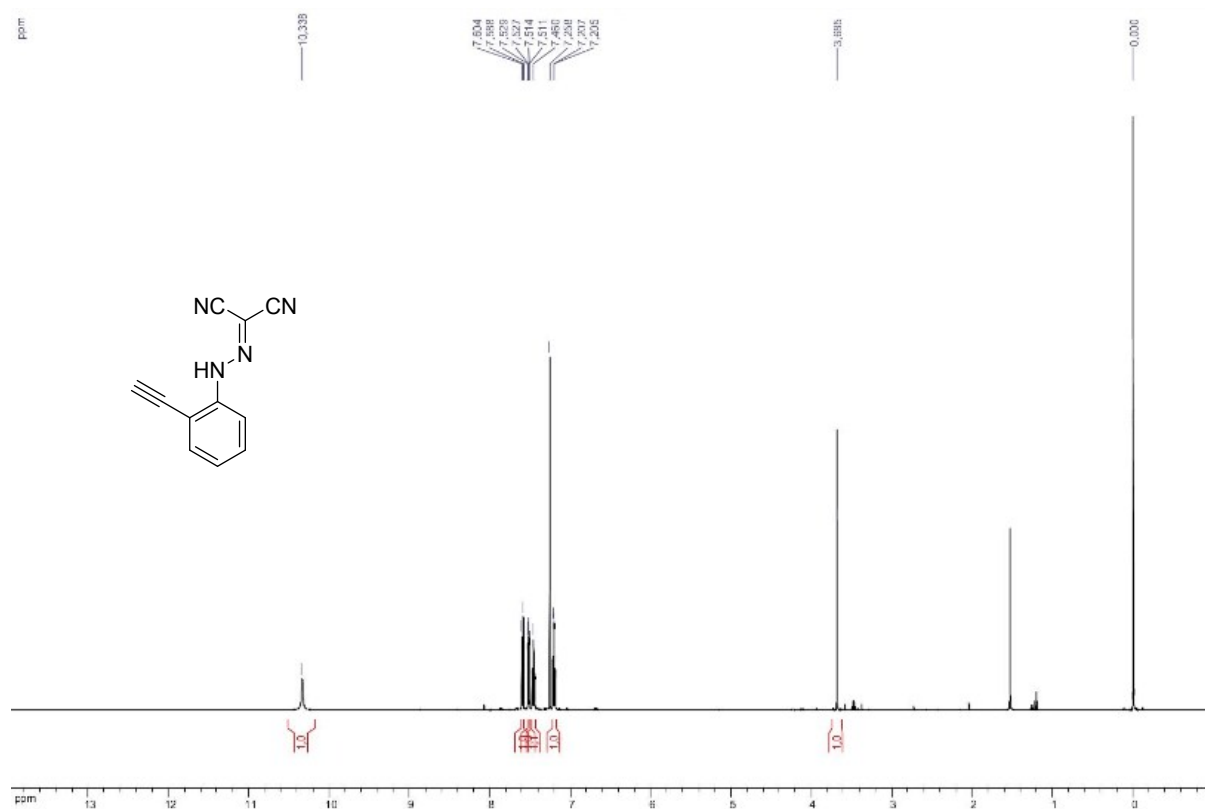
¹H NMR compound II.25



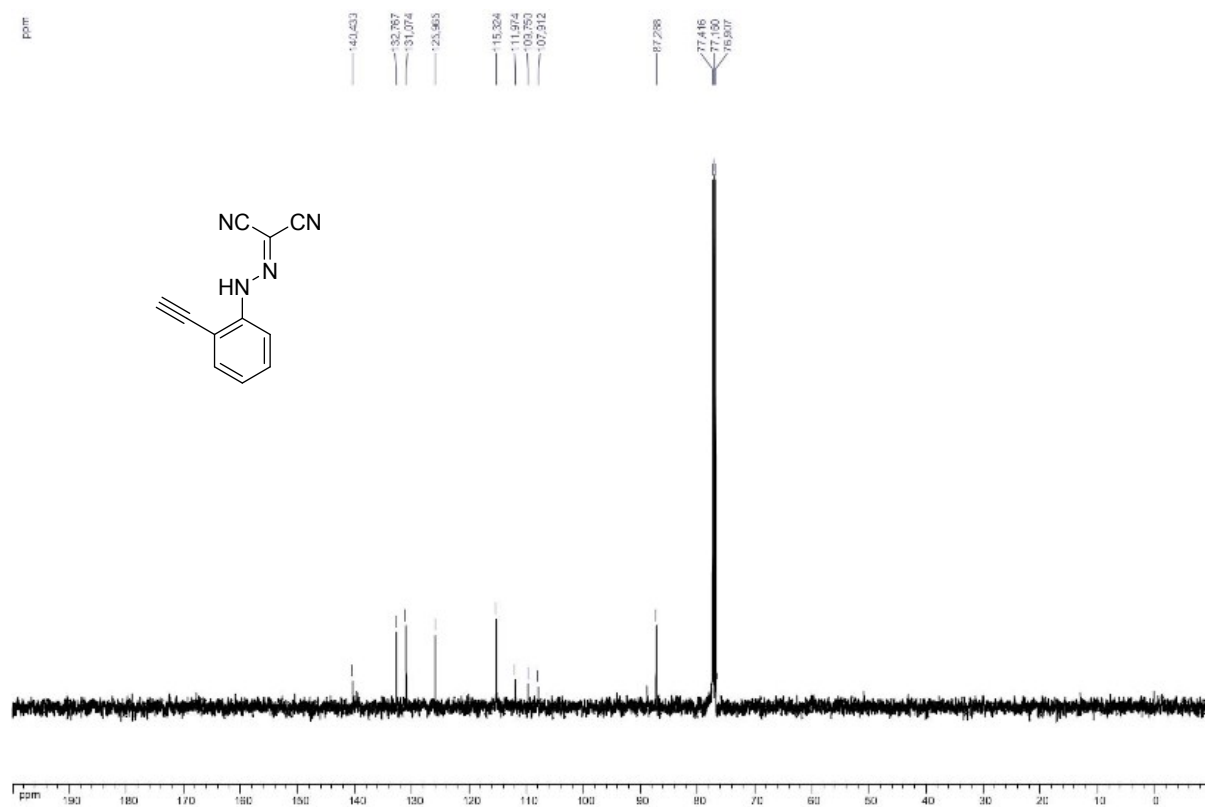
¹³C NMR compound II.25



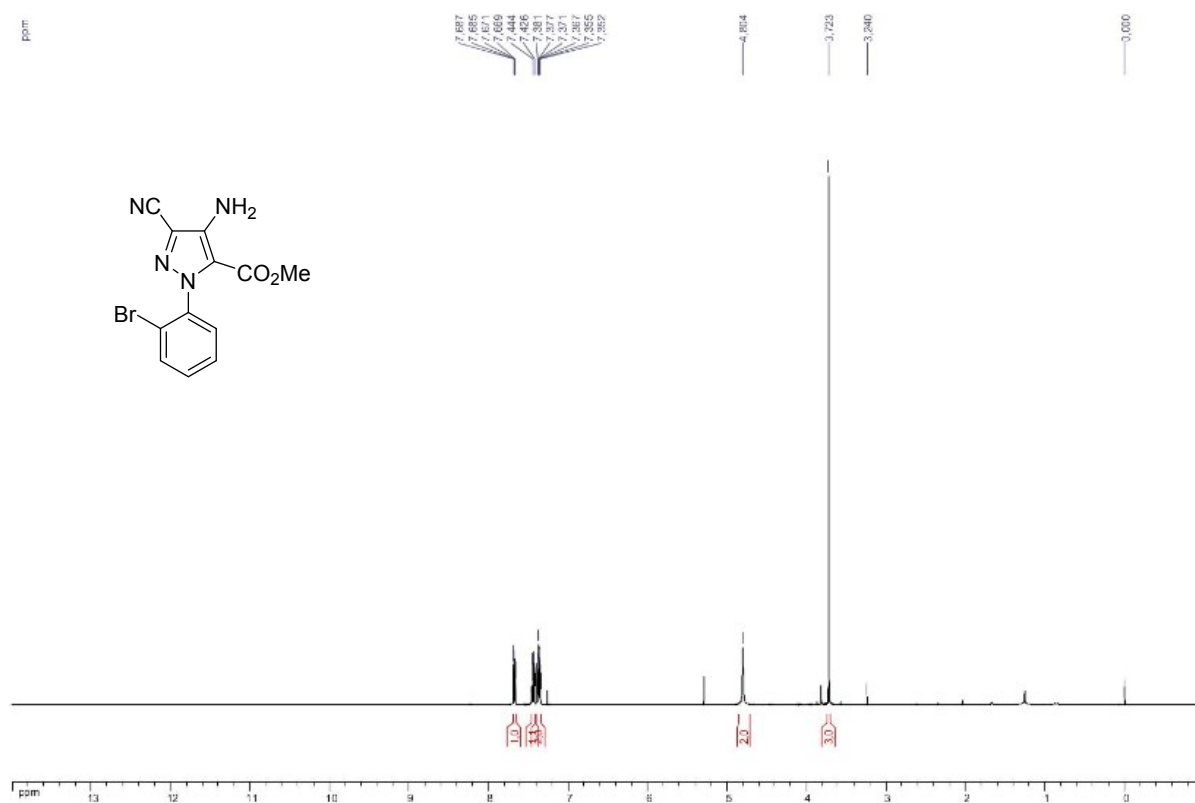
¹H NMR compound II.26



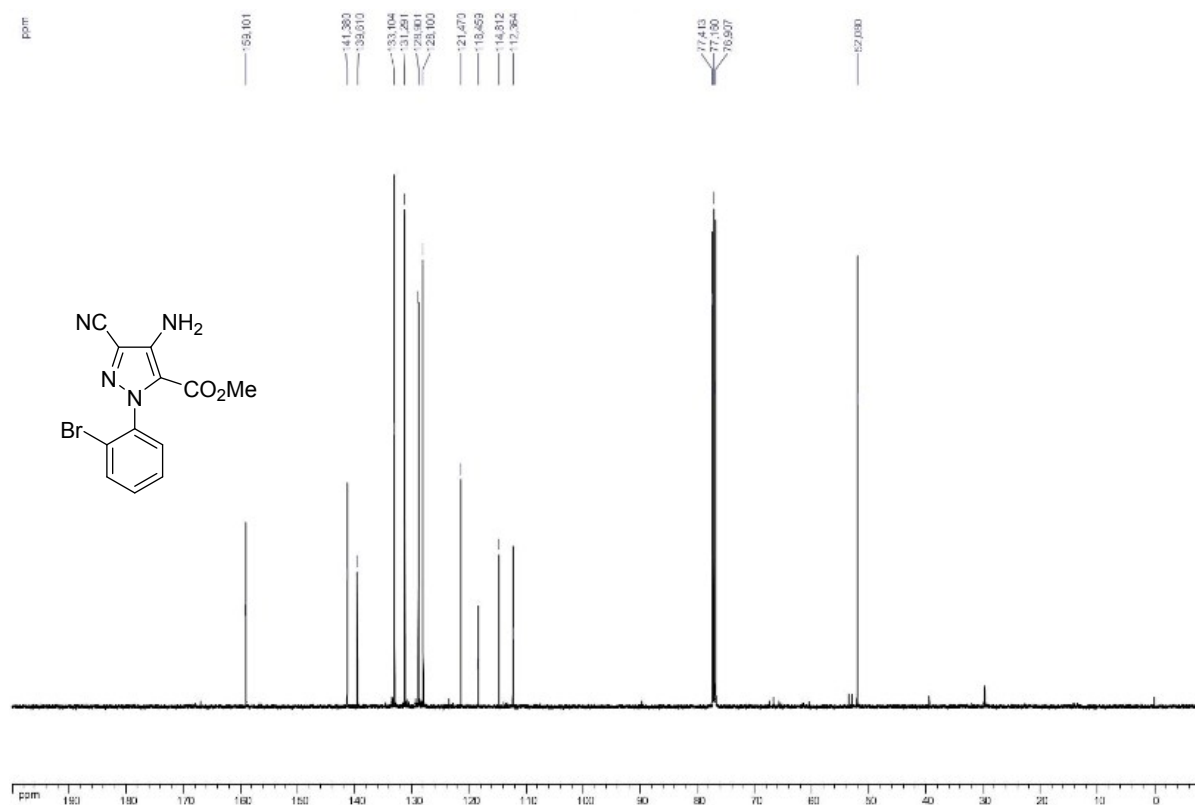
¹³C NMR spectrum of compound II.26



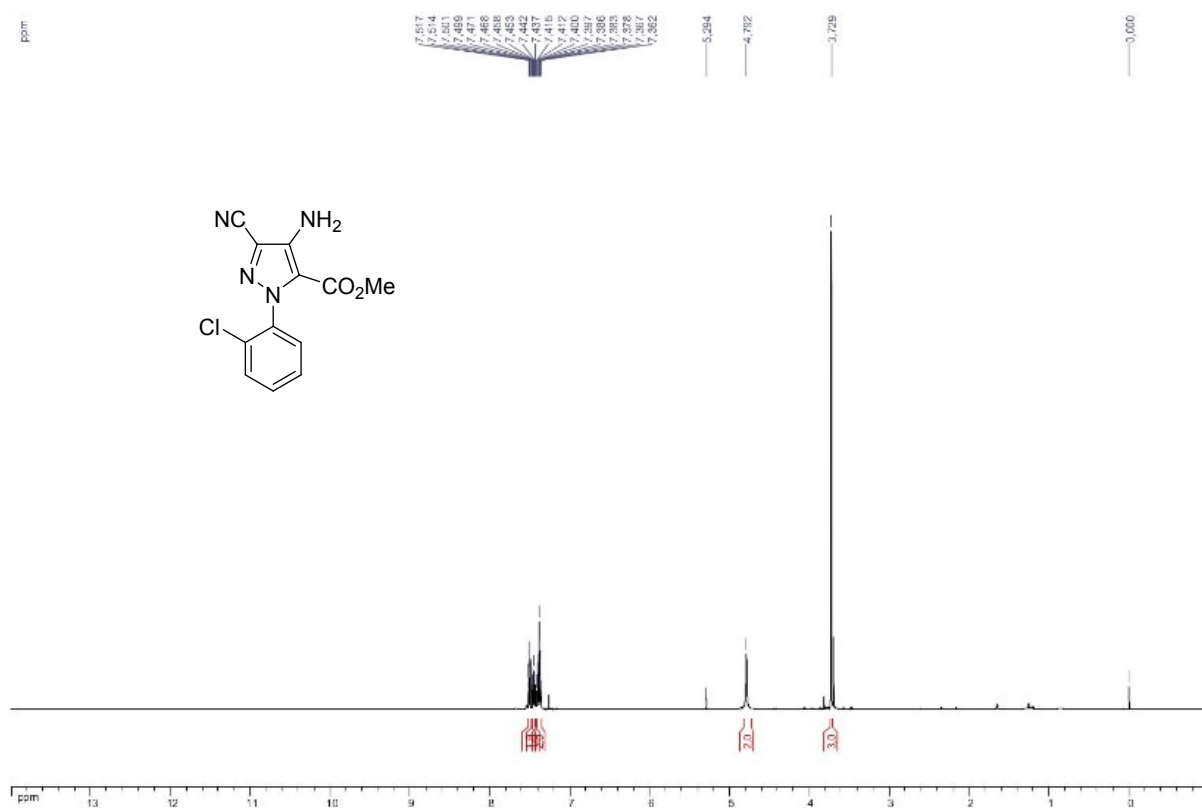
¹H NMR compound A.5



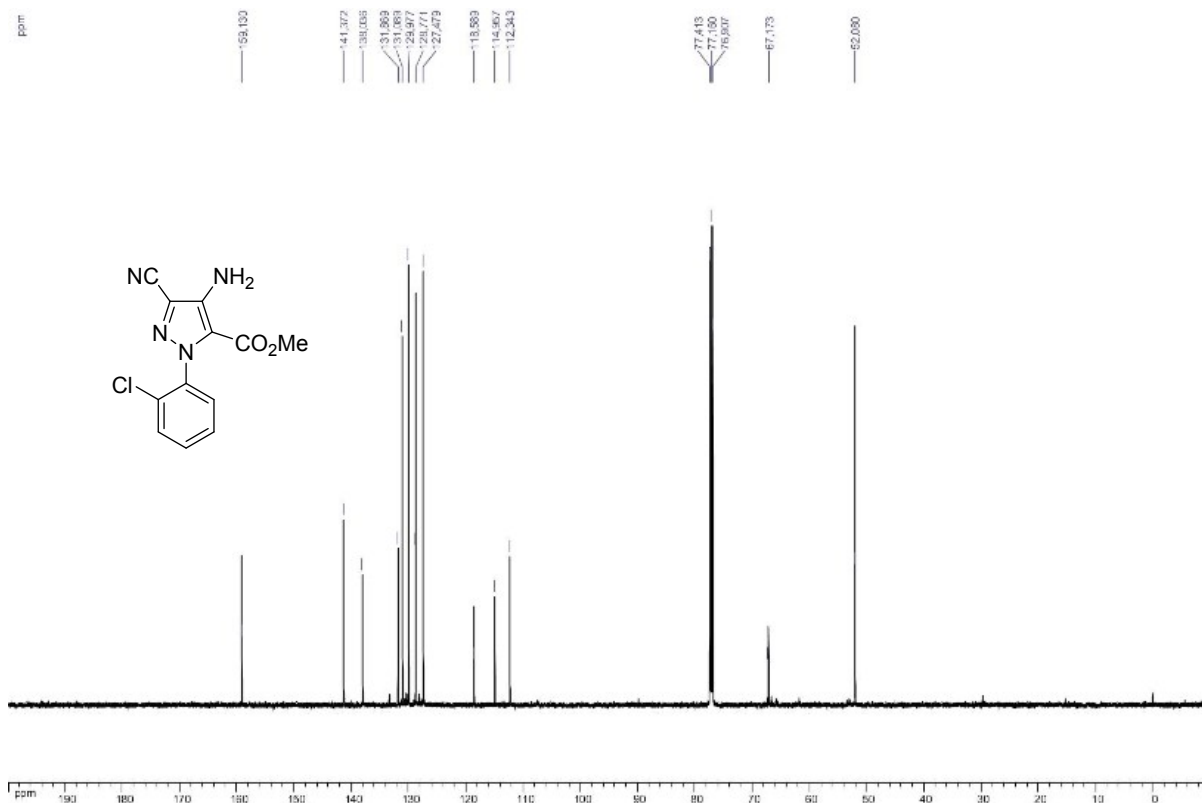
¹³C NMR spectrum of compound A.5



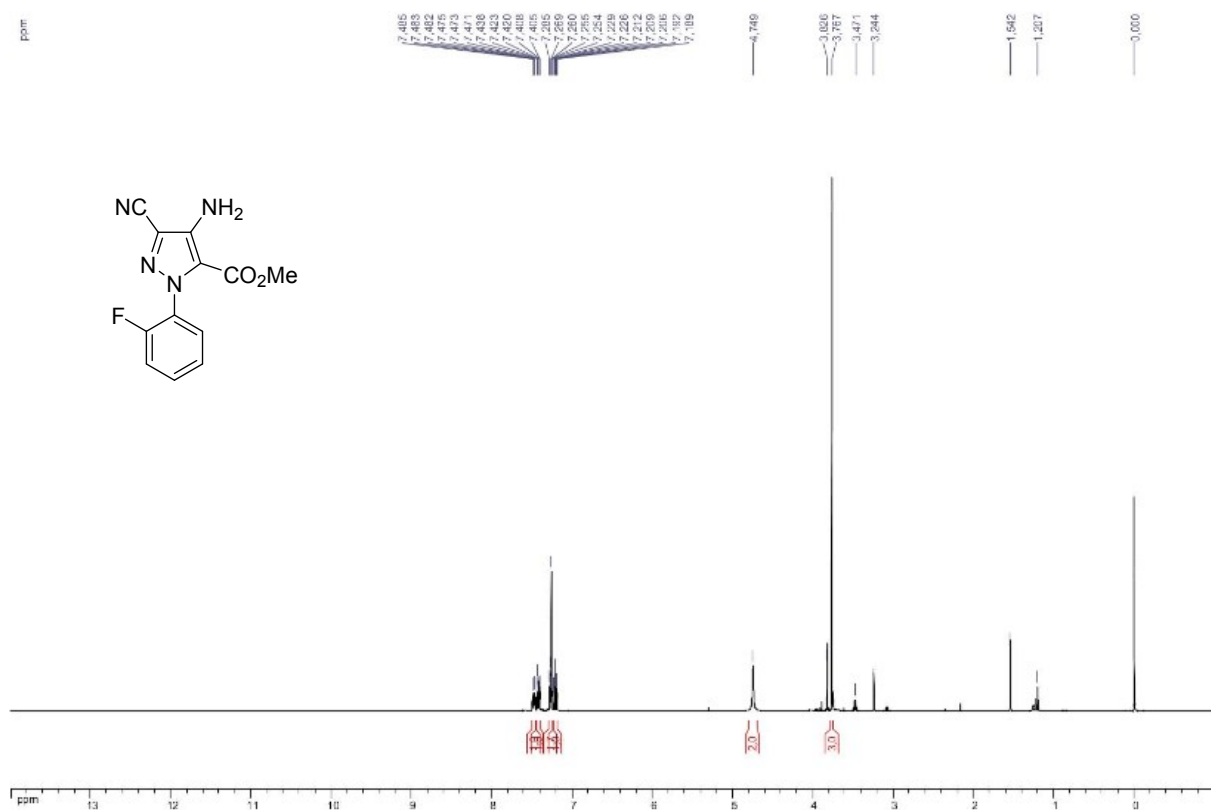
¹H NMR compound A.8



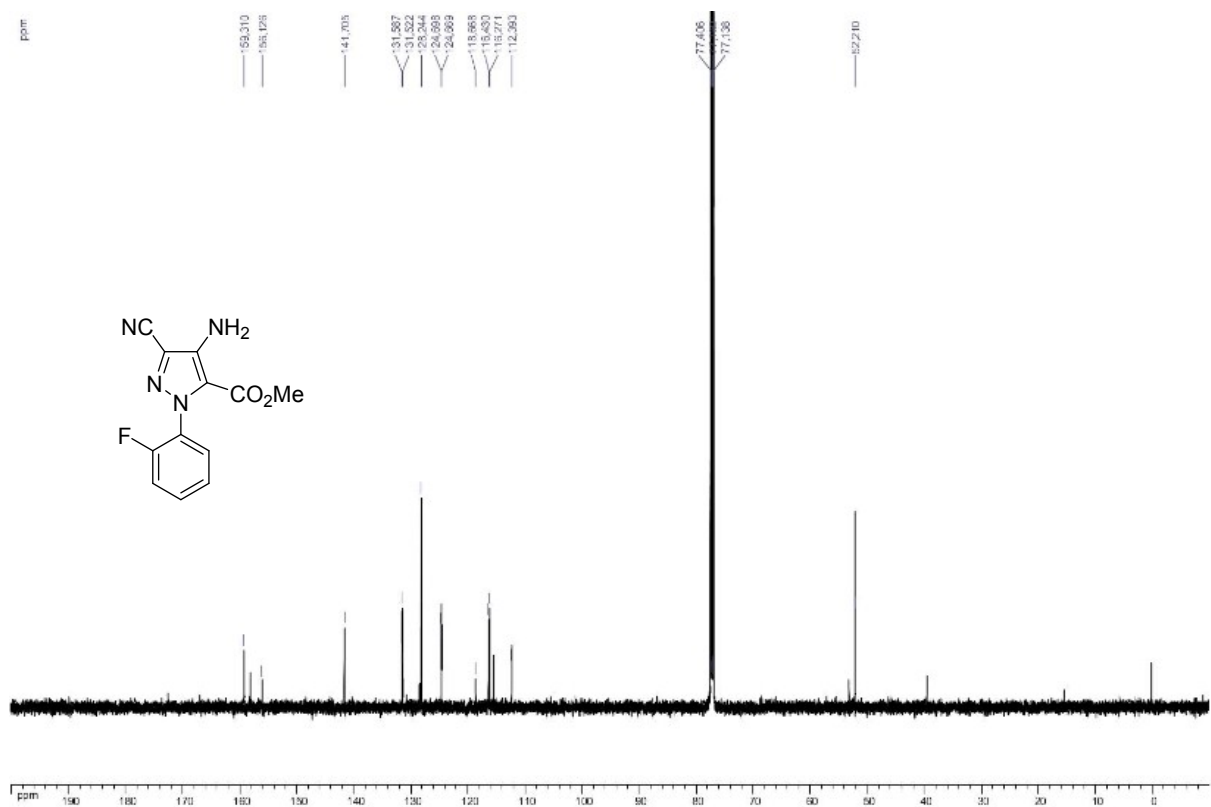
¹³C NMR compound A.8



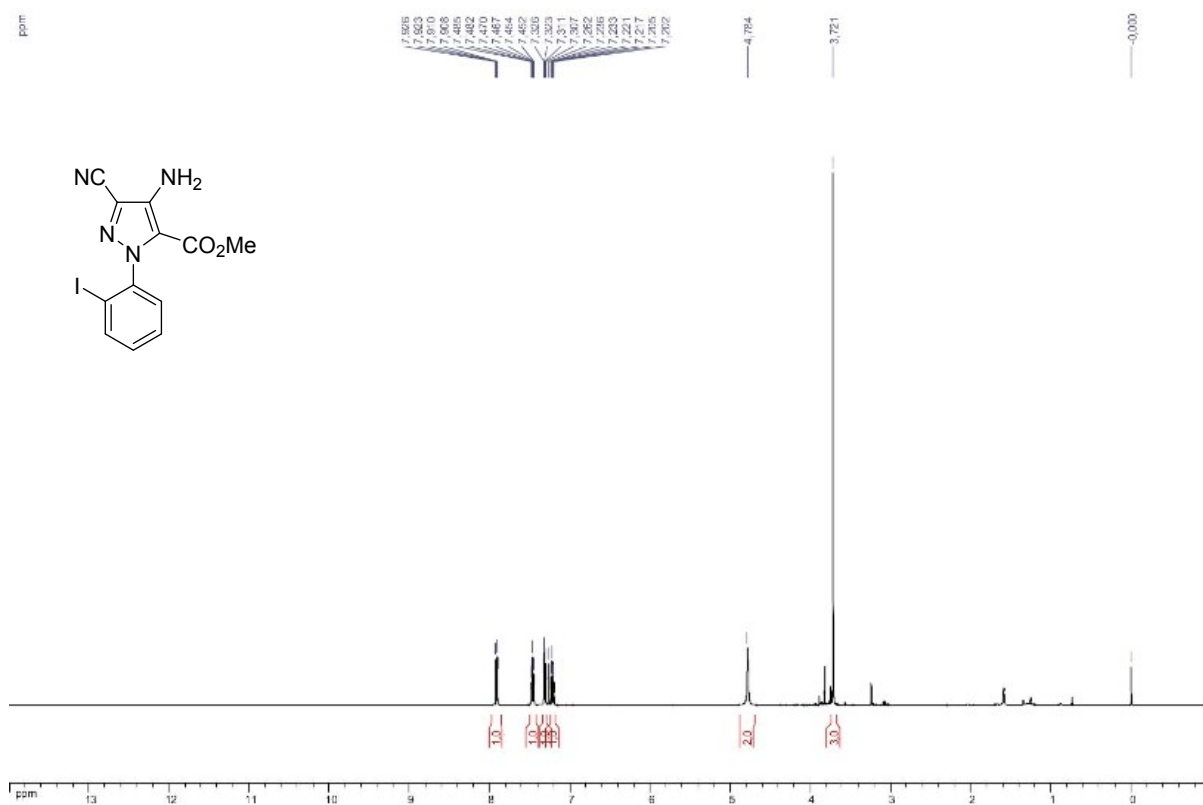
¹H NMR compound A.11



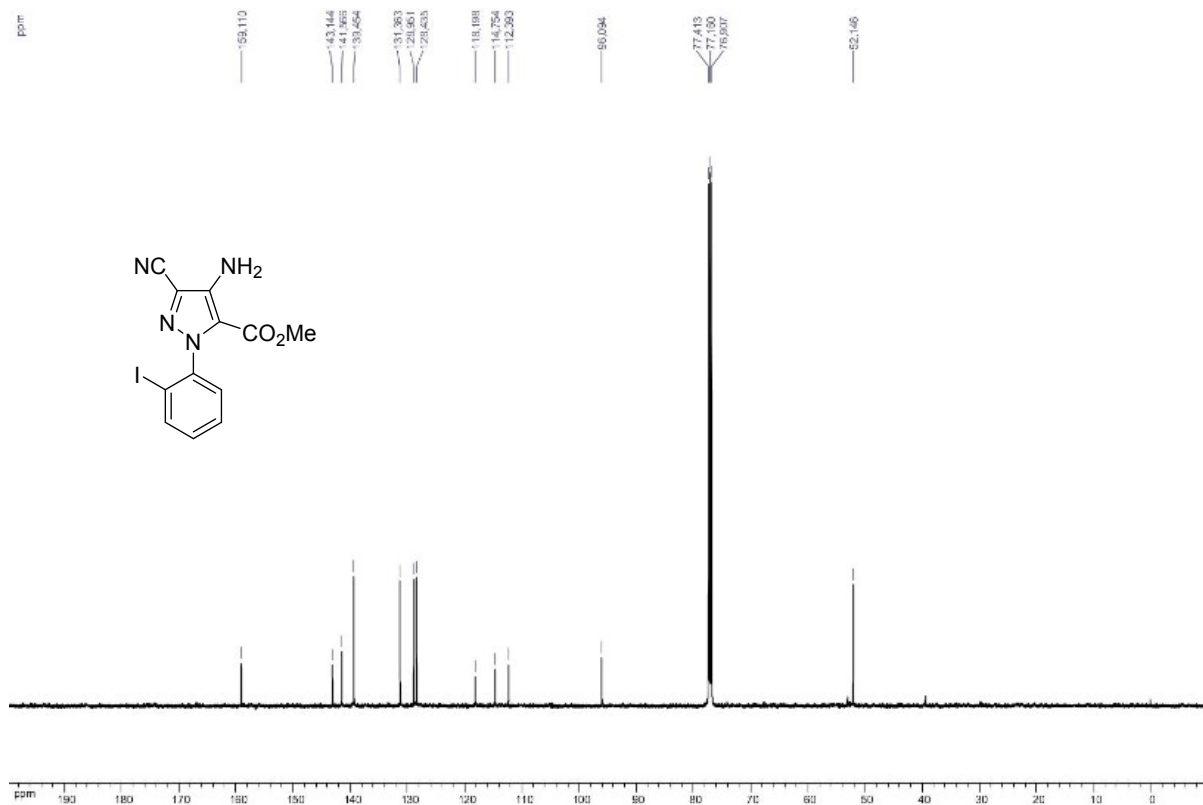
¹³C NMR compound A.11



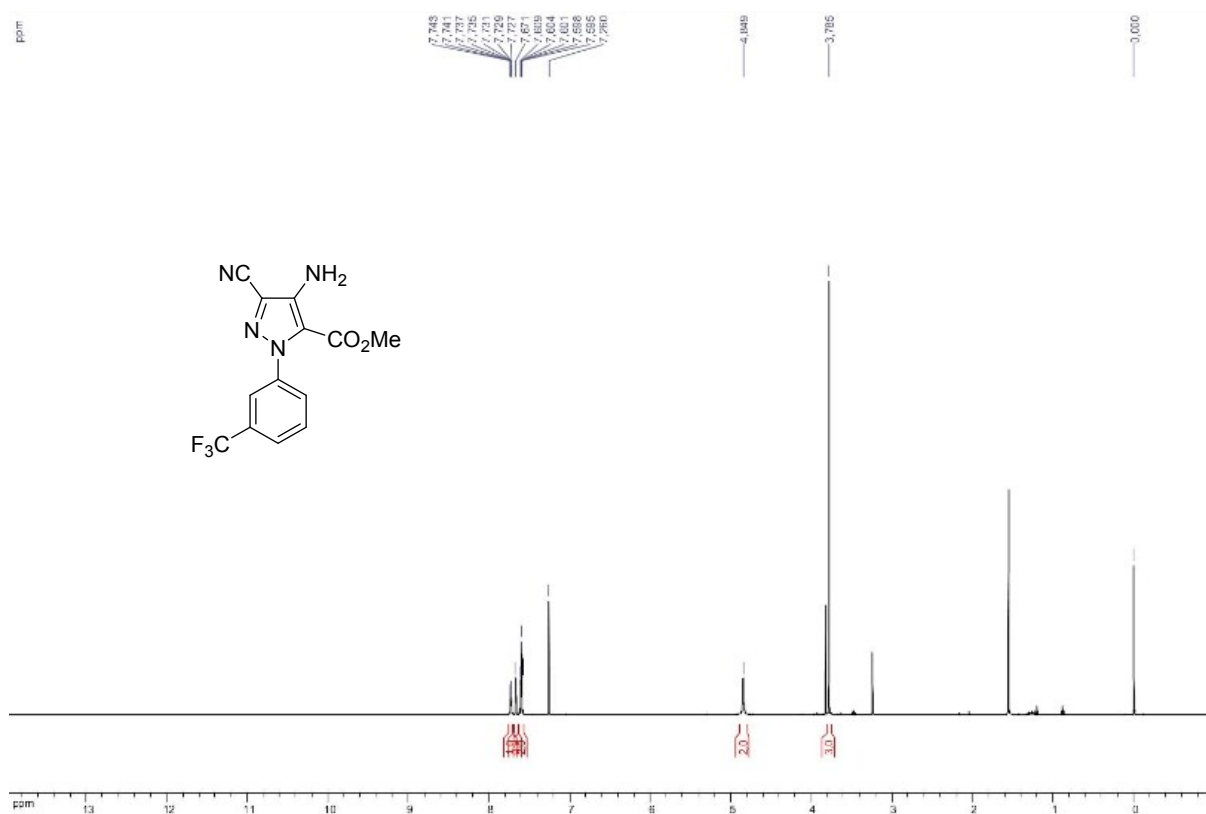
¹H NMR compound A.14



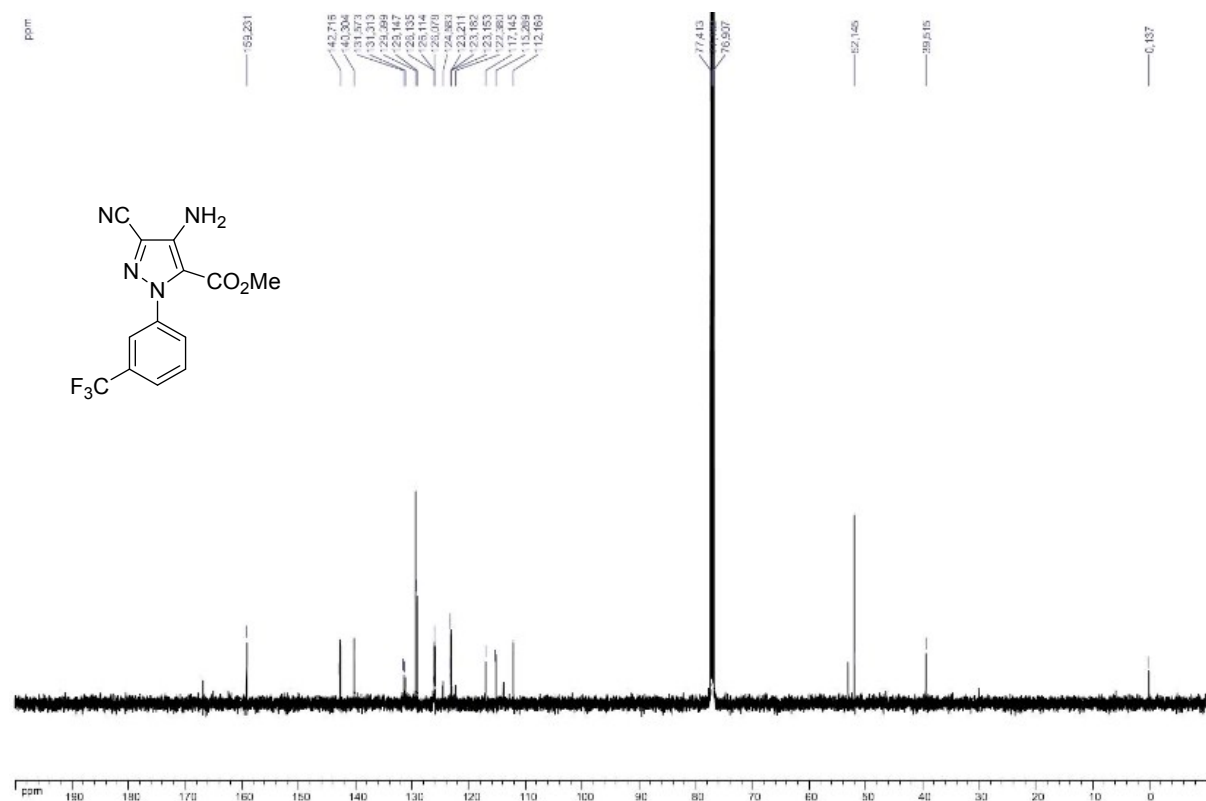
¹³C NMR spectrum of compound A.14



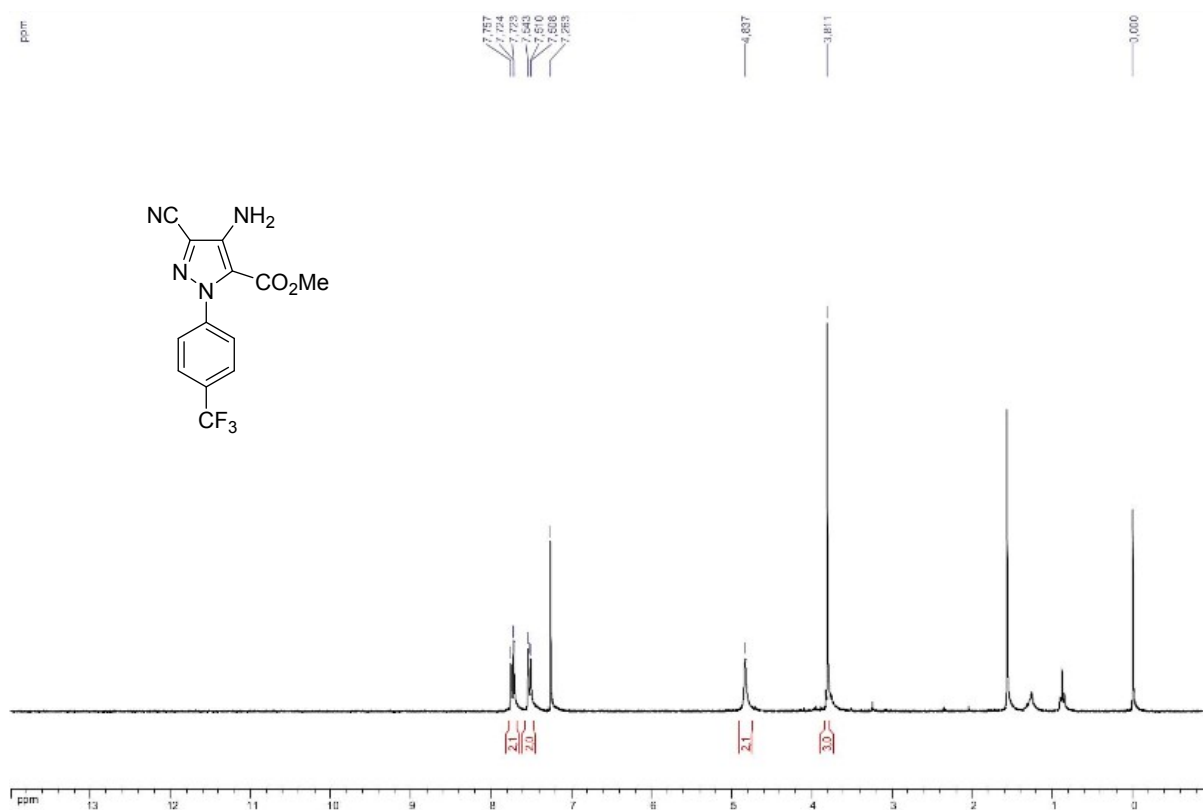
¹H NMR compound A.15



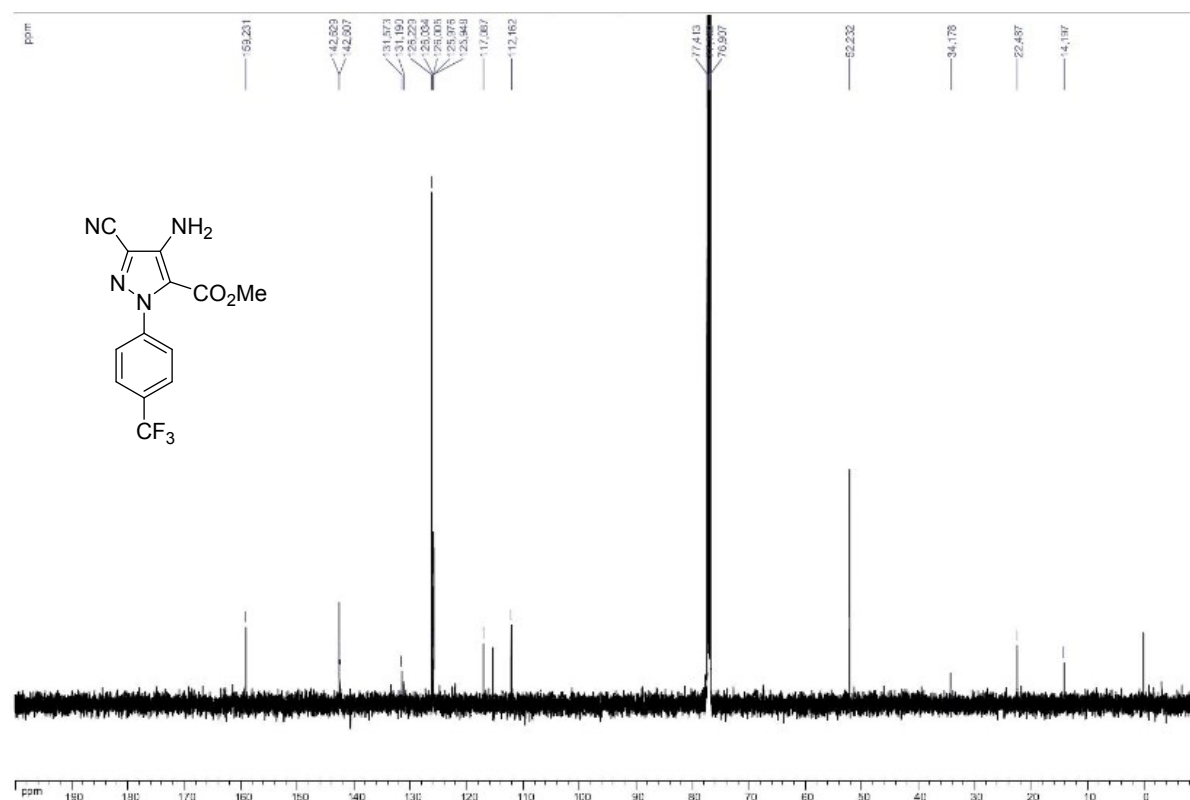
¹³C NMR spectrum of compound A.15



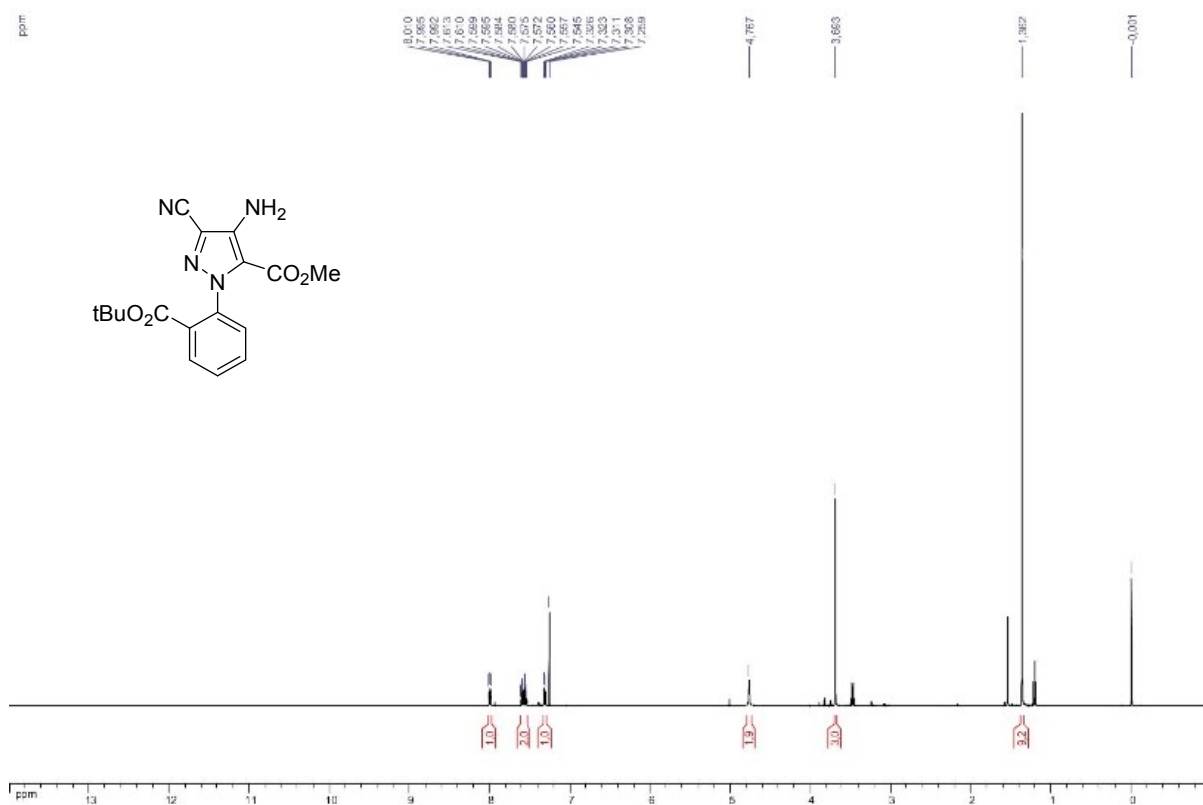
¹H NMR compound A.16



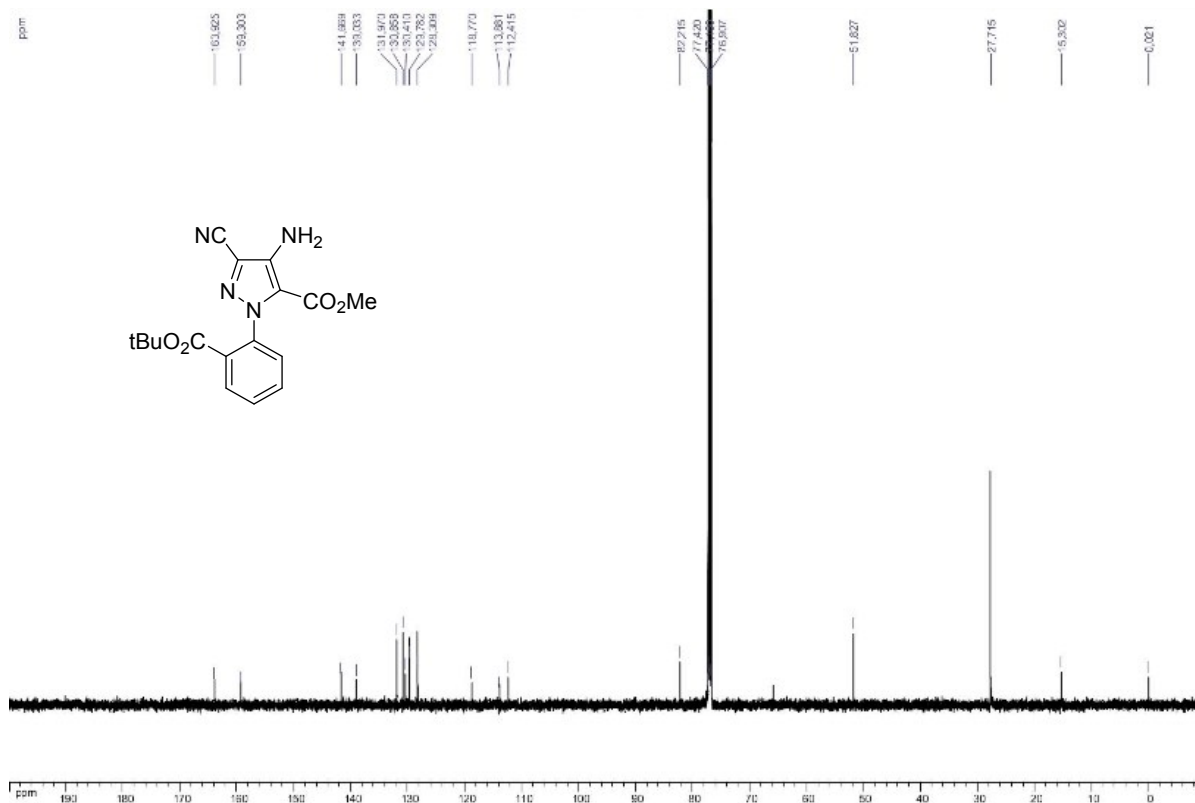
¹³C NMR spectrum of compound A.16



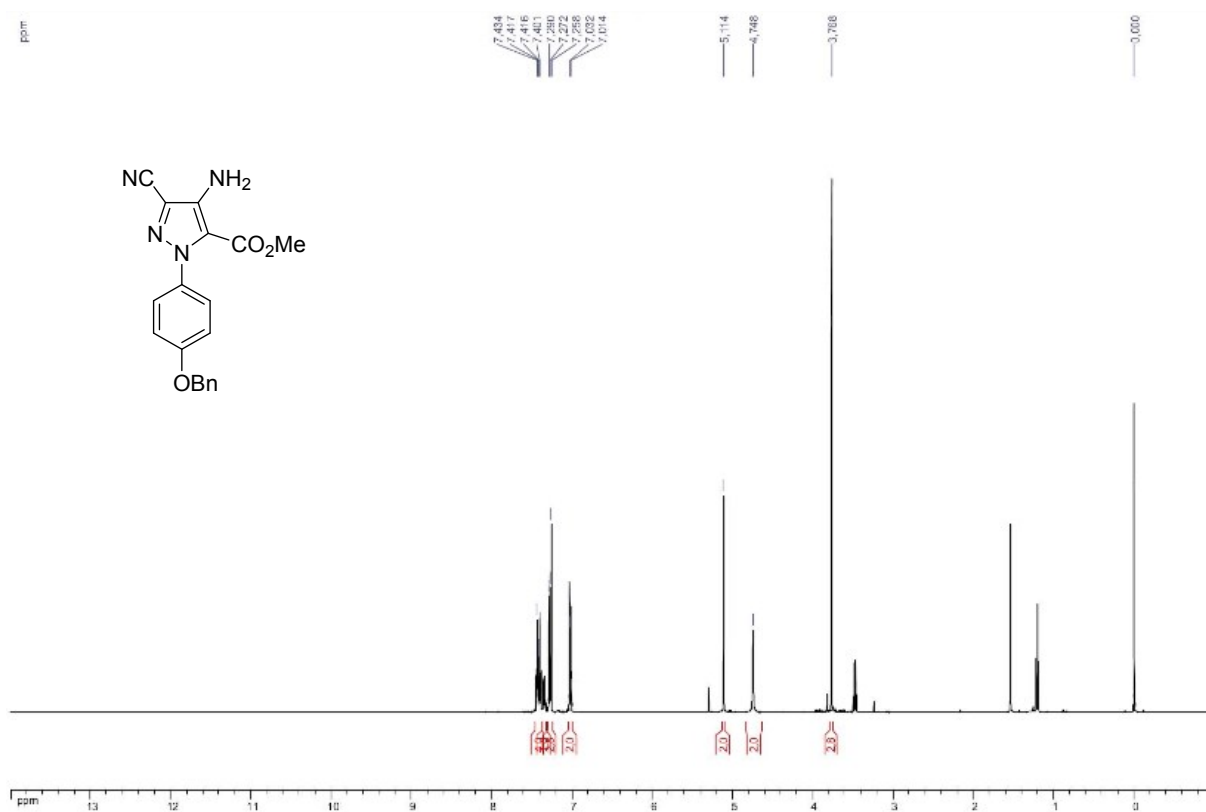
¹H NMR compound A.17



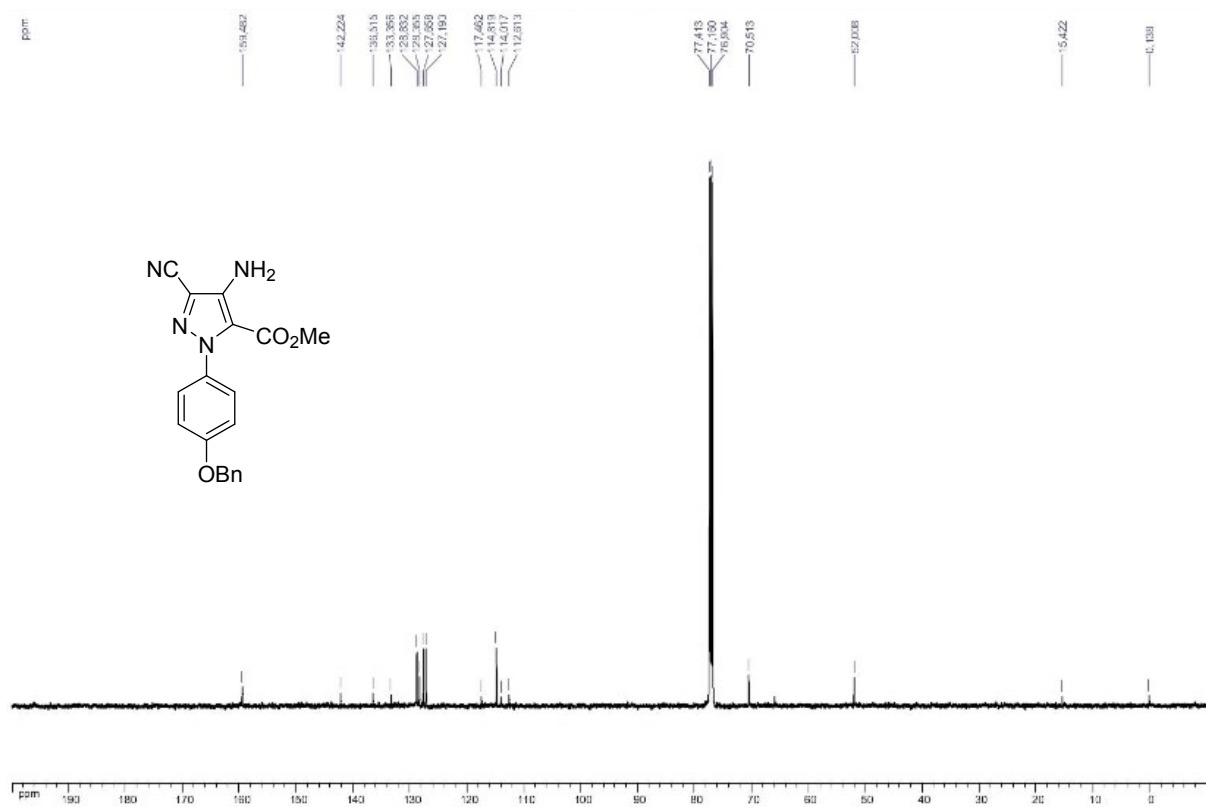
¹³C NMR compound A.17



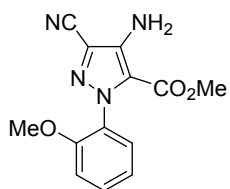
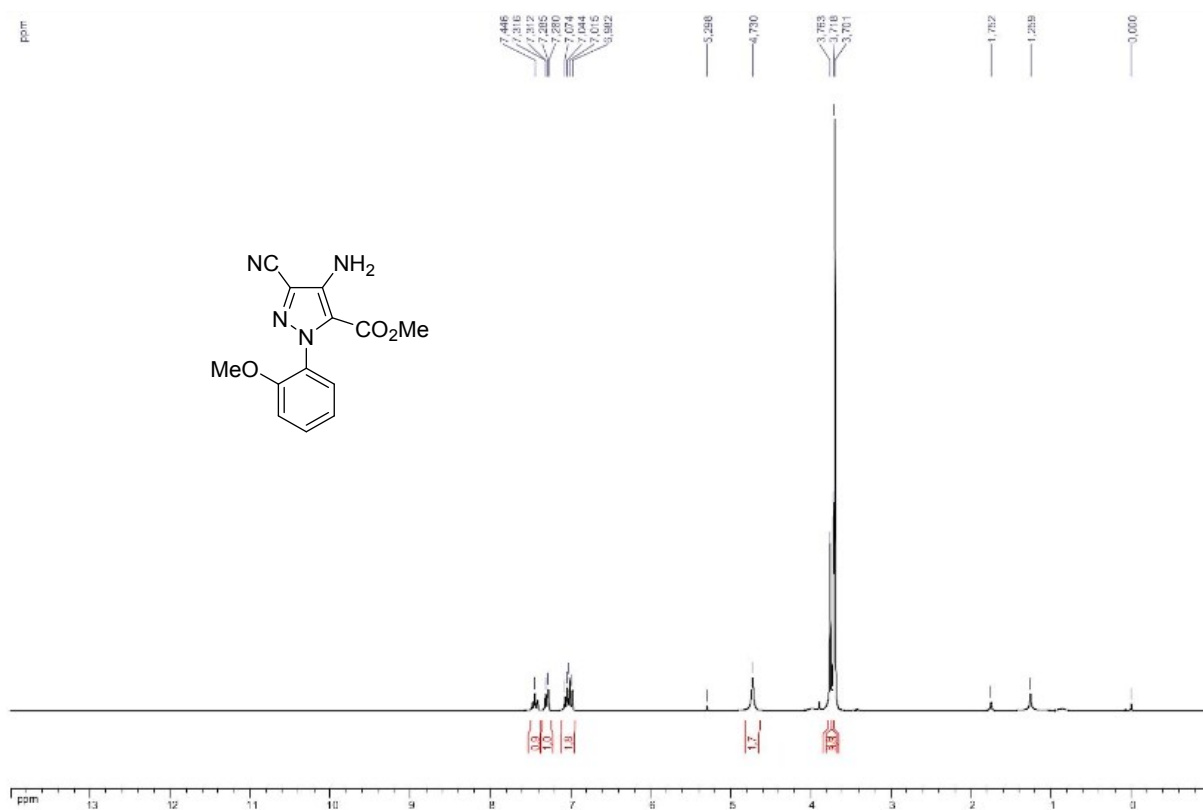
¹H NMR compound A.22



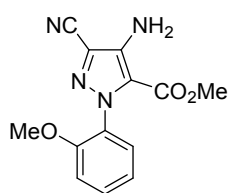
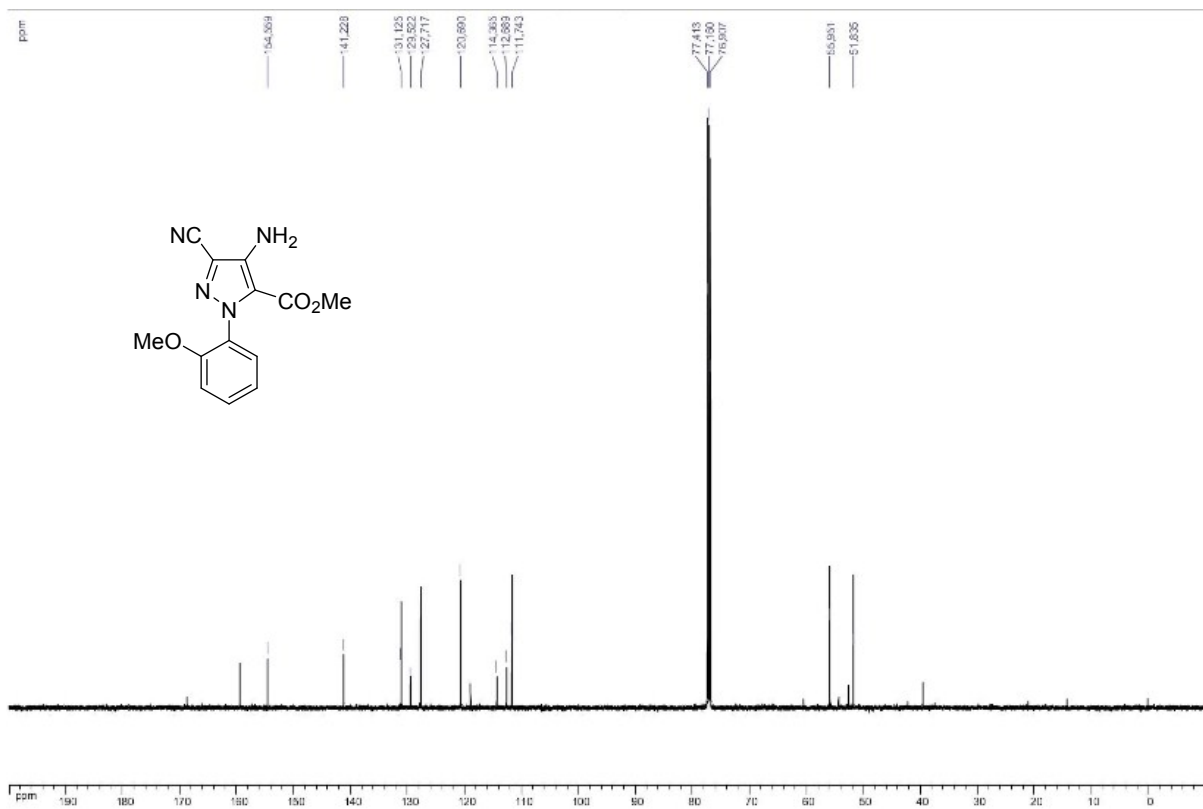
¹³C NMR spectrum of compound A.22



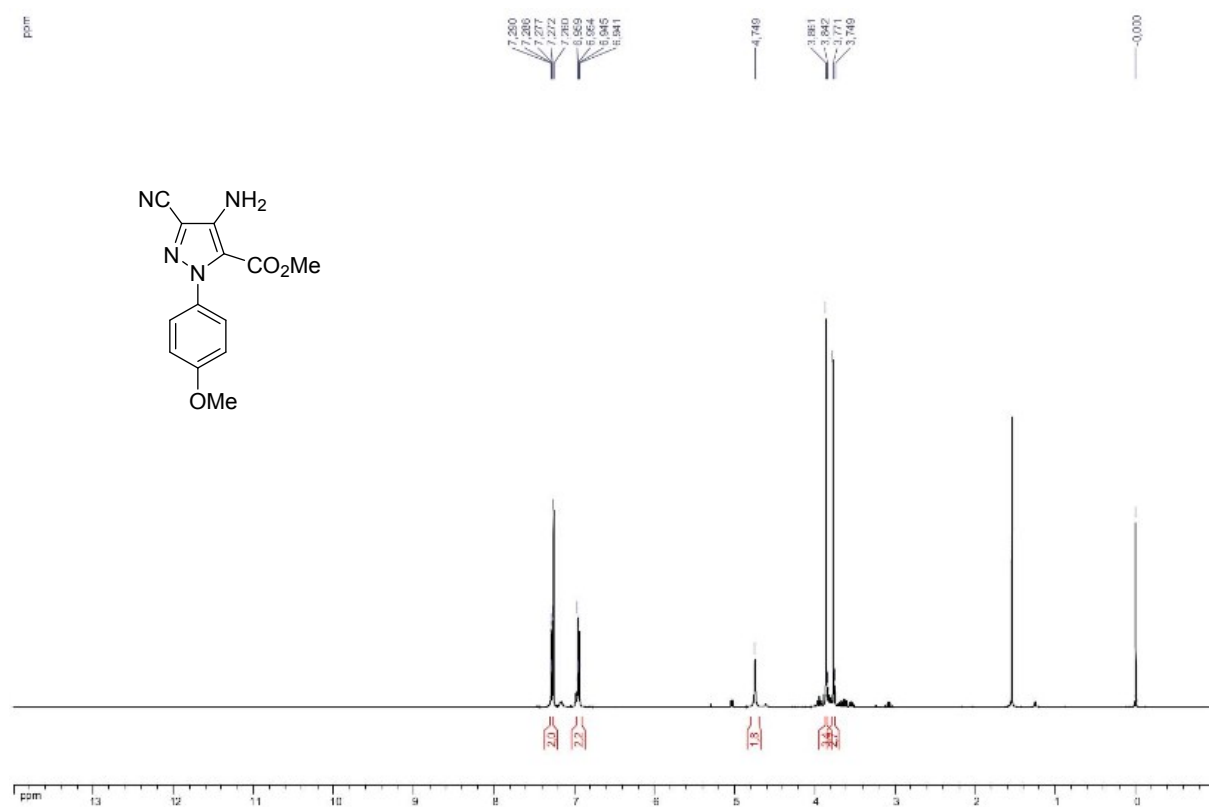
¹H NMR compound A.23



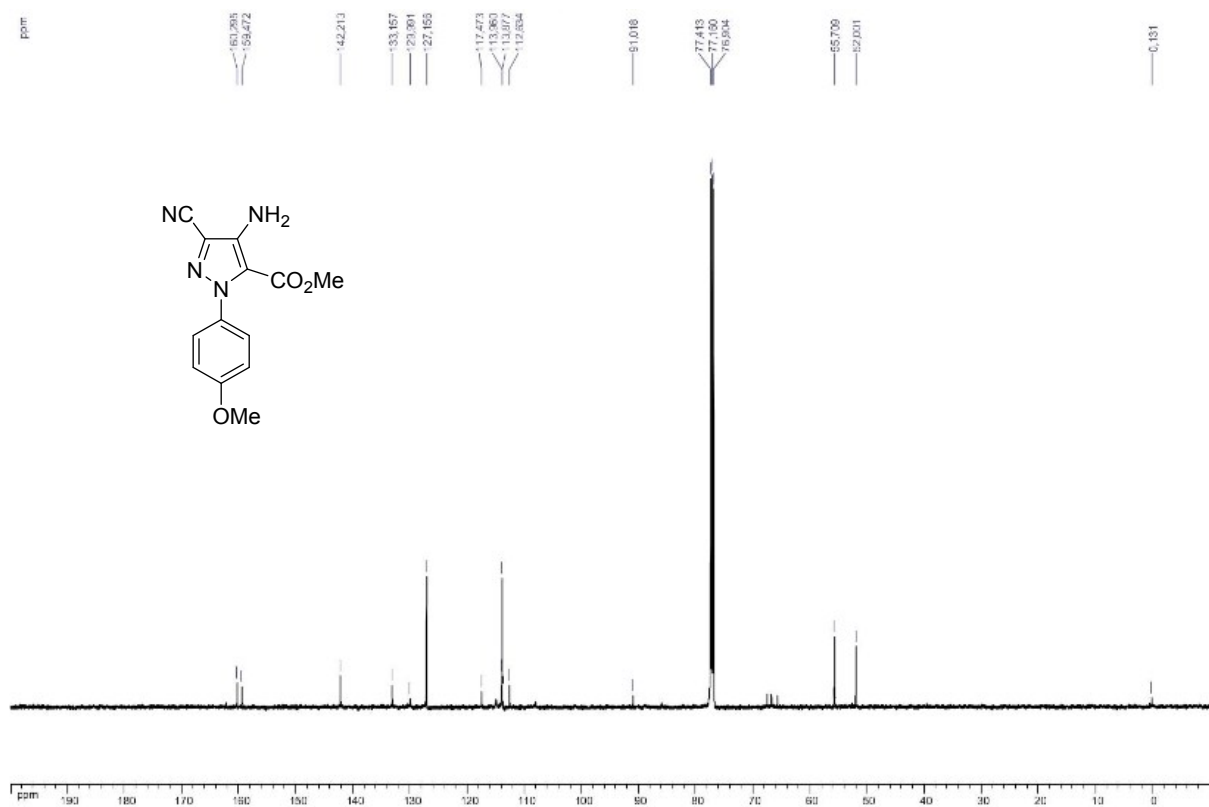
¹³C NMR compound A.23



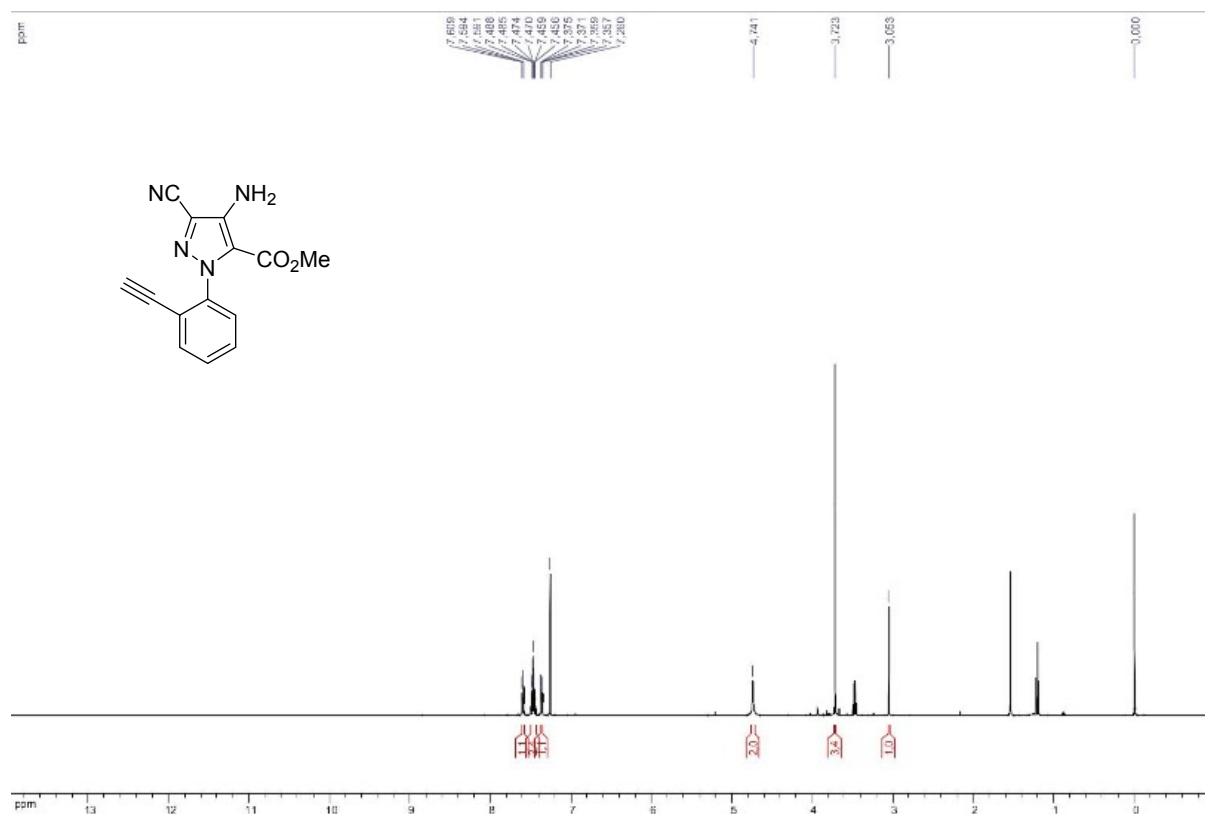
¹H NMR compound A.25



¹³C NMR spectrum of compound A.25



¹H NMR compound A.26



¹³C NMR compound A.26

